

**TERESA CRISTINA FONSECA DA SILVA**

**ADVANCED APPLICATIONS AND STUDIES OF  
LIGNOCELLULOSIC MATERIALS FOR ACHIEVING THE  
BIOREFINERY MODEL**

Tese apresentada à Universidade Federal de Viçosa, como parte das exigências do Programa de Pós-Graduação em Agroquímica, para obtenção do título *Doctor Scientiae*.

VIÇOSA  
MINAS GERAIS – BRASIL  
2011

**Ficha catalográfica preparada pela Seção de Catalogação e  
Classificação da Biblioteca Central da UFV**

T

S586a  
2011

Silva, Teresa Cristina Fonseca da, 1981-  
Advanced applications and studies of lignocellulosic  
materials for achieving the biorefinery model / Teresa  
Cristina Fonseca da Silva. – Viçosa, MG, 2011.  
xi, 105f. : il. ; 29cm.

Inclui apêndice.

Orientador: Jorge Luiz Colodette.

Tese (doutorado) - Universidade Federal de Viçosa.

Inclui bibliografia.

1. Materiais biomédicos. 2. Hemicelulose. 3. Eucalipto.  
4. Celulose. 5. Lignina. 6. Pirólise. I. Universidade Federal  
de Viçosa. II. Título.

CDD 22. ed. 630.2

**TERESA CRISTINA FONSECA DA SILVA**

**ADVANCED APPLICATIONS AND STUDIES OF  
LIGNOCELLULOSIC MATERIALS FOR ACHIEVING  
THE BIOREFINERY MODEL**

Tese apresentada à Universidade Federal de Viçosa, como parte das exigências do Programa de Pós-Graduação em Agroquímica, para obtenção do título *Doctor Scientiae*.

APROVADA: 06 de maio de 2011.

---

Prof<sup>a</sup>. Maria Eliana Lopes Ribeiro de  
Queiroz

---

Prof. Laurent Frederic Gil

---

Prof. Lucian Amerigo Lucia

---

Prof. Sebastião Tavares de Rezende

---

Prof. Jorge Luiz Colodette  
(Orientador)

Dedico esta tese aos meus pais **ANTÔNIO** e **OLÍVIA** e ao meu marido **LEONARDUS**,

*“You must be the change you wish to see  
in the world”*

Mahatma Ghandi

## AGRADECIMENTOS

À Deus, por me guiar e abençoar nessa caminhada;

Ao meu marido, pelo carinho, amor, paciência e pelo companheirismo em todos os momentos;

Aos meus pais, pelo amor incondicional, paciência, apoio e incentivo;

Aos meus irmãos e sobrinhos, pelo companheirismo, apoio e alegrias;

À Universidade Federal de Viçosa e ao Programa de Pós-graduação em Agroquímica, pela oportunidade oferecida;

Ao *Department of Forest Biomaterials* da *North Carolina State University* (NCSU) nos Estados Unidos, pela oportunidade de participação no programa Doutorado – Sanduíche do CNPq;

À CAPES e ao CNPq, pela concessão das bolsas de estudo;

Ao meu orientador, professor Dr. Jorge Luiz Colodette, pela orientação e pelos ensinamentos passados a mim durante o desenvolvimento deste trabalho;

Ao professor Dr. Lucian A. Lucia, pela orientação, incentivo, amizade e apoio;

Ao professor Dr. Youssef Habibi, pelos ensinamentos, orientação e apoio durante a realização das atividades na NCSU;

Aos professores Dr. Luis Henrique Mendes da Silva e Dra. Maria do Carmo Hespagnol, pela paciência, ensinamentos e incentivo no decorrer do doutorado;

Aos colegas da NCSU e as amizades construídas nos EUA, Soledad, Ilari, Ricardo, Emília, Justin, Cristina, Linda, Jim, Desiree e Colin;

Aos colegas do curso e funcionários do Laboratório de Celulose e Papel, em especial a Flávia, Bianca, Maurício, Bittencourt, Dora, Vanessa, Carolina, Dalton, Larisse e Fernando;

Finalmente, a todos que direta e indiretamente deram apoio e incentivo, meus sinceros agradecimentos.

## **BIOGRAFIA**

Teresa Cristina Fonseca da Silva, filha de Antônio Higino da Silva e Olívia Maria Fonseca da Silva, nasceu em 21 de dezembro de 1981, em Juiz de Fora - MG.

Em 2003, graduou-se no curso de Química no Centro Universitário de Patos de Minas.

Em 2005, iniciou os estudos em nível de mestrado pelo programa de pós-graduação em Agroquímica pela Universidade Federal de Viçosa, desenvolvendo trabalhos na remediação de efluentes de indústrias de celulose e papel. Defendeu a dissertação em fevereiro de 2007.

No mesmo ano, ingressou no doutorado, atuando na área de química da madeira e biorefinaria para desenvolvimento de novos materiais a partir da biomassa. Em setembro de 2009, iniciou o programa de doutorado sanduíche, tendo desenvolvido pesquisas na “North Carolina State University” até dezembro de 2010. Defendeu a tese em maio de 2011.

## SUMÁRIO

RESUMO.....	viii
ABSTRACT.....	x
INTRODUCTION.....	1
CHAPTER 1. ADSORPTION OF CHEMICALLY MODIFIED XYLANS ON EUCALYPTUS PULP AND ITS EFFECT ON THE PULP PHYSICAL PROPERTIES (ORIGINAL RESEARCH PAPER – <i>Industrial &amp; Engineering Chemistry Research (2011), 50 (2), 1138- 1145</i> .....	3
ABSTRACT .....	3
1. INTRODUCTION .....	4
2. METHODS.....	6
2.1 Xylan Preparation.....	6
2.2 Xylan Analysis.....	6
2.3 Adsorption Experiments .....	7
2.4 Pulp Analysis .....	7
2.4.1 Chemical Analysis .....	7
2.4.2 Surface Analysis .....	8
2.4.3 Hand Sheet Physical Properties.....	8
3. RESULTS AND DISCUSSION.....	8
3.1 Xylan Characterization.....	8
3.2 Adsorption of xylans onto pulp fibers.....	10
3.3 Surface Morphology.....	13
3.4 Pulp beatability and properties.....	16
4. CONCLUSIONS.....	20
ACKNOWLEDGEMENTS.....	20
REFERENCES.....	20
CHAPTER 2. NANOFIBRILLATED CELLULOSE-BASED AEROGELS: A NEW CHEMICAL APPROACH FOR TUNING THEIR MICRO-ARCHITECTURES.....	25
ABSTRACT.....	25
1. INTRODUCTION.....	26
2. MATERIALS AND METHODS.....	27
2.1. Materials.....	27
2.2 Isolation of Nanofibrillated Cellulose (NFC) .....	27
2.3 NFCs modifications.....	28
2.4 Preparation of NFC-based aerogels.....	28
2.5 Conductimetry.....	28
2.6 Infrared Spectroscopy.....	29
2.7 Scanning Electron Microscopy (SEM) .....	29
2.8 BET Measurements.....	29
2.9 Physical Properties (Rheology and Density) .....	29
3. RESULTS AND DISCUSSION.....	30

3.1 NFC modification and drying .....	30
3.2 Surface area, pore volume and density of the aerogels .....	33
3.3 Morphology and rheological properties .....	34
CONCLUSIONS.....	38
REFERENCES.....	39
CHAPTER 3. THE INFLUENCE OF THE CHEMICAL AND STRUCTURAL FEATURES OF XYLAN ON THE PHYSICAL PROPERTIES OF ITS DERIVED HYDROGELS (ORIGINAL RESEARCH PAPER – <i>Soft Matter</i> (2011), 7, 1090-1099).....	42
ABSTRACT.....	42
INTRODUCTION.....	43
RESULTS AND DISCUSSION.....	45
Extraction and derivatization of the xylans.....	48
Morphology, bounded water and rheological properties .....	45
Swelling behavior.....	54
Post-acetylated xylan based hydrogels .....	55
Drug release.....	57
CONCLUSION.....	58
MATERIAL AND METHODS.....	59
Materials.....	59
Isolation of xylans.....	59
Xylan Acetylation.....	60
Sugar Analyses.....	60
Size Exclusion Chromatography (SEC).....	60
Hydrogel Synthesis .....	60
<sup>1</sup> H NMR Measurements.....	61
Hydrogel swelling ratio measurements.....	61
Scanning Electron Microscopy (SEM).....	62
Bounded water content.....	62
Rheological Properties.....	62
Doxorubicin Release from xylan-based hydrogels.....	63
ACKNOWLEDGEMENTS.....	63
REFERENCES.....	63
CHAPTER 4. A FACILE APPROACH FOR THE SYNTHESIS OF XYLAN- DERIVED HYDROGELS.....	67
ABSTRACT.....	67
INTRODUCTION.....	68
EXPERIMENTAL PART .....	70
Material .....	70
Isolation and characterization of xylan .....	70
Hydrogel Synthesis and Characterization.....	71
RESULTS AND DISCUSSION.....	73

Isolation and characterization of xylans .....	73
Preparation and characterization of xylan-based hydrogel .....	75
Morphology and rheological properties.....	76
Swelling behavior.....	78
CONCLUSION.....	79
ACKNOWLEDGEMENTS.....	79
REFERENCES.....	79
CHAPTER 5. A QUANTITATIVE MOLECULAR STRUCTURE- PYROLYTIC ENERGY CORRELATION FOR HARDWOOD LIGNINS.....	81
ABSTRACT.....	81
1. INTRODUCTION.....	82
2. MATERIALS AND METHODS.....	83
2.1 Materials .....	83
2.2 Chemical/Structural analysis of lignin.....	84
2.3 Thermal Analysis of lignin.....	84
3. RESULTS AND DISCUSSION.....	85
3.1 Lignin Quantification by <sup>13</sup> C NMR .....	85
3.2 Pyrolysis of lignins in TGA/DSC.....	91
3.2.1 TGA experiments.....	91
3.2.2 DSC experiments.....	92
3.3 Analysis of the enthalpy and correlation with lignin substructures / content.....	94
4. CONCLUSIONS.....	97
ACKNOWLEDGEMENTS.....	98
REFERENCES.....	98
OVERALL CONCLUSION.....	102
APPENDIX .....	103

## RESUMO

SILVA, Teresa Cristina Fonseca da, D.Sc., Universidade Federal de Viçosa, maio de 2011. **Aplicações avançadas e estudos de materiais lignocelulósicos para alcançar o modelo de biorrefinaria.** Orientador: Jorge Luiz Colodette. Co-orientadores: Luis Henrique Mendes da Silva, Luiz Cláudio de Almeida Barbosa e José Lívio Gomide.

Celulose, hemiceluloses e lignina são os três principais componentes da biomassa. Esses componentes foram detalhadamente estudados e explorados com o objetivo de se alcançar o modelo de biorrefinaria. Celulose e hemiceluloses foram extraídas da madeira de *Eucalyptus urograndis* enquanto a lignina foi extraída dessa mesma espécie e de outras três espécies de folhosas (*Eucalyptus globulus*, *Eucalyptus nitens*, *Populus trichocarpa*). Celulose nanofibrilada (NFC) foi modificada usando TEMPO e hidroxiapatita (HAp) e posteriormente usada para produzir aerocelulose através de secagem direta por liofilização. A morfologia dos aerogéis de celulose oxidados mostraram uma distribuição homogênea no tamanho dos pores. Tal distribuição foi mantida após adição de HAp. Aerogels de celulose modificada também apresentaram-se mais resistentes a pressão que os seus correspondentes não modificados. Xilanas foram usadas tanto como aditivos na polpa celulósica como para produção de materiais com alto valor agregado – hidrogéis. Para o uso como aditivos, as xilanas foram modificadas para produzir diferentes quantidades e tipos de ácidos urônicos e o efeito da modificação química, temperatura e tempo de adsorção na polpa de eucalipto foi investigada. Os resultados mostraram que altas temperaturas aumentam significativamente a adsorção, enquanto tempo de adsorção não apresenta o mesmo efeito na adsorção. Xilanas com baixo teor de ácidos urônicos tiveram foram melhor adsorvidas, seguidas por xilanas enriquecidas com ácidos hexenurônicos e finalmente, xilanas com alto teor de ácidos metilglicurônicos. Xilanas também foram usadas para produzir hidrogéis em duas rotas diferentes: i) hidrogéis de xilana/poli(2-hidroxietilmetacrilato) foram preparados após reticulação induzida por monômeros metacrílicos e ii) hidrogéis de xilana ligadas a lignina (complexo lignina-carboidrato) usando monômeros metacrílicos. Propriedades dos hidrogéis puderam ser facilmente modificadas de acordo com a presença dos grupos acetila e do grau de substituição dos monômeros metacrilato ligados as cadeias de xilana. Grupos acetila introduziram compactação e rigidez aos hidrogéis, reduzindo a capacidade de inchamento dos

mesmos e também, melhorando propriedades tais como liberação do medicamento (doxorubicin) adicionados previamente nos hidrogéis. Para a segunda rota de produção de hidrogéis, polimerização radicalar com hidroxietilmetacrilato (HEMA) foi realizada com sucesso por meio de uma etapa facilitada devido a presença de duplas ligações formadas durante a deslignificação (usando ácidos peracético) dos complexos lignina-carboidratos, que foi a razão atribuída à formação da reticulação. Finalmente, ligninas isoladas do licor kraft (lignina técnica – TL) e suas estruturas foram correlacionadas com a energia da pirólise medida por “differential scanning calorimetry” (DSC). Correlações negativas foram encontradas entre energia da pirólise e estruturas da lignina tais como grupos metoxila, siringil/guaiacil e hidroxila alifáticas enquanto correlações positivas foram encontradas entre estruturas condensadas e valores de entalpia.

## ABSTRACT

SILVA, Teresa Cristina Fonseca da, D.Sc., Universidade Federal de Viçosa, May, 2011. **Advanced applications and studies of lignocellulosic materials for achieving the biorefinery model.** Adviser: Jorge Luiz Colodette. Co-advisers: Luis Henrique Mendes da Silva, Luiz Cláudio de Almeida Barbosa and José Lívio Gomide.

Cellulose, hemicelluloses and lignin are the three structural components of biomass. They were detailed studied and exploited to achieve the biorefinery model. Cellulose and hemicelluloses were extracted from *Eucalyptus urograndis* hardwood specimens while lignin was extracted from *Eucalyptus urograndis*, *Eucalyptus globulus*, *Eucalyptus nitens* and *Populus trichocarpa* specimens. Nanofibrillated cellulose (NFC) was modified with TEMPO and hydroxyapatite (HAp) and then, used to produce cellulose-based aerogels by direct freeze-drying. Oxidized aerogels morphology shows a homogeneous pore size distribution which was maintained after HAp addition. Modified aerogels produced also displayed higher strength than the non-modified one. Xylans polysaccharides were either used as an additive on cellulose pulp and also as basis for production add-value materials - hydrogels. For the primary use, xylans were modified to produce different amounts and types of uronic acids and the effect of the chemical modification, temperature and time of adsorption onto eucalyptus pulp was investigated. Higher temperatures greatly improved adsorption whereas adsorption time had no significant effect on adsorption. Low uronic acid-xylan had greater adsorption on pulp, followed by enriched hexenuronic acid xylan and xylan enriched with methylglucuronic acid groups. Xylans were also used to produce hydrogels in two different ways *via* radical polymerization: i) Xylan/poly(2-hydroxyethylmethacrylate)-based hydrogels were prepared after crosslinking induced by methacrylic monomers and ii) lignin-carbohydrate complex-based hydrogels using methacrylic monomers. Hydrogels properties could be easily tuned according to the presence acetyl groups and degree of substitution of methacrylate monomers attached to the xylan chain. Acetyl groups introduced compactness and stiffness to the hydrogels which ultimately reduced their water swelling capacity and moreover, enhanced their drug release properties. For the second path, a facile step to form hydrogels by radical polymerization with HEMA was successfully accomplished. The presence of double

bonds formed during mild delignification (using peracetic acid) of lignin-carbohydrate complex (LCC) was the reason attributed to the crosslinking. Once again, the presence of acetyl groups in xylan chains played an important role for tuning hydrogel properties. Finally, lignin from kraft liquor was isolated (technical lignin – TL) and its structure was correlated to the pyrolysis energy measured by differential scanning calorimetry (DSC). Negative relationships were found between lignin substructures such as methoxyl groups, syringyl/guaiacyl and aliphatic OHs whereas positive correlation was found between condensed structures and enthalpy values.

## INTRODUCTION

The biorefinery concept has become a hot research topic because integrates value-added materials from biomass, biofuel and bioenergy. Lignocellulosic biomass is one of the most available and renewable resources which represent a promising low cost raw material for renewable energy production. Producing multiple products and maximizing the value derived from the biomass feedstock are economically and sustainably advantageous. Moreover, decreasing the dependency on fossil fuel reserves by developing a sustainable society and boosting rural development are important goals of modern society.

Biomass is mainly constituted by three structural components (polysaccharides cellulose, hemicelluloses and aromatic polymer lignin) as well as by some minor nonstructural components. Cellulose, which represents over 50% of biomass, is a linear polymer of cellobiose (D-glucopyranosyl- $\beta$ -1,4-Dglucopyranose) units and presents a highly ordered structure. By contrast, lignin, the most recalcitrant plant constituent, forms a 3-D network including a variety of C-C and ether linked substructures. Hemicelluloses present an intermediate complexity degree, being formed by pentose and hexose units (often acetylated) in branched chains.

Cellulose and hemicellulose (xylans) from hardwood (eucalyptus urograndis) were used to produce added-value products such as aerogels and hydrogels, respectively. Besides, studies on hemicelluloses (xylans) adsorption onto cellulose pulp were carried out in this study.

Xylans are considered to be very important for production of printing and writing paper grades because they facilitate pulp refining and increase fiber bonding. Taking this fact into consideration, the effect of the different types of uronic acid linked to the xylan chain was investigated. During kraft pulping, methylglucuronic acid groups are almost completely converted into hexenuronic acid groups and this situation may affect the adsorption of xylans onto pulp and subsequently effect on pulp yield and properties. On Chapter 1, chemically modified xylans were adsorbed on eucalyptus pulp and the effects on the pulp physical properties were investigated.

Focus on development of added-value products derivatives from wood feedstock for advanced applications play an important role on the biorefinery perspective. In this context, one of the goals of this work was to develop hydrogels from xylans, the most common hemicellulose of eucalyptus wood, by exploiting

xylan's chemical features that allows for tuning their properties. Due to its characteristics, hydrogels constitute the basis for a variety of applications including, especially in biomedical and pharmaceutical use: controlled drug release, contact lenses, and soft tissue mimicking.

This work is comprised of two chapters dealing with hydrogels production from xylans (Chapters 3 and 4). On Chapter 3, xylans with and without acetyl groups were used to form hydrogels with particular characteristics. It was demonstrated for the first time the effect of acetyl groups on the morphology, physical properties and drug delivery system. Chapter 4 reveals a new approach for producing hydrogels in a facile route by likely initiating the crosslinking *via* radical polymerization from an oxidized lignin fragment.

Aerogels were fabricated from cellulose nanofibers (NFCs) and modified by TEMPO-mediated oxidation and addition of hydroxyapatite (Chapter 2). The primary goal of the aerogels produced was to reach high-resistance (strength) for further tests as bone substitute material. In fact, aerogels have attractive features leading to the development of applications such as storage media for gases, filter materials carrier for catalysis, scavengers for dust particles, shock absorbers and heat and sound insulators. Cellulose has emerged as a promising candidate for aerogels production because of their abundance and also because their properties may be similar to their inorganic counterparts such as silica and alumina.

Lignin has a rather high heat value, which makes it interesting to use as a biofuel. In pulp mills, lignin from kraft liquor is largely recovered as a byproduct to be used as a solid fuel, minimizing environmental impacts by closing the green house gas (CO<sub>2</sub>) loop. Developing a better understanding of lignin structures present on kraft pulp would be extremely helpful to exploit the potential lignin as renewable and readily available feedstock. On Chapter 5, lignin from kraft liquor was isolated (called "technical lignin" - TL) and its structure was quantitatively determined. Then, energy changes during heating and weight loss were associated to the chemical structure in order to identify the driving factors for energy changes. Correlations found between lignin structure and enthalpy values may represent important ramifications for the overall efficiency and energetics of thermochemical biomass transformation.

## CHAPTER 1

Published as original paper (*Industrial & Engineering Chemistry Research* (2011), 50 (2), 1138-1145)

### ADSORPTION OF CHEMICALLY-MODIFIED XYLANS ON EUCALYPTUS PULP AND ITS EFFECT ON THE PULP PHYSICAL PROPERTIES

*Teresa Cristina Fonseca Silva,<sup>1</sup> Jorge Luiz Colodette,<sup>1</sup> Lucian A. Lucia,<sup>2</sup> Rubens Chaves de Oliveira<sup>3</sup>, Flávia Natalino Oliveira<sup>1</sup>, Luis Henrique Mendes Silva<sup>1</sup>*

<sup>1</sup>Departamento de Química, Universidade Federal de Viçosa, Viçosa, MG, 36570-000; Brazil

<sup>2</sup>Laboratory of Soft Materials & Green Chemistry, Department of Forest Biomaterials, North Carolina State University, Raleigh, North Carolina 27695-8005

<sup>3</sup>Departamento de Engenharia Florestal, Universidade Federal de Viçosa, Viçosa, MG, 36570-000; Brazil

E-mail: [lucian.lucia@ncsu.edu](mailto:lucian.lucia@ncsu.edu)

#### Abstract

Three different birchwood-based xylan biomaterials were used in the current study to deconvolve the heretofore unknown effects of these modified adsorbed xylans on the processability of eucalyptus pulp: a 4-O-methylglucuronic acid xylan (MeGlcA-xylan); then, the MeGlc moiety was modified to provide an enriched hexenuronic acid xylan (HexA-xylan), and a low uronic acid content xylan (LowUrA-xylan). The study illustrates how the composition of xylan, in terms of the type and content of uronic acid, strongly influences the physical properties of cellulose fibers. NMR was used to confirm these structures and their  $M_w$ s were measured by GPC. The three different xylan types were adsorbed onto bleached kraft pulp under controlled times and temperatures and examined by AFM and SEM. It was found that LowUrA-xylan had greater adsorption on eucalyptus pulp, especially at high temperatures and times, while HexA-xylan adsorbed more onto eucalyptus pulp than MeGlcA-xylan. Water Retention Values (WRV) of xylan-enriched eucalyptus pulps increased, while their hornification decreased. In general, xylan-enriched pulps demonstrated improved

processability (beatibility) while displaying acceptable physical properties. These findings may have important implications for the overall efficiency and energetics of downstream biomass transformation processes such as pretreatment within the context of a biofuel application.

**Keywords:** *Eucalyptus*, *xylans*, *chemical modification*, *adsorption*, *water retention*, *hornification*

## 1. Introduction

Xylans are the most abundant heteropolysaccharides (hemicelluloses) found in angiosperms and terrestrial plant cell walls and are among the most abundant biomaterials on the planet. Due to xylans abundance in nature and their inherent affinity to cellulose, they can be used as biodegradable and renewable cellulose fiber modifying agents<sup>1-3</sup>. From a chemical engineering perspective, the relative importance of maintaining a high retention of xylans during the pulping of hardwoods has very high economic considerations because it directly affects overall materials output or pulp yield<sup>4, 5</sup>. Structurally, xylans are comprised of linear chains of  $\beta$ -D-(1,4)-linked D-xylopyranosyl residues that are assembled in a branched array. On average, every tenth xylosyl residue possesses an  $\alpha$ -4-O-methylglucuronyl residue that branches off at O-2<sup>6-10</sup>. During the kraft pulping process, wood xylan is extensively modified<sup>11-14</sup>. It is believed that the dissolved xylan, modified or not, is adsorbed onto the cellulose-based fibers at the end of the pulping phase<sup>13, 15-17</sup>.

Molecular structural investigations of polysaccharide interactions have revealed that the level of interaction between the cellulose-based fibers and hemicelluloses is a function of pH, temperature, and time of adsorption<sup>18-21</sup>. Additionally, another consideration during the pulping of hardwoods is that the methylglucuronic acid groups of xylan are almost completely converted into hexenuronic acid groups during pulping<sup>22, 23</sup>. This situation may affect the adsorption of xylans onto pulp and its subsequent effect on pulp yield and pulp properties are important questions to resolve. Answers to questions such as the latter can influence the methodology (time, temperature, pH) of hardwood pulping for maximum output and physical properties of the pulp.

It is well known that adsorption of xylans onto cellulose fibers improves the physical processability (beatibility) of the pulp which directly saves energy<sup>24</sup> but, many contradictions are found in terms of whether or not the mechanical properties of

the fibers are affected by the xylan adsorbed<sup>21, 25, 26</sup>. Many authors<sup>19, 23, 27, 28</sup> differ on the contribution of glucuronic acid groups to swelling properties and cell wall cohesion. A recent study showed that 4-*O*-methylglucuronoxylans have little effect on pulp handsheet properties<sup>29</sup>, while Lindstrom<sup>30</sup> concluded that the presence of glucuronic acid groups on the fiber surface is important for papermaking wet-end chemistry due to increased fiber surface charge.

A great advantage for using hemicelluloses to modify cellulose fiber is because of its natural affinity to cellulose<sup>18-21</sup>. Many authors pointed to the importance of preserving xylans during pulping process because xylan–cellulose interactions result in a final paper structure that possesses good tensile properties and wettability<sup>21, 26, 31</sup>. However, the contribution of hemicellulose to fiber strength is not yet clear; hemicellulose may act as an effective stress-transfer matrix while any mechanical damage to the bulk fibers may impair the stress transfer mechanism<sup>32, 33</sup>. A recent study using different cellulose/hemicelluloses ratios in fiber reported that the fiber and bond strength were not influenced by the hemicellulose content in the fiber<sup>34</sup>. It has been suggested that bleached pulp tensile strength is more a function of cellulose properties than xylan content and minimizing the degradation of cellulose and hemicelluloses is more important for pulp quality than increasing the amount of hemicelluloses in the fiber<sup>25</sup>. The minimization of sugar degradation in woody pulp also has important implications for the overall efficiency of downstream bioprocessing technologies that focus on energy production (bioethanol).

Therefore, it becomes critical to understand the mechanism of the adsorption of hemicelluloses to cellulose-based fibers. Few studies have been discussed the effect of side groups such as arabinolyl and *O*-acetyl during the adsorption of xylans onto cellulose fibers; as well as the effect of interaction in absence of branched groups<sup>19, 28</sup>. Thus, it is difficult to derive the key factors governing the xylan–cellulose interactions.

Several early studies have shown a mechanism for xylan retention on cellulose fibers. The mechanism is based on the tendency of xylan to self-associate and agglomerate onto cellulose fibers<sup>23, 28, 35</sup>. Kabel et al.<sup>19</sup> have concluded that arabinolyl and *O*-acetyl substituents on xylan were detrimental for the adsorption of xylan to bacterial cellulose. Further increases in the number of unsubstituted xylosyl residues induced the formation of xylan-xylan interaction which contributed to adsorption. Also, heat cleaves glucuronic acid groups from the xylans and thereby increases the aggregate size which contributes to greater hemicellulose sorption<sup>28</sup>.

In this study we evaluated the relative importance with respect to kraft bleached pulp fibers adsorption of three types of xylan solutions from birch wood, time, and temperature. Xylan solutions were made using modified and native xylans (high content of 4-O-methylglucuronic acid) from birchwood. The original xylan, rich in 4-O-Me-glucuronic acid (MeGlcA-xylan) was modified to produce a xylan enriched in hexenuronic acid (HexA-xylan) and containing low amounts of uronic acids (LowUrA-xylan).

The aims of this work were: to compare and quantify the adsorption level of different structural xylans solutions onto bleached kraft pulp fibers, verify the influence of time and temperature on the adsorption rates, and investigate the role of adsorbed xylans on the physical properties of bleached kraft pulp fibers.

## **2. Methods**

### *2.1. Xylan Preparation*

Xylan from birchwood purchased from Sigma-Aldrich (product No. X-0502) was used as the source of 4-O-methylglucuronoxylan (MeGlcA-xylan) without further purification. Xylan with a high degree of hexenuronic acid (HexA-xylan) was prepared using the method according to Teleman et al.<sup>36</sup>. 4-O-Methylglucuronoxylan (15 g) and NaBH<sub>4</sub> (0.2 g) were dissolved in 1 M NaOH (300 mL) and kept overnight under N<sub>2</sub>. The solution was heated to 150°C for 2 h. After cooling, glycerol (15 mL) was added and the solution was neutralized (pH 7) with formic acid. The xylan was precipitated by slow addition of MeOH (300 mL). The precipitate was separated by centrifugation, washed with MeOH-water (1:1, 300 mL), and MeOH (300 mL), and dried under vacuum at room temperature. Another xylan solution was prepared with a low degree of uronic acids (LowUrA-xylan) which followed a procedure similar to that of Teleman et al.<sup>36</sup>, but with the following modifications to guarantee degradation of uronic acids: the concentration of sodium hydroxide solution was 2.0 mol L<sup>-1</sup> instead of 1.0 mol L<sup>-1</sup>, and the time of reaction was 4 instead of 2h. Figure A.1.1 (Appendix) illustrates the preparation of the xylans used in this work.

### *2.2. Xylan analysis*

Xylans structures were confirmed by <sup>1</sup>H-NMR. NMR spectra were obtained using a Varian Mercury 300 instrument (300 MHz), using D<sub>2</sub>O as solvent and tetramethylsilane (TMS) as the internal standard ( $\delta=0$ ).

The GPC analysis of three xylans was performed on four serially connected columns PLgel 20 mm Mixed B 300x7.5 mm columns protected by a PLgel 20 mm pre-column (Polymer Laboratories Ltd, UK ). The temperatures of the pre-column and columns, the injector, and the detector (RI) were kept constant at 80°C. N,N-dimethylacetamide (DMA) with 0.5% of LiCl (w/v) was used as the eluent at a rate of 1.0 mL min<sup>-1</sup> and the injection volume was 100 µL. The xylans (50 mg) were dissolved in DMA containing 8% LiCl (w/v) (500 µL) and the temperature of the solutions were kept constant at 70°C until complete dissolution of samples. The samples were diluted with DMA to a xylan concentration of about 0.25%. The calibration of the GPC columns was made with Pullulan reference materials (Polymer Laboratories) in the range 0.8–100 kDa. Data analysis was performed with Cirrus GPC software (Polymer Laboratories).

### *2.3. Adsorption Experiments*

Xylans solutions were made by the addition of 5.0 g xylan in 80 mL deionized water at 90°C for 30 minutes under stirring to allow the xylan to dissolve. After cooling, pH of the solution was adjusted to 12 using sodium hydroxide. The solutions were then directly poured into a glass vial containing 5 g of ECF (OD(EPO)DP) pulp bleached substrate. The glass vial was placed in a bath under careful temperature control (25°C, 75°C and 125°C). The treatment time varied between 60 and 240 minutes (at intervals of 60 minutes). After adsorption of the xylan to the fibers, the fibers were thoroughly washed with hot deionized water, 1% acetic acid, suspended in deionised water for 10 min, and then washed again. The amount of adsorbed xylan was quantified by carbohydrate analysis of the modified fibres. The reference pulp was subjected to the same treatment except it was not subjected to xylan addition.

### *2.4. Pulp Analysis*

#### *2.4.1. Chemical Analysis*

The xylan content of the reference and modified pulp samples was established by High Performance Anion Exchange Chromatography with Pulse Amperometric Detection (HPAEC-PAD) after pre-treatment (30°C, 1 h) with aqueous 72% H<sub>2</sub>SO<sub>4</sub><sup>37</sup> followed by hydrolysis with 3% H<sub>2</sub>SO<sub>4</sub> in an autoclave (100°C, 3 h). HPAEC-PAD was carried out in a Dionex ICS-3000 system equipped with a CarboPac PA1 (250 x 4mm) analytical column. The total uronic acids contents of pulps were calculated

taking into account both the uronic acid content linked to xylan and xylan adsorbed onto pulp. Uronic acid content was determined by the colorimetric method involving 3,5-dimethylphenol addition<sup>38</sup>. The viscosity of all pulps was determined by a capillary viscometer method according to TAPPI standard methods<sup>37</sup>.

#### 2.4.2. Surface Analysis (AFM/SEM)

The surface morphology of the reference and modified pulp samples was determined using Scanning Electron Microscopy (SEM). The surfaces were coated with gold for analysis and visualized with a LEO 1430VP operated at 20 kV. Additionally, pieces of the substrate were cut and mounted on a magnetic holder for surface morphology measurements using an Atomic Force Microscopy (AFM) in tapping mode on a Digital Instruments NT-MDT Ntegra model.

#### 2.4.3. Hand Sheet Physical Properties

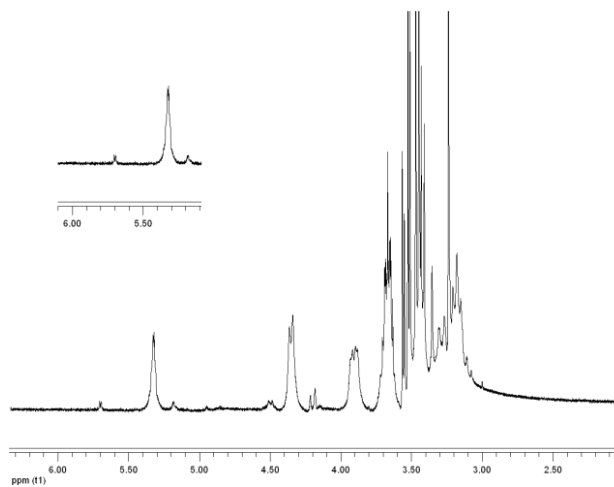
Three samples of modified pulps (three xylan solutions, 125°C and treatment time of 240 minutes) and a reference pulp were granulated by hand, air dried at room temperature, disintegrated (ISO 5263), PFI beaten from reference treatment and MeGlcA-xylan were 1000, 2000 and 3000 revolutions; 1000, 2000 and 2500 for HexA-xylan treatment and 500, 1000 and 2000 revolutions for xylan with LowUrA-xylan (ISO 5264-2), hand sheet prepared (ISO 5269-1) and tested for strength and density properties. Water retention values (WRV) and hornification were determined for unbeaten pulps. The degree of pulp hornification was determined based on the Water Retention Value (WRV) of never-dried and dried pulps according to the method of Weise<sup>39</sup>.

### 3. Results and Discussion

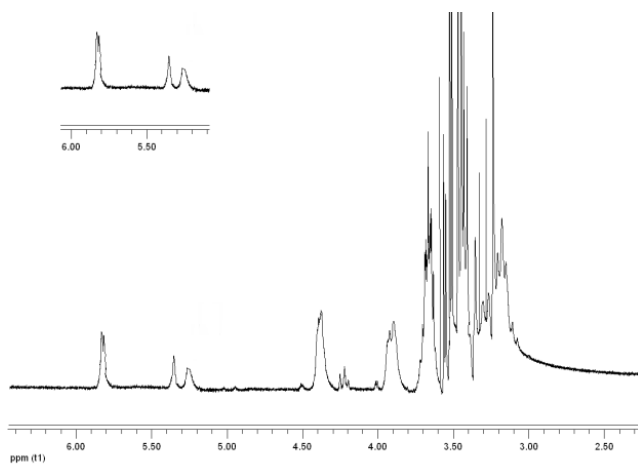
#### 3.1. Xylans' characterization

The <sup>1</sup>H-NMR spectra (2.5 – 6.0 ppm) of xylans are illustrated in Figure 1. Confirmation for the chemical modifications obtained in these studies was validated. For example, the resonance of H-1 at 5.32 ppm of MeGlcA (Fig. 1a) that is due to the MeGlcA residues is evident for MeGlcA-xylan, while it is diminished in the HexA-xylan and LowUr-xylan samples. Also, no proton signals appear in the region of 4.6 – 5.2 ppm clearly indicating the absence of acetylated xylopyranose units.

a)



b)



c)

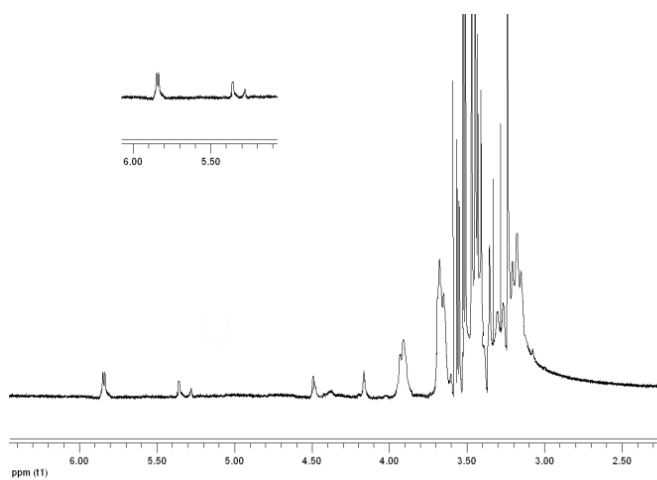


**Figure 1.** <sup>1</sup>H-NMR spectra of xylans, a) MeGlcA-xylan; b) HexA-xylan, and c) LowUrA-xylan.

Evidence from  $^1\text{H-NMR}$  spectra was also found supporting the formation of the 4-O-methyl- $\alpha$ -D-glucopyranosyluronic acid (MeGlcA) units that occurs through a  $\beta$ -elimination of a methoxyl group under alkaline conditions. Specifically, analysis of the sugar anomeric region demonstrates the obvious signature for the latter formation because of the new signals at 5.23 and at 5.83 ppm in HexA-xylan and at 5.28 and at 5.82 ppm in LowUrA-xylan. These latter signals are normally assigned to H-1 and H-4, respectively, in the 4-deoxy- $\beta$ -L-threo-hex-4-enopyranosyluronic acid (hexenuronic acid, HexA) residues <sup>40</sup>. The spectra in Figure 1 illustrate the main chain of xylan that displays linear (1 $\rightarrow$ 4)- $\beta$ -linked D-xylopyranose units with the already mentioned (*vide infra*) 4-O-methyl- $\alpha$ -D-glucuronic acid groups and HexA groups linked to the 2-position of the xylose units.

The GPC elution curves for the xylans (not shown) exhibit a unimodal Gaussian molecular weight distribution indicating the structural homogeneity of the isolated polysaccharide sample. The  $M_w$  for each of the samples for GlcA-xylan, HexA-xylan and LowUrA-xylan correspond to familiar xylan-based molecular weights of 16000 – 22000 Da<sup>11</sup> with  $M_w$ s and polydispersity indices of 21800 Da and 1.19; 19565 Da and 1.14; 16183 Da and 1.16, respectively.

The small  $M_w$  variation between MeGlc-xylan and HexA-xylan may be explained by invoking differences in their stability in alkaline conditions during short times (120 min) that results in dissolved polysaccharides that contribute to lower molecular weights <sup>41</sup>. The lower molecular weight of LowUrA-xylan indicated that extending treatment and increasing alkali concentration causes degradation of the xylan chain likely by the well known  $\beta$ -elimination mechanism <sup>7</sup>.

### 3.2. Adsorption of xylans to pulp fibers

Three temperatures (25°C, 75°C and 125°C) and four reaction times (60, 120, 180 and 240 min) were investigated for adsorption of the three xylan types. Pulp xylan content (% weight) and uronic acids content (% weight) were plotted against temperature and time (Fig. 2 and 3) for each of the three xylan types. The xylan content and uronic groups content for the pulp without treatment were 14.2% and 0.95%, respectively.

A significant increase of pulp xylan content was achieved in the adsorption experiments carried out at 75°C and 125°C. In fact, the highest pulp xylan content was

obtained at the highest temperature and the longest time, in agreement with previous work<sup>15, 23</sup> (Fig. 2). However, the experimental design indicates a greater influence of temperature than treatment time on the xylan adsorption. Nevertheless, the time effect is seemingly more significant at high temperatures, especially for sample C. Xylan aggregation occurs more easily at higher temperatures leading to improved precipitation onto the pulp surface. According to Linder et al.<sup>28</sup>, treatment at high temperature and pH leads to decreased amounts of 4-O-MeGlcA groups on the xylan backbone, thereby increasing the driving force for xylan aggregation because xylan molecules can associate through interactions between the unsubstituted linear regions of the chains<sup>19, 23</sup>.

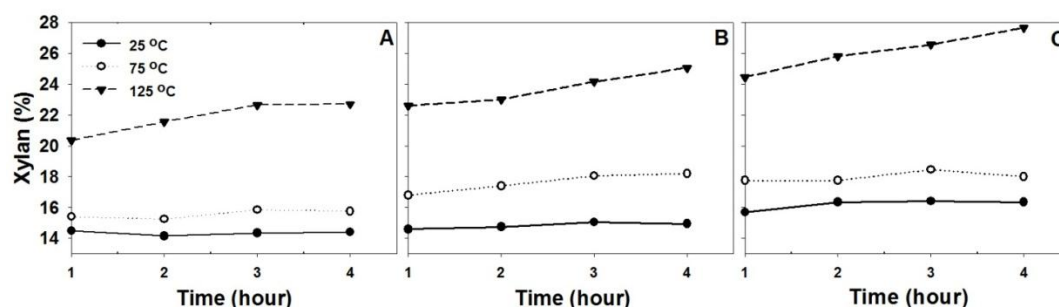


**Figure 2.** Xylan content on pulp (%) after adsorption treatment: A) MeGlcA-xylan solution, B) HexA-xylan solution and C) LowUrA-xylan solution.

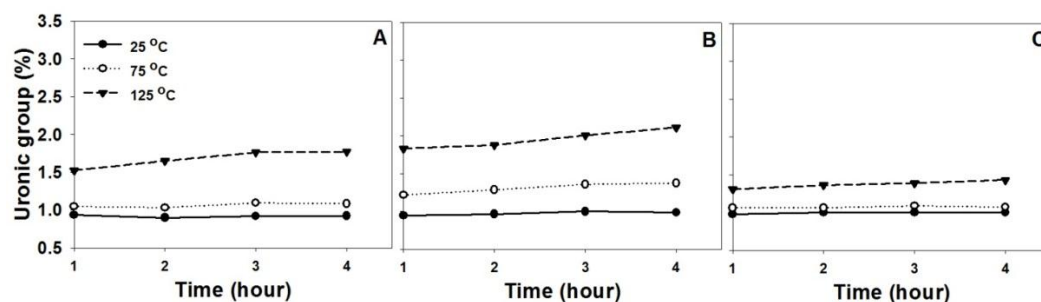


**Figure 3.** Uronic group content (%) on pulp after adsorption treatment: A) MeGlcA-xylan solution, B) HexA-xylan solution and C) LowUrA-xylan solution.

It is well known that aggregates constitute the major part of the adsorbed xylan and the presence of negatively charged uronic substituents on the xylan chains increases repulsion between xylan molecules and favors dissolution, thereby decreasing xylan adsorption onto pulp<sup>28, 42, 43</sup>. The aggregation kinetics depends on the activity of xylans in solution, concentration of xylan in solution, and temperature<sup>44</sup>.

This study shows (Fig. 2) that xylans with low uronic groups content (LowUrA-xylan) produced the highest adsorption, particularly at 125°C, in agreement with literature<sup>19, 42, 45</sup>. Similar results were found<sup>44</sup>. However, others authors have concluded that smaller molecules tend to adsorb less to the cellulose surface than the larger ones, which was not the case here<sup>19</sup>. At 25 °C, treatment with LowUrA-xylan had an increase in the xylan content after adsorption showing the ease in this species adsorbed on the pulp. The effect of absorption of Low-UrA-xylan seems to be more related with the low uronic acid content than with the molecular weight because the amount of uronic acids in different xylans contribute to a large difference among them. However, at this time, these differences have not been ascribed in terms of molecular weight.

The effect of uronic groups on adsorption can be observed by measuring the content of uronic groups on pulp after treatment (as shown in Fig. 3). The amount of uronic acid on pulp increased by increasing of MeGlcA-xylan, HexA-xylan and LowUrA-xylan adsorbed and as can be observed in Fig. 3 in which HexA-xylans showed to be more stable in higher temperatures.<sup>36</sup>

HexA-xylan attached to pulp to a greater extent than MeGlcA-xylan. Two reasons to this behavior are suggested: a) lower molecular weight of xylan and b) easier formation of aggregates by reducing the molecular weight and size of the uronic group in the formation of HexA. Thus, to the extent that smaller fragments are generated from xylan and the distance between molecules becomes small enough, molecules will start to aggregate. Certainly, this aggregate could more easily penetrate the fiber wall than larger ones.

Pulp viscosity was largely dependent on the amount of xylan adsorbed onto the pulp (Fig. 4). The highest xylan adsorption resulted in the lowest pulp viscosity (6 mPa.s) which represents a loss of 33% in relation to original value (9 mPa.s). This resulted is explained by the low molecular weight of the xylans in relation to that of the cellulose chains. The low original pulp viscosity derives from the bleaching procedure used to prepare the pulp which was aimed at creating a material that contained low hexenuronic and 4-O-methylglucuronic acid contents.

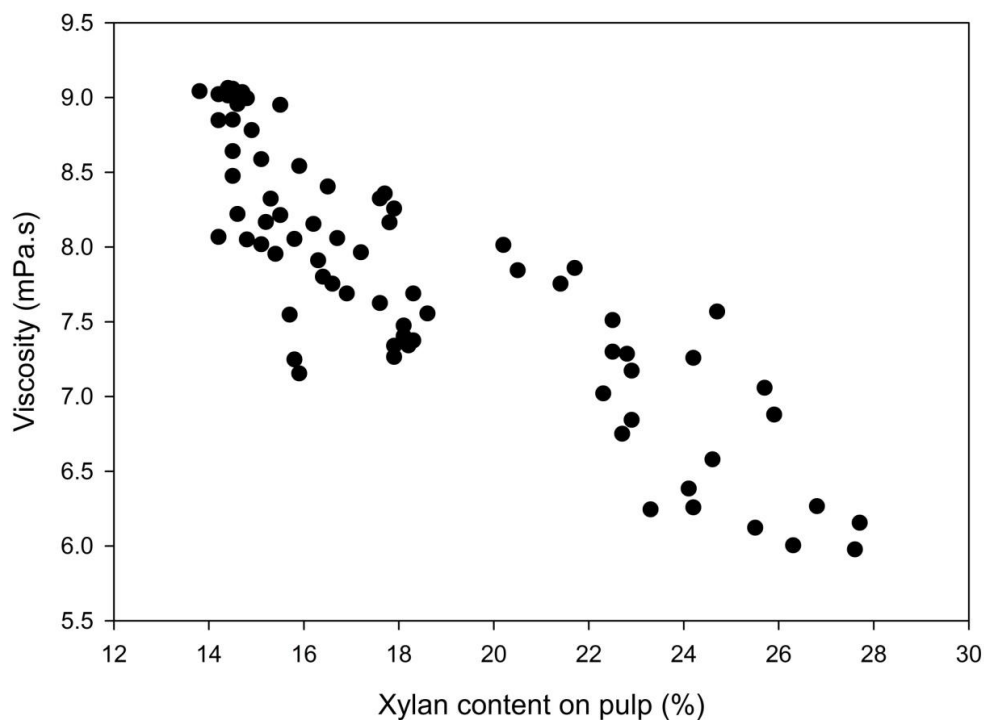


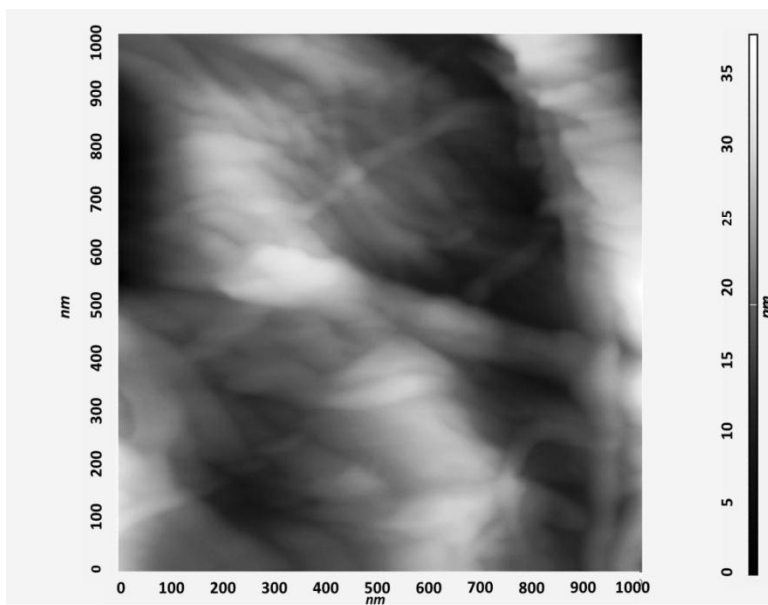
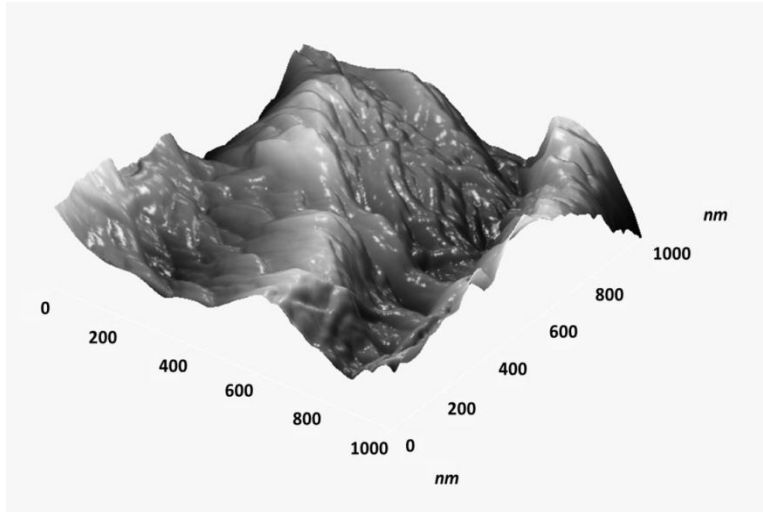
**Figure 4.** Viscosity vs. xylan content on pulps.

### 3.3. Surface morphology

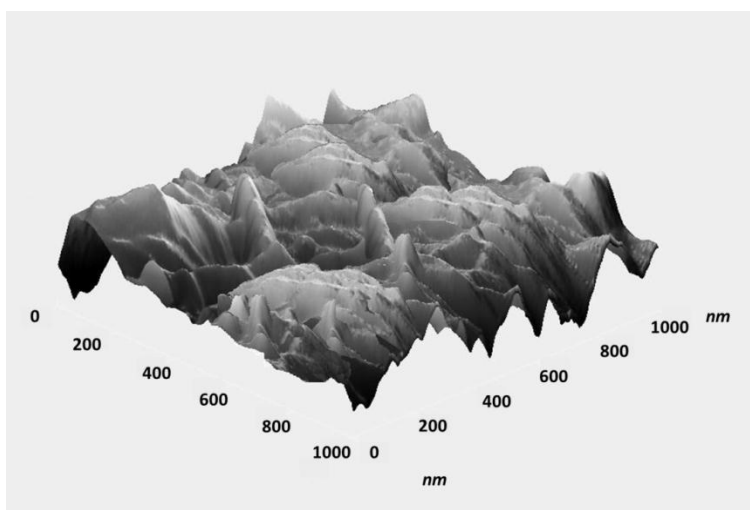
The xylans that were adsorbed onto pulp fibers can be visualized by Atomic Force Microscopy (AFM) in tapping mode and Scanning Electron Microscopy (SEM). The appearance of the untreated and treated (with low uronic xylan solution) pulp samples were examined. The pulp reference has 14.2% of xylan, but the pulp with adsorbed xylan (27.5% of xylan) shows a completely different topography (Fig. 5). AFM shows topography with particles visible as protuberances on the fiber surface. The treated pulp is still rather smooth, but appears to have a higher surface roughness.

On the treated pulp, fragments of xylan set up a net between fibers surfaces that could be seen by SEM (Fig. 6).

**A**



**B**



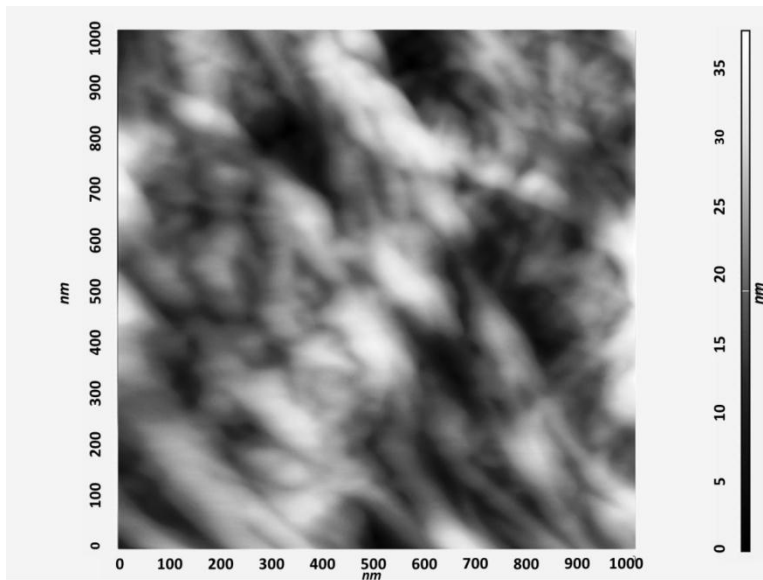
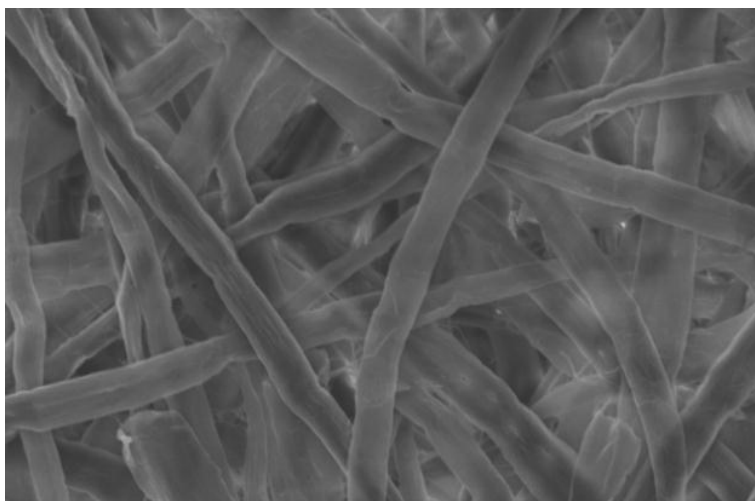


**Figure 5.** AFM image of a bleached pulp A) untreated (14.2% of xylan) and B) treated pulp by LowUrA-xylan solution at 125°C and 4 h (27.5% of xylan). Scaling vs. axis 1000 nm/div, z axis 40nm/div.

**A**



**B**

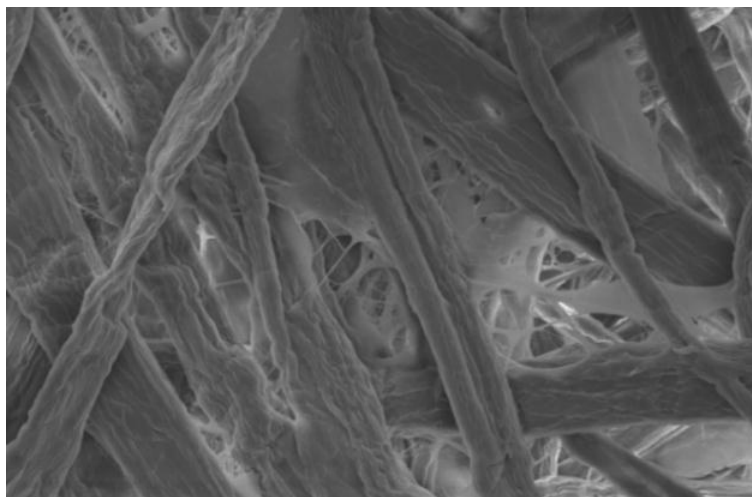


**Figure 6.** A SEM micrograph of: A) untreated pulp (14.5% of xylan) and B) treated pulp by LowUrA-xylan solution at 125°C and 4 h. (27.5% of xylan) (1000 X)

#### *3.4. Pulp beatability and properties*

The pulp samples treated with MeGlcA-xylan, HexA-xylan and LowUrA-xylan solutions at 125°C for 240 min and the reference pulp were tested for WRV, hornification (morphological pore diminution phenomenon in microfibrils induced by loss of bound water molecules), energy consumption during beating (beatability), tensile index, tensile energy absorption, burst index, tear index, specific elastic modulus, and hand sheet density. All tests, except WRV and hornification, were done on pulps before and after being beaten at three different levels of PFI revolution.

Not surprisingly, the pulps containing adsorbed xylans required less beating energy than the reference. At the same energy consumption level, higher Schopper-Riegler values were reached for the xylan treated pulp in relation to the reference (Fig. 7). The Schopper-Riegler is a term that provides a summary of the relationship of the refining degree to the rate of the drainage of the diluted fibers suspension. The rate of drainage is related to the surface conditions and the expansion of fibers and it is considered a useful indicator of the amount of mechanical treatment (refining) of the pulp. The largest energy savings of about 40% were achieved in the post-refining stage for pulp treated to LowUrA-xylan because the xylan content of this pulp is superior to the others. Addition of hemicelluloses favors interfiber bonding due to its hydrophilic properties which cause greater swelling of cell walls in water imparting fiber flexibility<sup>46</sup>. As a result of the development of fibrillation, the energy consumption was reduced during beating. This helps in better fiber conformation and more interfiber bonding

during sheet formation. Similar results were found <sup>47</sup>, using Ramie hemicelluloses during the beating operation.

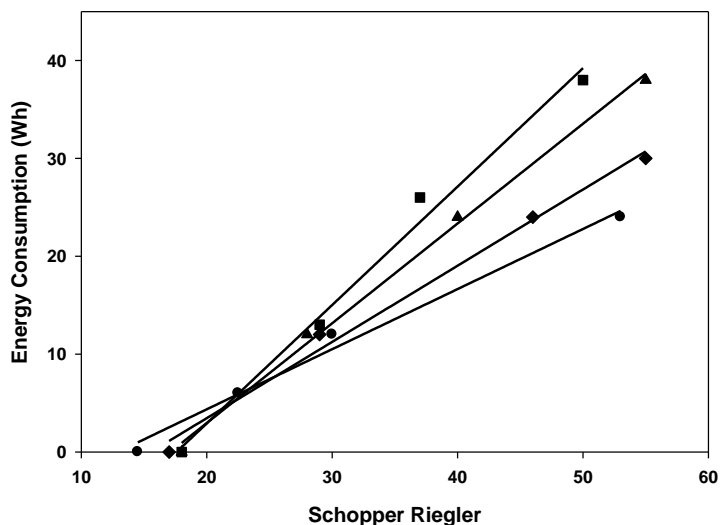


**Figure 7.** Energy Consumption during beating in a PFI mill versus Schopper-Riegler. Untreated (■), MeGlcA-xylan-treated pulp (▲), HexA-xylan-treated pulp (◆), Low UrA-xylan-treated pulp (●).

Many authors <sup>21, 26, 43, 44, 47</sup> emphasize that hemicelluloses adsorbed on pulp, mainly xylans, increase the tensile strength by acting as an adhesive and binder. However, it has been concluded that xylan content adsorbed in pulp does not affect tensile index <sup>25</sup>. The results show that the physical properties of pulp sheets depend on the degree of beatability of the pulp. Indeed, xylans' adsorption on pulp provides higher Schopper-Riegler values and so, improvements on the properties can be seen. As the physical properties of paper sheets made from the bleached pulp with xylan were evaluated (Figure 8) and haven't shown any significant difference in terms of the properties (even with higher xylan content), the data obtained were tested by non-linear regression model in order to adjust all samples according to just one equation. It is worth mentioning that just small differences among parameters of the chosen model for different pulps were observed. Figure 8 shows strength properties plotted against Schopper-Riegler.

It is well known that the chemical composition of pulp greatly affects its fiber strength. Both increased cellulose and hemicelluloses <sup>31</sup> content have been reported to give an increased fiber strength <sup>34</sup>. The likely reason for the discrepancies found in this system is differences in the hemicellulose content. If there were enough hemicelluloses

in the matrix between the fibril aggregates, an increased cellulose content is positive, i.e., more fibril aggregates to bear the load. However, if the hemicellulose content is too low, the load transfer between the fibril aggregates decreases and so will the fiber strength<sup>48</sup>.

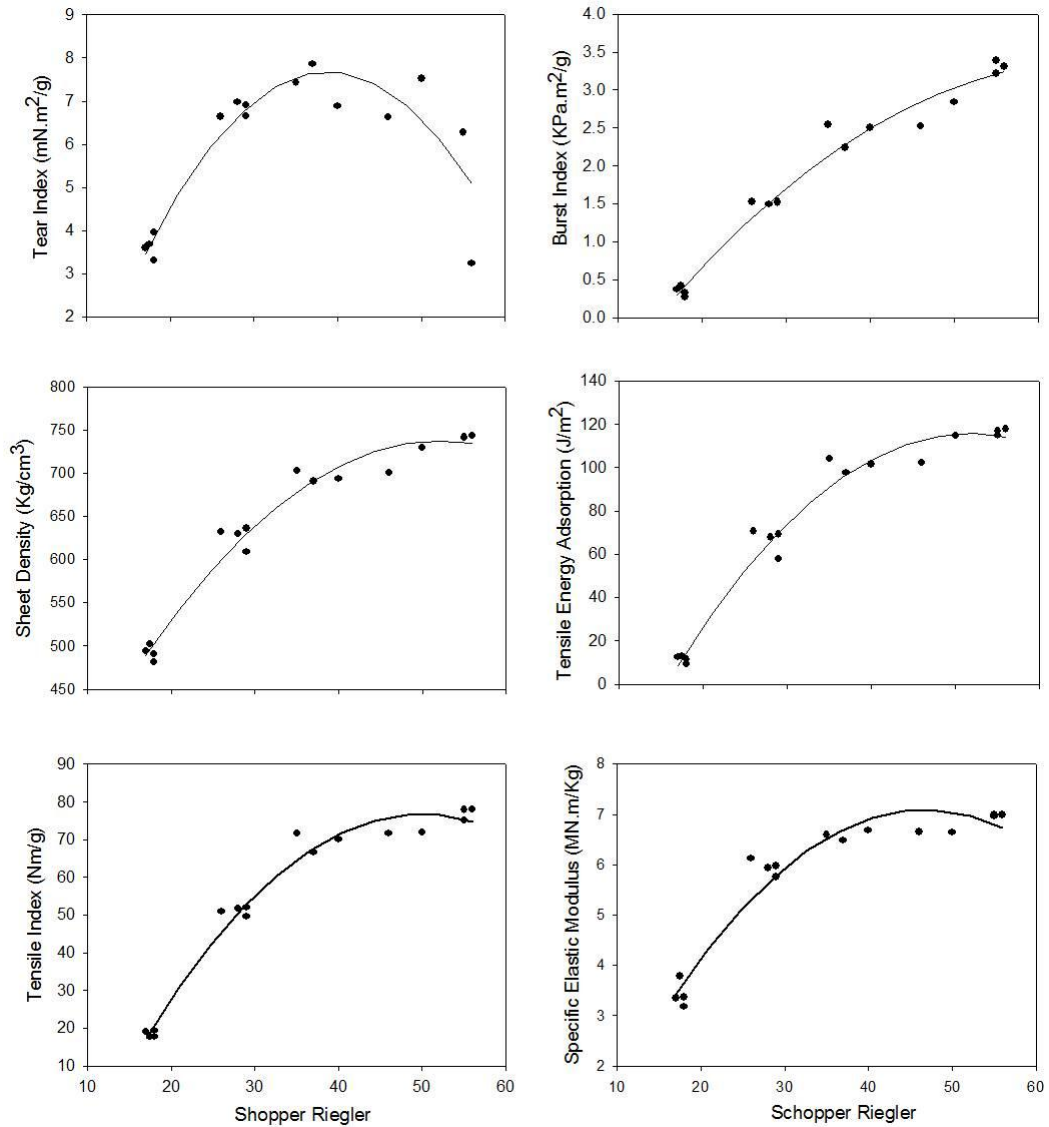


**Figure 8.** Physical properties versus Schopper-Riegler of treated and untreated pulps.

In this case, the xylan content of the reference (14.2%) seems to have been sufficient for the maintenance of strength properties of the pulp. The slight increase of the tensile index and sheet density in addition to the other physical properties measured after treatment show that addition of xylan in a pulp that has a reasonable quantity of hemicelluloses does not justify the improvement in physical properties. The type and quantity of xylan adsorbed does not seem to considerably influence these properties. For instance, a study employing different cooking conditions which vary the amount of

both hemicelluloses and cellulose in the fiber reported that the fiber strength and bond strength were not influenced by the hemicellulose content of fiber <sup>49</sup>.

The slight increase of sheet density can be attributed to a reduction of fiber wall pores by small xylan aggregates <sup>50</sup>. No significant increase of tensile was seen. However, tear index decreased slightly due to fiber structure damage. Analysis of the behavior of fibers showed that treatment had a slight protective effect on the fibers in facilitating fibrillation without significant cutting. This behavior could explain the improvement of the tensile and burst index. According to Molin <sup>34</sup> these properties were more affected by the cellulose/hemicellulose ratio. In addition, Shin and Stromberg <sup>25</sup> suggested that the bleached pulp tensile strength is more dependent on cellulose characteristics than xylan content.

Water retention value (WRV) of the differently treated pulps correlated with the total xylan content or with the total charges of fibers <sup>26</sup>. The WRV values increased with increasing pulp-xylan content (Table 1). The xylan adsorbed increased both never-dried and once-dried bleached pulp WRV, thus reducing the degree of hornification. Xylan in pulps promote better swelling of dried fibers by forming a hydrophilic xylan layer on the fibril surface facilitating water attraction and preventing strong interactions between the crystalline regions of adjacent fibrils. The decreased hornification extent of treated pulp could be attributed to higher xylan and uronic contents <sup>30</sup>. Both uronic acid and hemicelluloses prevent pulp hornification via diminishing interfibril aggregation in fibres <sup>51</sup>. The results show a decrease in the hornification degree of pulps that have higher xylan contents. The slight decrease between pulps treated with HexA-xylan versus LowUrA-xylan treatment show the effect of the absence of uronic acids <sup>52</sup> which indicates that xylan in kraft pulp is strongly bonded to cellulose fibril surfaces and covers larger fibril areas.

**Table 1.** WRV (g/g) and degree of hornification (%) of untreated and treated pulps.

Pulp	Xylan Content (%)	WRV (g/g)	S.D <sup>a</sup>	Hornification (%)	S.D <sup>a</sup>
Reference	14.2	112.0	4.10	15.8	2.2
MeGlcA-xyl. pulp	22.7	115.0	2.56	13.0	2.86
HexA-xyl. pulp	25.05	125.0	6.07	9.6	0.59
LowUrA-xyl. pulp	27.65	137.0	5.34	9.0	1.28

<sup>a</sup>Standard Deviation

#### 4. Conclusions

The birchwood-based xylan biomaterials used in the current study (MeGlcA-xylan, HexA-xylan, and LowUrA-xylan) provided key data on their effects on the processability of eucalyptus pulp by setting up high ratio xylans: pulp (5g/ 5g) during the experiments. More specifically, the composition of xylan, in terms of the type and content of uronic acid, influences the adsorption and properties of cellulose fibers. Under controlled times and temperatures, it was found that LowUrA-xylan had greater adsorption on eucalyptus pulp, especially at high temperatures and times, while HexA-xylan adsorbed more onto eucalyptus pulp than MeGlcA-xylan. Water Retention Values (WRV) of xylan-enriched eucalyptus pulps increased, while their hornification decreased. In addition, not only does temperature have an important influence on the adsorption, but so does the type of uronic acid linked to the xylan chain. Xylans containing low uronic groups displayed higher adsorption rates relative to those xylans substituted with HexA (HexA-xylan). Finally, xylan adsorption of any type onto pulp fibers decreases beating energy demand and hornification without affecting pulp strength properties. In general, xylan-enriched pulps demonstrated improved processability (beatibility), while displaying acceptable physical properties. Given the great abundance of xylan in the biosphere, these latter findings may be key to developing appropriate processing strategies when considering hardwood (angiosperm)-based biomass for biomass transformation technologies.

#### Acknowledgements

We would like to gratefully acknowledge the CAPES (Coordenação de Aperfeiçoamento de Pessoal de Nível Superior) for the generous provision of a research fellowship to TCFS that allowed parts of this work to be realized. We also thank the Núcleo de Microscopia e Microanálise – NMM, Universidade Federal de Viçosa – UFV.

#### References

1. Uhlin, K. I.; Atalla, R. H.; Thompson, N. S., Influence of hemicelluloses on the aggregation patterns of bacterial cellulose. *Cellulose* **1995**, 2, (2), 129-144.

2. Henriksson, Å.; Gatenhalm, P., Surface properties of CTMP fibers modified with xylans. *Cellulose* **2002**, 9, (1), 55-64.
3. Atalla, R. H.; Hackney, J. M.; Uhlin, I.; Thompson, N. S., Hemicelluloses as structure regulators in the aggregation of native cellulose. *International Journal of Biological Macromolecules* **1993**, 15, (2), 109-112.
4. Dillen, S.; Noreus, S., Kraft pulping with recirculation of cooking liquor containing hemicellulose. *Svensk Papperstidning* **1968**, 71, (15), 509.
5. Sjöblom, K., Extended delignification in kraft cooking through improved selectivity. Part 3. The effect of dissolved xylan on pulp yield. *Nordic Pulp & Paper Research Journal* **1988**, 3, (1), 34-37.
6. Evtuguin, D.; Tomás, J.; Silva, A. S.; Neto, C., Characterization of an acetylated heteroxylan from *Eucalyptus globulus* Labill. *Carbohydrate Research* **2003**, 338, (7), 597-604.
7. Sjöstrom, E., The behavior of wood polysaccharides during alkaline pulping processes. *Tappi Journal* **1977**, 60, (9), 151-154.
8. Hon DN-S., S. N., Wood and cellulosic chemistry In *Chemistry of hemicelluloses*, Shimizu, K., Ed. Marcel Dekker: New York, 1991; pp 177-214.
9. Aspinall, G. O., Chemistry of cell wall polysaccharides. *Biochemistry Plants* **1980**, 3, 473-500.
10. Timell, T. E., Recent progress in the chemistry of wood hemicelluloses. *Wood Science and Technology* **1967**, 1, (1), 45-70.
11. Pinto, P. C.; Evtuguin, D. V.; Neto, C. P., Structure of hardwood glucuronoxylans: modifications and impact on pulp retention during wood kraft pulping. *Carbohydrate Polymers* **2005**, 60, (4), 489-497.
12. Aurell, R.; Karlsson, K., The 4-O-methyl-D-glucuronic acid content of xylan isolated from birch kraft pulps. *Svensk Papperstidn* **1964**, (67), 167-169.
13. Danielsson, S.; Lindström, M., Influence of birch xylan adsorption during kraft cooking on softwood pulp strength. *Nordic Pulp & Paper Research Journal* **2005**, 20, (4), 436-441.
14. Danielsson, S.; Kisara, K.; Lindström, M. E., Kinetic study of hexenuronic and methylglucuronic acid reactions in pulp and in dissolved xylan during kraft pulping of hardwood. *Industrial & Engineering Chemistry Research* **2006**, 45, (7), 2174-2178.
15. Hansson, J. A.; Hartler, N., Sorption of hemicelluloses on cellulose fibers. I. sorption of xylans. *Svensk Papperstidning* **1969**, 72, (17), 521-530.

16. Hartler, N.; Lund, A., Sorption of xylan on cotton. *Svensk Papperstidning* **1962**, 65 (23), 951-955.
17. Yllner, S. a. B. E., Adsorption of xylan on cellulose fibers during the sulfate cook I. *Svenska Papperstidning* **1956**, 59, 229-232.
18. Dammström, S.; Salmén, L.; Gatenhalm, P., On the interactions between cellulose and xylan, a biomimetic simulation of the hardwood cell wall. *BioResources* **2009**, 4, (1), 3-14.
19. Kabel, M. A.; van den Borne, H.; Vincken, J.-P.; Voragen, A. G. J.; Schols, H. A., Structural differences of xylans affect their interaction with cellulose. *Carbohydrate Polymers* **2007**, 69, (1), 94-105.
20. Le Moigne, N.; Navard, P., Dissolution mechanisms of wood cellulose fibres in NaOH–water. *Cellulose* **2010**, 17, (1), 31-45.
21. Köhnke, T.; Pujolras, C.; Roubroeks, J.; Gatenholm, P., The effect of barley husk arabinoxylan adsorption on the properties of cellulose fibres. *Cellulose* **2008**, 15, (4), 537-546.
22. Buchert, J.; Teleman, A.; Harjunpää, V.; Tenkanen, M.; Viikari, L.; Vuorinen, T., Effect of cooking and bleaching on the structure of xylan in conventional pine kraft pulp. *Tappi Journal* **1995**, 78, (11), 125-130.
23. Henriksson, Å.; Gatenholm, P., Controlled Assembly of Glucuronoxylans onto Cellulose Fibres. *Holzforschung* **2001**, 55, (5), 494-502.
24. Bhaduri, S. K.; Ghosh, I. N.; del Sarkar, N. L., Ramie hemicelluloses as beater additive in paper making from jute – stick kraft pulp. *Industrial Crops and Products* **1995**, 4, 79-84.
25. Shin, N. H.; Stromberg, B. In *Xylan's impact on eucalyptus pulp yield and strenght – myth or reality?*, International Colloquium on Eucalyptus Pulp., Belo Horizonte, Brazil, 2007.
26. Schönberg, C.; Oksanen, T.; Suurnäkki, A.; Kettunen, H.; Buchert, J., The Importance of Xylan for the Strength Properties of Spruce Kraft Pulp Fibres. *Holzforschung* **2005**, 55, (6), 639-644.
27. Kerr, E. M.; Fry, S. C., Pre-formed xyloglucans and xylans increase in molecular weight in three distinct compartments of a maize cell-suspension culture. *Planta* **2003**, 217, (2), 327-339.
28. Linder, Å.; Bergman, R.; Bodin, A.; Gatenholm, P., Mechanism of Assembly of Xylan onto Cellulose Surfaces. *Langmuir* **2003**, 19, (12), 5072-5077.

29. Saake, B.; Kruse, T.; Puls, J., Investigation on molar mass, solubility and enzymatic fragmentation of xylans by multi-detected SEC chromatography. *Bioresource Technology* **2001**, 80, (3), 195-204.
30. Lindström, T., Chemical factors affecting the behavior of fibers during papermaking *Nordic Pulp & Paper Research Journal* **1992**, 7, 181–192.
31. Spiegelberg, H., Effect of hemicelluloses on mechanical properties of individual pulp fibers. *Tappi Journal* **1966**, 49, (9), 388-396.
32. Suurnaekk, A.; Oksanen, T., The effect of mannan on physical properties of ECF bleached softwood kraft fibre handsheets. *Nordic Pulp and Paper* **2003**, 18, (4), 429-435.
33. Kersavage, P., Moisture content effect on tensile properties of individual Douglas-fir latewood tracheids *Wood and Fiber* **1973** 5 (2), 105-117.
34. Molin, U.; Teder, A., Importance of cellulose/hemicellulose-ratio for pulp strength. *Nordic Pulp & Paper Research Journal* **2002**, 17 (1), 14-19.
35. Linder, Å.; Gatenholm, P., Effect of Cellulose Substrate on Assembly of Xylans. In *Hemicelluloses: Science and Technology*, American Chemical Society: Washington, DC, 2003; pp 236-253.
36. Teleman, A.; Hausalo, T.; Tenkanen, M.; Vuorinen, T., Identification of the acidic degradation products of hexenuronic acid and characterisation of hexenuronic acid-substituted xylooligosaccharides by NMR spectroscopy. *Carbohydrate Research* **1996**, 280, (2), 197-208.
37. Tappi, Carbohydrate composition of extractive-free wood and wood pulp by gas liquid chromatography. In *Tappi Method T 249*, Tappi Press: Atlanta, Georgia, 1985; Vol. cm-85.
38. Scott, R. W., Colorimetric determination of hexuronic acids in plant materials. *Analytical Chemistry* **1979**, 51, (7), 936-941.
39. Weise, U. P. H., Hornification mechanisms and terminology. *Paperi Ja Puu-Paper and Timber* **1998**, 80, (2).
40. Teleman, A., Harjunpaa V., Tenkanen, M., Buchert, J., Hausalo, T., Drakenberg, T., Vuorinen, T., Characterization of 4-deoxy-β-L-threohex-4-enopyranosyluronic acid attached to xylan in pine kraft pulp and pulping liquor by carbon-13 and proton NMR spectrometry. *Carbohydrate Research* **1995**, 272, (1), 55-71.

41. Lisboa, S. A.; Evtuguin, D. V.; Neto, C. P.; Goodfellow, B. J., Isolation and structural characterization of polysaccharides dissolved in Eucalyptus globulus kraft black liquors. *Carbohydrate Polymers* **2005**, 60, (1), 77-85.
42. Westbye, P.; Svanberg, C.; Gatenholm, P., The effect of molecular composition of xylan extracted from birch on its assembly onto bleached softwood kraft pulp. *Holzforschung* **2006**, 60, (2), 143-148.
43. Hannuksela, T.; Tenkanen, M.; Holmbom, B., Sorption of dissolved galactoglucomannans and galactomannans to bleached kraft pulp. *Cellulose* **2002**, 9, (3), 251-261.
44. Danielsson, S. Xylan reactions in kraft cooking process and product considerations. Thesis KTH - Royal Institute of Technology, Stockholm 2007.
45. Walker, E. F., Effects of the uronic acid carboxyls on the sorption of 4-O-methylglucuronoarabinoxylans and their influence on papermaking properties of cellulose fibers. *Tappi* **1965**, 48, (5), 298-303.
46. Pettersson, S. E.; Rydholm, S. A., Hemicelluloses and paper properties of birch pulps III. *Svensk Papperstidning* **1961**, 64, 4-17.
47. Bhaduri, S. K.; Ghosh, I. N.; Deb Sarkar, N. L., Ramie hemicellulose as beater additive in paper making from jute-stick kraft pulp. *Industrial Crops and Products* **1995**, 4, (2), 79-84.
48. Page, D. H., Seth, R. S., El-Hosseiny, F., Strength and chemical composition of wood pump fibres. In *8th Fundamental Research Symposium - Papermaking Raw Materials*, Mechanical Engineering Publications Ltd.: Oxford, 1985; Vol. 1, pp 77-91.
49. Luce, J. E., Radial Distribution of Properties through the Cell Wall. *Pulp and Paper Magazine of Canada* **1964**, 65, T419-T423.
50. Danielsson, S.; Lindström, M. E. In *Utilization of black liquor xylan to increase tensile properties of kraft pulp*, International Colloquium on Eucalyptus Pulp (III ICEP), Belo Horizonte, Brazil, 2007.
51. Fernandes Diniz, J.; Gil, M.; Castro, J., Hornificationits origin and interpretation in wood pulps. *Wood Science and Technology* **2004**, 37, 489-494.
52. Rebutzi, F.; Evtuguin, D. V., Effect of Glucuronoxylan on the Hornification of Eucalyptus globulus Bleached Pulps. *Macromolecular Symposia* **2005**, 232, (1), 121-128.

## CHAPTER 2

### NANOFIBRILLATED CELLULOSE-BASED AEROGELS: A NEW CHEMICAL APPROACH FOR TUNING THEIR MICRO-ARCHITECTURES

Teresa Cristina Fonseca Silva<sup>1,2</sup>, Youssef Habibi<sup>2</sup>, Jorge Luiz Colodette<sup>1</sup>, Lucian A. Lucia<sup>2</sup>

<sup>1</sup>*Departamento de Química, Universidade Federal de Viçosa, Viçosa, MG, 36570-000; Brazil*

<sup>2</sup>*Laboratory of Soft Materials & Green Chemistry, Department of Forest Biomaterials, North Carolina State University, Raleigh, North Carolina 27695-8005; USA*

Email: [lucian.lucia@ncsu.edu](mailto:lucian.lucia@ncsu.edu)

**Abstract:** Freeze-dried nanofibrillated cellulose based-aerogels were produced using hardwood as a raw material. Nanofibers were isolated under high pressure and modified with TEMPO-mediated oxidation and/or hydroxyapatite (HAp). Different degrees of oxidation (DO) were reached and measured by conductimetric titration (~ 0.1 and 0.2). Oxidized and non-oxidized samples were modified with HAp in a level of HAp:cellulose ratio of 0.2:1. Morphology (FE-SEM), rheological and physical properties were used to characterize produced aerogels. The results shown a well-organized morphology for aerogels fabricated with oxidized nanofibers. TEMPO-oxidation and addition of HAp resulted in aerogels with great mechanical strength, increasing the stress from approximately 7500 Pa to 20000 Pa when compressed to 50% of the original height. However, the oxidation effect was more pronounced than the addition of HAp. Density of the aerogels varied from 0.008 to 0.011 g/cm<sup>3</sup>. Slightly lightweight aerogels were produced by increasing the degree of oxidation whereas the use of HAp as modifying agent contributed to higher densities.

*Keywords : NFC, aerogels, TEMPO, Hydroxyapatite.*

## 1. Introduction

Aerogels are highly porous materials possessing low solids content, considerably lightweight, high strength and good dimensional stability. In a “nano” perspective, the extensive interconnected chains confers stable three-dimensional network due to the linkage of the nanoparticles to each other with inter-chain distances typically being in order of 10-100 nm.<sup>1</sup> For being promptly accessible, these structures have attractively led to the development of variety of applications such as storage media for gases, filter materials, carrier for catalysis, scavengers for dust particles, shock absorbers and heat and sound insulators<sup>2,3</sup>.

Although aerogels can be prepared from an extensive range of materials, a particular promising candidate for addressing novel applications is cellulose. Cellulose is the most abundant sustainable material in the biosphere, but it has not been as exploited for novel materials as may be surmised; yet, with the pressing concerns surrounding petroleum supplies and increasing environmental consciousness, it has been slowly gaining ascendancy as a raw material for various market applications. Aerogels-based nanofibrillated cellulose, for example, has gained increasing attention because their properties may be similar to their inorganic counterparts such as silica and alumina with additional advantage of employing a substrate that is renewable, abundant and biodegradable.<sup>4-6</sup> In addition to that, excellent mechanical properties of cellulose have produced several works using cellulose nanofibers as a reinforcing material.<sup>7-11</sup>

Aerogels are obtained by carefully drying wet gels. Drying methods such as freeze drying or supercritical drying have been applied to maintain the openness of the structure. These methods preserve intramolecular hydrogen bonding and the entangled long partly amorphous nanofibers<sup>12</sup>.

Tuning the properties of any chemical assembly such as an aerogel to obtain specific applications may require chemical tweaking of the existing structure(s).<sup>13</sup> Such modifications of cellulose are interesting approaches for value-added products. One common modification is its catalytic oxidation using 2,2,6,6-tetramethylpyperidine-1-oxyl radical (TEMPO) to introduce functionalities such as aldehyde and carboxyl groups and thus derive new industrial use<sup>14,15</sup>. For instance, improvements on the physical properties of handsheets have been observed when TEMPO-oxidized pulps are used because inter-fiber bond is formed.<sup>16</sup> Also, it has been found that regenerated cellulose could be

completely converted into water-soluble polyglucuronic acid,<sup>17, 18</sup> which might contribute to the formation of highly viscous hydrogels to be further converted in resistant aerogels. Another alternative for cellulose modification, relatively unexplored until the present, is the use of hydroxyapatite (HAp),  $(\text{Ca}_{10}[\text{PO}_4]_6(\text{OH})_2)$ . HAp has biochemical and mechanical properties that make its use attractive for applications as artificial bones and scaffolds for tissue engineering.<sup>19, 20</sup> A range of features have been beneficially expected due to HAp combination with cellulose such as high mechanical properties, sufficient porosity, high water holding capability, excellent biocompatibility and bone-bonding ability.<sup>20</sup> However, not much has been found on the literature regarding to HAp and cellulose.<sup>20</sup> Cellulose composites can be formed in a variety of shapes and it is biocompatible. However, many studies have been carried out to address the limitation of using cellulose as artificial bone since it does not bond directly to it.<sup>21</sup>

The aim of this work is to produce, characterize and explore aerogels prepared from nanofibrillated cellulose (NFC) extracted from hardwood by freeze-drying for direct water removal. The study emphasizes on the effects of modifications on nanofibrillated cellulose-based aerogel using TEMPO and/or hydroxyapatite as modifier agent. The aerogels produced are characterized according to their morphology (FE-SEM), mechanical properties and water bound.

## **2. Materials and Methods**

### **2.1. Materials**

Potassium hydroxide (99%), hydrogen peroxide (30%), acetic acid (99.5%), hydroxyapatite, sodium hydroxide (0.01 N) and hydrochloric acid (0.01 N), TEMPO, sodium bromide, sodium hypochlorite solution were all purchased from Sigma-Aldrich.

### **2.2. Isolation of Nanofibrillated Cellulose (NFC)**

The starting cellulose material was hardwood *Eucalyptus urograndis* specimens. Extratives-free sawdust of wood samples was subjected to delignification with peracetic acid at 15% to yield holocellulose. Then, hemicelluloses were removed by using KOH 24% at room temperature. Cellulose fibers left were washed several times and swollen for 1 day in deionized water until a w/v ratio of 2.0% was achieved. Next, the sample was dispersed using a blender for 5 minutes to get a consistent fiber suspension. Nanofibrillated cellulose (NFCs) aqueous gel was obtained by passing the suspension formed through a

high pressure homogenizer (15MR two-stage Manton-Gaulin homogenizer - APV, Delavan, WI, USA) at approximately 0.8% solids content. The operating pressure was maintained at 55 MPa and the suspension was collected after 20 passes through the homogenizer and stored at 4°C in cold storage until needed. Cellulose structure is presented in Figure A.2.1 (Appendix)

### 2.3. NFCs modifications

#### *TEMPO-mediated oxidation of NFCs*

Nanofibrillated celluloses (2g) in 250 mL of suspension, TEMPO (0.058 g, 0.095 mmol) and sodium bromide (0.635 g, 1.57 mmol) were added to the suspension. The TEMPO-mediated oxidation was started by adding the desired amount of the 1.24 M NaClO solution (1.6 – 5.0 mmol NaClO per gram of cellulose). The pH of the mixture was maintained to 10 at room temperature by adding 0.5 M NaOH while stirring the suspension. After 45 minutes, the oxidation was terminated by adding drops of methanol and the pH was adjusted to 7 with 0.5M HCl. The oxidized samples were dialyzed against deionized water.

#### *NFCs modification with hydroxyapatite (HAp)*

HAp aqueous solutions (pH ~ 4) were prepared in concentration of 0.5 mol L<sup>-1</sup> and a volume of 1.0 mL of each solution was added to NFCs oxidized and non-oxidized after their centrifugation to reach a weight ratio HAp:cellulose of 0.2:1.

### 2.4. Preparation of NFC-based aerogels

After removing the excess of water by centrifugation of NFC's suspension, the aqueous gel were placed on cylindrical molds and quickly plunged in liquid nitrogen at the temperature of ca. -190°C. The frozen sample in the mold was transferred into a pre-cooled glass bottle and subjected to freeze drying in a vacuum oven for 30 hours.

### 2.5. Conductimetry

Conductimetric titration was used to determine carboxyl content of oxidized NFC. The samples (30, 50 and 100 mg) were suspended into 15 ml of 0.01 M hydrochloric acid solutions and stirring for 10 minutes. After, the suspensions were titrated with 0.01 M NaOH and titration curves were created (Figure 2). From the curves, it is possible to

calculate the amount of carboxyl groups and therefore the degree of oxidation (DO), according to the following equation,<sup>22</sup>

$$DO = \frac{162 \times C \times (V_2 - V_1)}{w - 36 \times C \times (V_2 - V_1)}$$

where C is the NaOH concentration (mol L<sup>-1</sup>), V<sub>1</sub> and V<sub>2</sub> are the initial and final amount of NaOH in L based on the plateau of the curve, w (g) the weight of the oven-dried sample.

## 2.6. Infrared spectroscopy

FT-IR spectroscopy was performed on a Thermo Nicolet NEXUS 670 FT-IR spectrophotometer. Spectra were obtained by accumulation of 128 scans, with a resolution of 4cm<sup>-1</sup> at 4000-650 cm<sup>-1</sup>.

Oxidized NFCs were converted to their acid form by ion exchange in order to displace the carboxyl absorption band toward higher wavelength and thus eliminate any interference with the absorbed water band (1640 cm<sup>-1</sup>).

## 2.7. Scanning Electron Microscopy (SEM)

The morphology of the hydrogels was controlled by field emission scanning electron microscopy (FE-SEM) using a JEOL 6400F microscope operated with an accelerating voltage of 5 kV and a working distance of 15 mm, and a 30 μm objective aperture. A small hydrogel sized sample was affixed onto conductive carbon tape and mounted on the support and then sputtered with an approximately 25 nm layer of gold/palladium (60/40).

## 2.8. BET Measurements

Specific surface area and pore volume of the cellulose aerogels analysis was carried out using the Brunauer–Emmett–Teller (BET) nitrogen adsorption/desorption method on a HORIBA SA-9601-MP. The samples were degassed under flowing UHP grade nitrogen for 2 h at a temperature of 100°C before used. The experiment was done in duplicate.

## 2.9. Physical Properties (Rheology and Density)

Stress (strength) and strain (deformability) of the aerogels were determined by compression testing. Gels were cut into cylinders (~23.5 mm in height) and compressed at

50% of the original length between plates using a universal testing machine (Model 5565, Instron Engr. Corp., Canton, Mass., U.S.A.) controlled with Bluehill® software version 2.0 (Instron Engr. Corp.). A 5 kN load cell was used for all samples. Rheological measurements were done in duplicates. Apparent density of aerogel was evaluated from mass (0.1 mg accuracy) and geometric dimensions avoiding deformation of soft specimens. Measurements were done in three replicates.

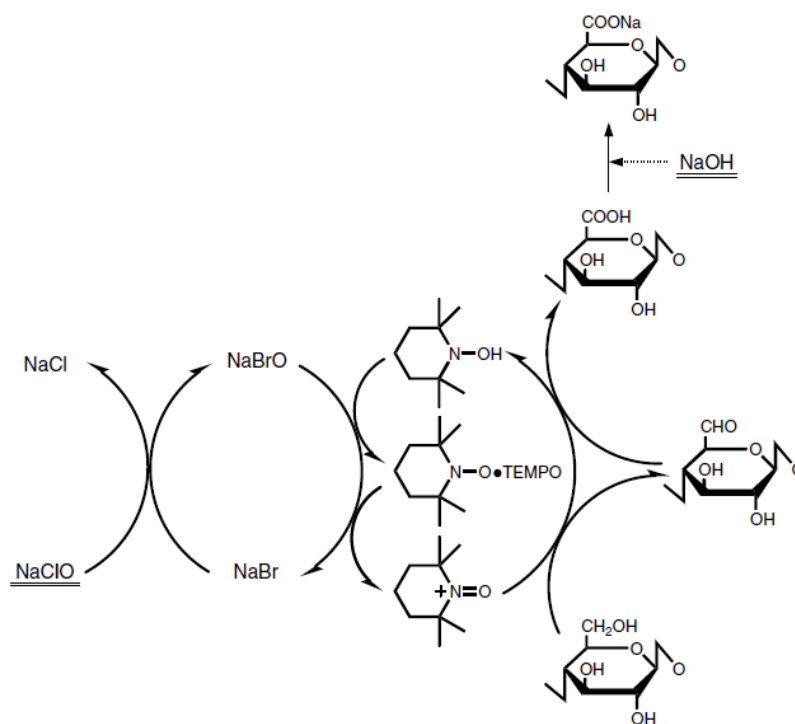
### **3. Results and Discussion**

Firstly, NFC suspensions were modified or not with TEMPO and/or HAP, generating cellulose dispersion with three degrees of oxidation. Then, HAP suspensions (in water) were also used to modify the NFC suspensions. At the end, six NFC based aerogels samples were produced and they were further characterized according to their density, surface area (BET), morphology (FE-SEM) and rheological properties.

#### **3.1. NFC modification and drying**

The TEMPO-mediated oxidation of NFC shown two different DO, measured by conductimetric titration (Figure 2). As shown in the scheme of the TEMPO-oxidation of cellulose (Scheme 1), 1 mol of carboxylate group is formed by consuming 2 mol of NaClO, while 1 mol aldehyde group is formed by 1 mol of NaClO.

The results indicated a DO of 0.1 and 0.2 for the two samples oxidized by TEMPO. The non-oxidized sample showed a little DO of 0.03, probably due to oxidation from the use of peracetic acid during the delignification of wood. Higher levels of oxidation were reached when increasing amounts of NaOCl were used. However, when the maximum DO of 0.2 was achieved; any additional increasing amounts of NaOCl did not lead to a higher DO.



**Scheme 1.** TEMPO-mediated oxidation of cellulose.<sup>23</sup>

Once TEMPO-oxidation of NFC dispersions was successfully accomplished, HAP was also used as a physical modifying agent at weight ratio HAP: cellulose of 0.2:1. Finally, NFC suspensions were direct freeze-dried for water removal.

One of the most common challenging on aerogel preparation is the drying process because direct drying of hydrogels usually results in total collapse of porosity caused by the strong surface tension of leaving water. However, mostly cellulose nanofibers dispersed in water can be obtained by TEMPO-mediated oxidation, producing a homogeneous suspension.<sup>24, 25</sup> Besides, tensile strength of the handsheets has been improved using TEMPO-oxidized pulps and the positive effect on cellulose fibers properties with the formation of carboxylic groups<sup>26</sup>.

Lightweight sponge-like aerogel was produced with no significant collapse or shrinkage. In fact, non-oxidized aerogel itself was slightly brittle than the oxidized ones. Figure 1 shows the pictures of the cylindrical shape aerogels produced by freeze-drying. Note that no shrinkage has occurred.



**Figure 1.** Macro structures of cellulose aerogels regenerated after freeze-drying. Left: cylindrical mold used during freeze-drying.

Resulting aerogels were analyzed by FTIR and the spectra of the oxidized and non-oxidized samples are shown in Figure 3. It is possible to notice some changes in bands due to the selective TEMPO oxidation in position 6 of the glucose ring. The band at  $1720\text{-}1740\text{ cm}^{-1}$  on the FT-IR spectra confirms the presence of carboxylic groups, and the higher the carboxylic content, the higher the degree of oxidation (Figure 3). Even for TEMPO non-oxidized NFC (DO~0.03), it is clearly observed the difference between the samples by observing the intensity of carboxylic band ( $1720\text{-}1740\text{ cm}^{-1}$ ) and its comparison with the characteristic cellulose band near  $1420\text{ cm}^{-1}$  (C-O stretching).

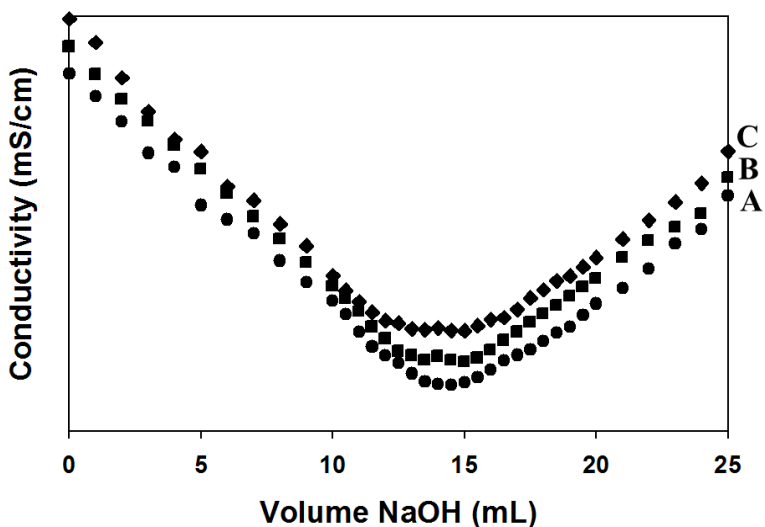


**Figure 2.** Conductimetric titration curves of oxidized NFCs with different DOs resulting from different ratio NaOCl/AGU. NFC non-oxidized by TEMPO (●), NFC TEMPO-mediated oxidation DO=0.1 (■), NFC TEMPO-mediated oxidation DO=0.2 (◆).

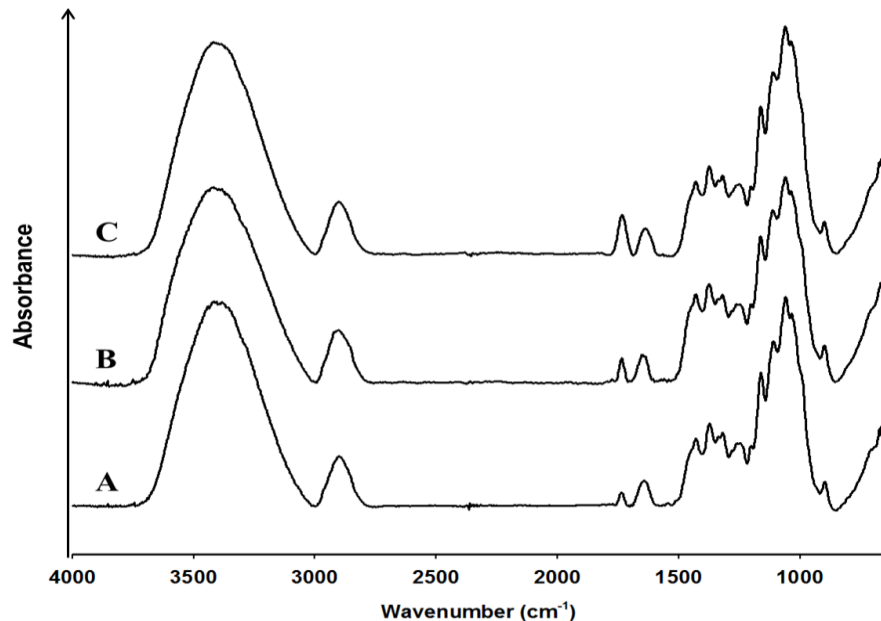


**Figure 3.** FTIR spectra of NFC: NFC non-oxidized by TEMPO (A), NFC TEMPO-mediated oxidation DO=0.1 (B), NFC TEMPO-mediate oxidation DO=0.2 (C)

### 3.2. Surface area, pore volume and density of the aerogels

Recently, many studies have been analyzing the influence of freeze-drying conditions as well as NFC concentration for cellulose based aerogel fabrication.<sup>13, 27-29</sup> In the present work, the same NFC suspension concentration (0.8 wt%) and the same drying conditions were used in all cases. This way, the changes on surface area, pore volume and density were uniquely attributed to the chemical/physical modifications placed on the aerogels. Surface area, pore volume and density of the aerogels are shown in Table 1.

The specific surface areas of the resulting aerogels are in agreement with those reported for freeze-dried NFC aerogels using liquid nitrogen for cooling.<sup>13</sup> Higher surface areas have been found earlier for aerocellulose rapidly cooling with propane before freeze-drying.<sup>6, 12</sup> Differences on the surface area of the aerogels can be noticed between oxidized and non-oxidized aerogels.

Highly viscous NFC suspensions were obtained after oxidation. Oxidized aerogels provide lower densities and therefore, an increasing on surface area/pore volume can be observed, as expected. Densities determinations were carefully carried out by weighting the same amount of NFC suspension before placing them in a vial for further freeze-drying. Thus, it was possible to note an increasing on the volume of the aerogels.

However, when HAp was used, the density of the aerogels started increasing. The addition of HAp would be the main contributor for increasing of weight considering the same volume.

**Table 1.** Surface area, pore volume and density of the NFC aerogels.

Sample	Surface Area (m <sup>2</sup> /g)	Pore Volume (cm <sup>3</sup> /g)	Density (g/cm <sup>3</sup> )
AG DO=0	13.6	0.008	0.0098
AG DO=0.1	15.8	0.010	0.0085
AG DO=0.2	18.4	0.012	0.0080
AG DO=0 + HAp	10.8	0.007	0.0108
AG DO=0.1 + HAp	16.5	0.009	0.0088
AG DO=0.2 + HAp	16.9	0.009	0.0090

### 3.3. Morphology and rheological properties

The aerogels presented diverse macroscopic morphologies, especially when contrasting samples with different DOs. It became clear that the samples with higher DOs displayed a more organized distribution of pores, revealing a hierarchical order of the open-porous cellulose network. The higher degree of oxidation (DO=0.2) of the aerogels, the higher homogeneous the morphology.

It is worth mentioning that the use of NFC suspension does form a hydrogel-like network. However, the oxidized samples provide more homogeneous and highly viscous hydrogels, thus contributing to the formation of a homogeneous aerogel network. Previous work has revealed that a combination of TEMPO-mediated oxidation and homogenizing treatment has better advantages to disintegrate cellulose fibers into microfibrillated suspension using mechanical treatment only.<sup>25</sup>

Interestingly, no collapse during the drying process was observed for the aerogels. A well aggregated-like structure was formed for the oxidized cellulose, especially for the one fabricated with DO=0.2.

A close view on the SEM images showing the aggregation of HAp in the cellulose fibers of the aerogels can be observed on Figure 5. Overall, HAp affects the aerogels

morphology, as it can be observed in Figure 4. The morphology shown by the non-oxidized NFC based aerogel without addition of HAp were at some point preserved observed after its addition. For both levels of TEMPO-oxidized aerogels, HAp affects the morphology creating a closer network which may have been induced by the presence of carboxylate groups present on cellulose structure.

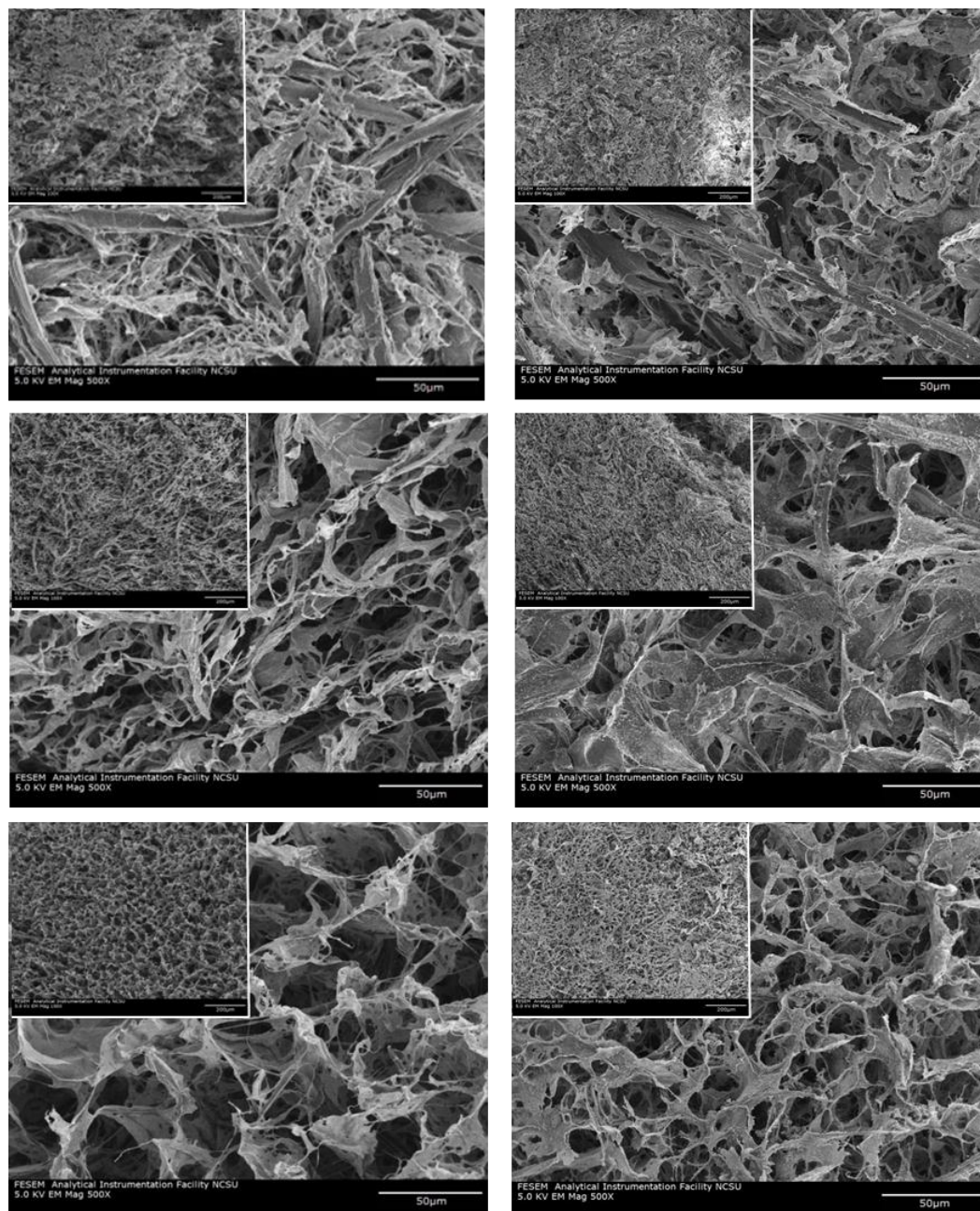


**Figure 4.** SEM of the aerogels. Left, from the top to the bottom: AG DO=0; AG DO=0.1; AG DO=0.2. Right, from the top to the bottom: AG DO=0 + HAp; AG DO=0.1 + HAp; AG DO=0.2 + HAp.

AG DO=0.2 + HAp.

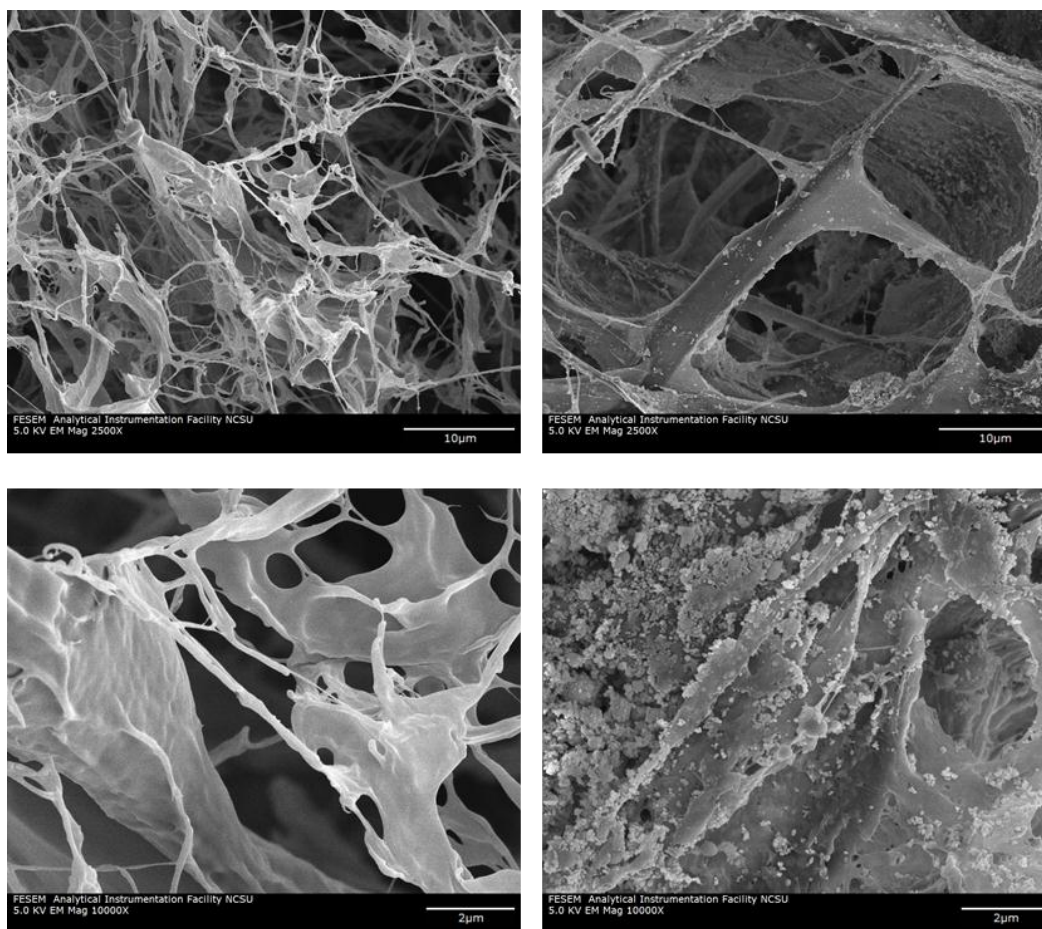


**Figure 5.** SEM images of the aerogels DO=0.2. Left: no HAp addition and Right: HAp addition.

The resulting aerogels were then analyzed according to their mechanical properties by measuring the force applied to compress the samples at 50% of their original length (Figure 6). After compression, the oxidized aerogels (without HAp) were able to bounce back a little and recovering approximately at 65% of the original length whereas the non-oxidized ones were able to reach 55% of the original length. The addition of HAp to the aerogels did not contribute as much as its absence on the recovering height of the aerogels. Oxidized aerogels were able to reach 55% of the original length but no significant height recovery was noticed for the non-oxidized aerogels.

Figure 6 shows the effect of the TEMPO-oxidation, leading to a more highly

compression-resistant sample. Ostensibly, the addition of HAp to all three oxidized samples increased the resistance of the NFC aerogels as well. The synergistic effect of oxidation and HAp on the resulting aerogels were able to increase the resistance of them up to 3-fold. Although, the oxidation effect was more pronounced, the HAp addition played a crucial role to enhance the resistance of these materials.

A combination of HAp and cellulose nanofibers is expected to offer striking features as high mechanical properties, excellent biocompatibility and bone-bonding ability. Even though HAp-NFC association to form aerogels has been expected high mechanical performance as alternative for bone tissue engineering fields, no work exploiting such properties has not been published so far.

According to the results obtained in this work, the addition of HAp in all oxidized and non-oxidized samples have given a significant strength to the NFC-based aerogels. This fact supports the supposition that NFC that is *a priori* modified by TEMPO can have viscoelastic properties improved by addition of HAp. Even though TEMPO-oxidized aerogels has been shown greater effectiveness on the strength properties, the use of HAp to modify the aerogels is also presented as an alternative to improve strength.

The addition of HAp on the non-oxidized aerogels was able to increase the strength from approximately 7500 Pa to 10000 Pa and this effect is less pronounced as the degree of oxidation increases.

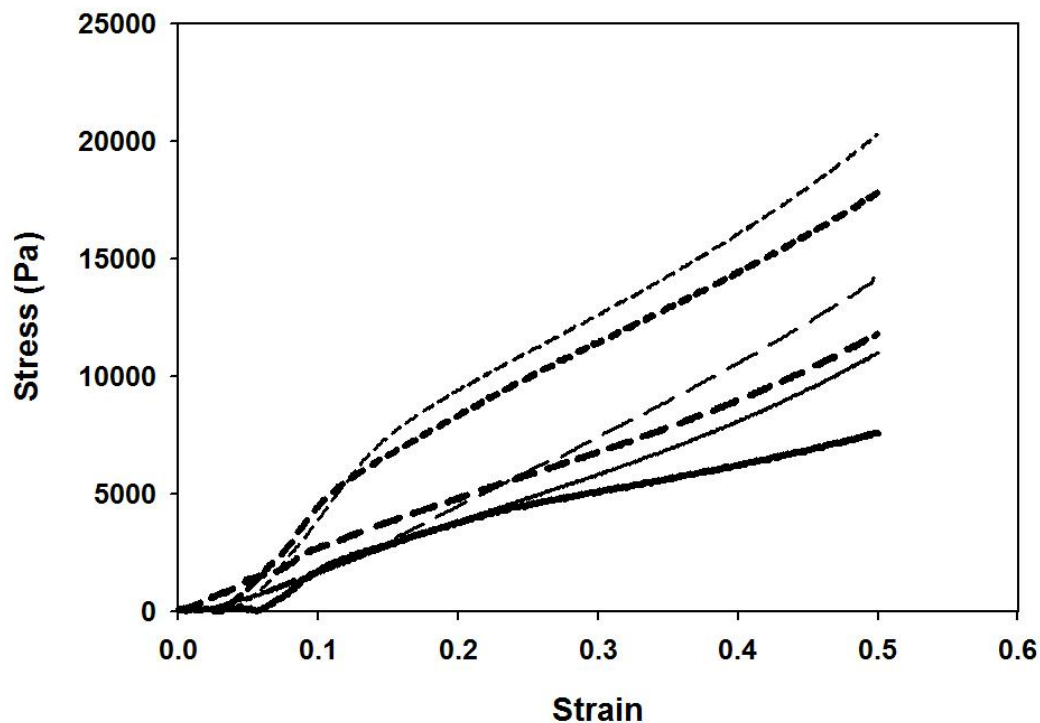


**Figure 6.** Rheological properties of the NFC-based aerogels. Bold lines represent the aerogels without HAp addition. Solid line: AG DO=0; long dashed line: AG DO=0.1; short dashed line: AG DO=0.2.

#### 4. Conclusions

Nanofibrillated cellulose based aerogels were prepared by vacuum freeze-drying of aqueous suspension of cellulose nanofibers prepared under high pressure homogenizer. The cellulose suspension was successfully modified either by TEMPO-oxidation and/or hydroapatite (HAp) addition, indicating that the resulting aerogel can be easily tuned by those modifications. Oxidized aerogels revealed lower densities whereas the use of HAp increased the density slightly. Morphology of oxidized aerogels presented high pore size homogeneity, which was nearly maintained by the addition of HAp. Both modifications applied were able to enhance the strength of the aerogels, even though the oxidation had the striking effect. Tuned NFC-based aerogels have been offered as a viable pathway for the production of high value cellulose aerogels.

## 5. References

1. Liebner, F.; Potthast, A.; Rosenau, T.; Haimer, E.; Wendland, M., Cellulose aerogels: Highly porous, ultra-lightweight materials. *Holzforschung* **2008**, 62, (2), 129-135.
2. Burchell, M. J.; Creighton, J. A.; Cole, M. J.; Mann, J.; Kearsley, A. T., Capture of particles in hypervelocity impacts in aerogel. *Meteoritics & Planetary Science* **2001**, 36, (2), 209-221.
3. Hüsing, N.; Schubert, U., Aerogels-airy materials: chemistry, structure, and properties. *Angewandte Chemie International Edition* **1998**, 37, (1-2), 22-45.
4. Innerlohinger, J.; Weber, H. K.; Kraft, G., Aerocellulose: Aerogels and Aerogel-like Materials made from Cellulose. *Macromolecular Symposia* **2006**, 244, (1), 126-135.
5. Cai, J.; Kimura, S.; Wada, M.; Kuga, S.; Zhang, L., Cellulose Aerogels from Aqueous Alkali Hydroxide–Urea Solution. *ChemSusChem* **2008**, 1, (1-2), 149-154.
6. Gavillon, R.; Budtova, T., Aerocellulose: New Highly Porous Cellulose Prepared from Cellulose–NaOH Aqueous Solutions. *Biomacromolecules* **2007**, 9, (1), 269-277.
7. Dufresne, A.; Dupeyre, D.; Vignon, M. R., Cellulose microfibrils from potato tuber cells: Processing and characterization of starch–cellulose microfibril composites. *Journal of Applied Polymer Science* **2000**, 76, (14), 2080-2092.
8. Iwamoto, S.; Nakagaito, A. N.; Yano, H., Nano-fibrillation of pulp fibers for the processing of transparent nanocomposites. *Applied Physics A: Materials Science & Processing* **2007**, 89, (2), 461-466.
9. Nakagaito, A. N.; Iwamoto, S.; Yano, H., Bacterial cellulose: the ultimate nanoscale cellulose morphology for the production of high-strength composites. *Applied Physics A: Materials Science & Processing* **2005**, 80, (1), 93-97.
10. Leitner, J.; Hinterstoisser, B.; Wastyn, M.; Keckes, J.; Gindl, W., Sugar beet cellulose nanofibril-reinforced composites. *Cellulose* **2007**, 14, (5), 419-425.
11. Zimmermann, T.; Pöhler, E.; Geiger, T., Cellulose Fibrils for Polymer Reinforcement. *Advanced Engineering Materials* **2004**, 6, (9), 754-761.
12. Paakko, M.; Vapaavuori, J.; Silvennoinen, R.; Kosonen, H.; Ankerfors, M.; Lindstrom, T.; Berglund, L. A.; Ikkala, O., Long and entangled native cellulose I nanofibers allow flexible aerogels and hierarchically porous templates for functionalities. *Soft Matter* **2008**, 4, (12), 2492-2499.

13. Aulin, C.; Netrval, J.; Wagberg, L.; Lindstrom, T., Aerogels from nanofibrillated cellulose with tunable oleophobicity. *Soft Matter* **2010**, 6, (14), 3298-3305.
14. Bragd, P. L.; van Bekkum, H.; Besemer, A. C., TEMPO-Mediated oxidation of polysaccharides: survey of methods and applications. *Topics in Catalysis* **2004**, 27, 49-66.
15. Varma, A. J.; Chavan, V. B., A study of crystallinity changes in oxidised celluloses. *Polymer Degradation and Stability* **1995**, 49, (2), 245-250.
16. Saito, T.; Isogai, A., Wet Strength Improvement of TEMPO-Oxidized Cellulose Sheets Prepared with Cationic Polymers. *Industrial & Engineering Chemistry Research* **2006**, 46, (3), 773-780.
17. Isogai, A.; Kato, Y., Preparation of Polyuronic Acid from Cellulose by TEMPO-mediated Oxidation. *Cellulose* **1998**, 5, (3), 153-164.
18. Tahiri, C.; Vignon, M. R., TEMPO-oxidation of cellulose: Synthesis and characterisation of polyglucuronans. *Cellulose* **2000**, 7, (2), 177-188.
19. Hong, L.; Wang, Y. L.; Jia, S. R.; Huang, Y.; Gao, C.; Wan, Y. Z., Hydroxyapatite/bacterial cellulose composites synthesized via a biomimetic route. *Materials Letters* **2006**, 60, (13-14), 1710-1713.
20. Wan, Y. Z.; Hong, L.; Jia, S. R.; Huang, Y.; Zhu, Y.; Wang, Y. L.; Jiang, H. J., Synthesis and characterization of hydroxyapatite-bacterial cellulose nanocomposites. *Composites Science and Technology* **2006**, 66, (11-12), 1825-1832.
21. Kwak, D. H.; Hong, S. J.; Kim, D. J.; Greil, P., The formation of hydroxyapatite on chemically-modified cellulose fibers. *Journal of Ceramic Processing Research* **2010**, 11, (2), 170-172.
22. da Silva Perez, D.; Montanari, S.; Vignon, M. R., TEMPO-Mediated Oxidation of Cellulose III. *Biomacromolecules* **2003**, 4, (5), 1417-1425.
23. Saito, T.; Okita, Y.; Nge, T. T.; Sugiyama, J.; Isogai, A., TEMPO-mediated oxidation of native cellulose: Microscopic analysis of fibrous fractions in the oxidized products. *Carbohydrate Polymers* **2006**, 65, (4), 435-440.
24. Saito, T.; Kimura, S.; Nishiyama, Y.; Isogai, A., Cellulose Nanofibers Prepared by TEMPO-Mediated Oxidation of Native Cellulose. *Biomacromolecules* **2007**, 8, (8), 2485-2491.

25. Saito, T.; Nishiyama, Y.; Putaux, J.-L.; Vignon, M.; Isogai, A., Homogeneous Suspensions of Individualized Microfibrils from TEMPO-Catalyzed Oxidation of Native Cellulose. *Biomacromolecules* **2006**, 7, (6), 1687-1691.
26. Laine, J.; Stenius, P., Effect of charge on the fibre and paper properties of bleached industrial kraft pulps. *Paperi ja puu* **1997**, 79, (7), 257-266.
27. Hoepfner, S.; Ratke, L.; Milow, B., Synthesis and characterisation of nanofibrillar cellulose aerogels. *Cellulose* **2008**, 15, (1), 121-129.
28. Jin, H.; Nishiyama, Y.; Wada, M.; Kuga, S., Nanofibrillar cellulose aerogels. *Colloids and Surfaces A: Physicochemical and Engineering Aspects* **2004**, 240, (1-3), 63-67.
29. Heath, L.; Thielemans, W., Cellulose nanowhisker aerogels. *Green Chemistry* **2010**, 12, (8), 1448-1453.

## CHAPTER 3

Published as original paper (*Soft Matter* (2011), 7, 1090-1099)

### THE INFLUENCE OF THE CHEMICAL AND STRUCTURAL FEATURES OF XYLAN ON THE PHYSICAL PROPERTIES OF ITS DERIVED HYDROGELS

Teresa Cristina Fonseca Silva,<sup>1,2</sup> Youssef Habibi,<sup>2</sup> Jorge Luiz Colodette,<sup>1</sup> and Lucian A. Lucia<sup>2</sup>

<sup>1</sup>Departamento de Química, Universidade Federal de Viçosa, Viçosa, MG, 36570-000; Brazil

<sup>2</sup>Laboratory of Soft Materials & Green Chemistry, Department of Forest Biomaterials, North Carolina State University, Raleigh, North Carolina 27695-8005

E-mail: [lucian.lucia@ncsu.edu](mailto:lucian.lucia@ncsu.edu)

**ABSTRACT:** Xylan polysaccharides, both with and without acetyl substituents, were obtained from the specific hardwood *Eucalyptus urograndis* by controlled extraction processes and eventually post-acetylated. They were subsequently functionalized with well-defined levels of methacrylic monomers to thereby provide different degrees of substitution of the functional group. These modified xylans were the basis to successfully prepare for the first time xylan/Poly(2-hydroxyethylmethacrylate)-based hydrogels via the radical polymerization of HEMA used as a crosslinking agent. The tuning of the crosslinking density of the hydrogel network was accomplished by preparing hydrogels that had two composition ratios of xylan to HEMA (60:40 and 40:60) and was also done by varying the degrees of substitution. The resulting hydrogels were characterized according to their morphology, swelling and rheological properties by field emission scanning electron microscopy (FE-SEM), gravimetric measurements after immersion in water, and dynamical mechanical analysis. Surprisingly, the presence of acetyl moieties leads to stiffer hydrogels which have a reduced capacity for water uptake. A natural

extension to the synthesis and characterization of the novel-based xylan hydrogels is examining one of their primary functionalities: encapsulation and release. This functionality was one of the drivers of this work when it was conceived given the inherent ability of hydrogels to act as cargo carriers. Therefore, a representative anticancer drug doxorubicin was loaded into these hydrogels and its release in different media was studied. Acetylated xylans showed high delivery ratios while non-acetylated samples leveled off at half the level of the acetylated samples.

**KEYWORDS.** Hydrogels, xylans, renewable resources, wood, *Eucalyptus urograndis*, rheology, drug release, doxorubicin

## **Introduction**

Hydrogels are three-dimensional stable networks formed from cross-linked hydrophilic homopolymers, or copolymers to form insoluble polymeric materials.<sup>1, 2</sup> They have received increasing interest over the last several years in part due to their hydrophilicity, soft tissue-mimicking consistency, high permeability to metabolites and oxygen, and resilience. Furthermore, due to their unique biocompatibility, flexible methods of synthesis, range of constituents, and desirable physical characteristics, hydrogels constitute the basis for numerous biomedical applications. For example, they have been the material of choice for such applications as witnessed by work in cartilage or tendons, in bio-adhesives, in tissue engineering, as ocular lenses, or as drug delivery matrices.<sup>3-5</sup>

A wide range of synthetic polymers have been used to develop advanced hydrogels with tailored properties.<sup>4</sup> However, with the onset of the new “bio-”energy portfolio focused on extracting energy from biomaterials, the use of renewable resources has surfaced as a potential alternative to fossil fuels, and recent advances have streamlined the development of renewable biomaterials for advanced applications.<sup>6</sup>

In addition to their inherent renewability, natural polysaccharide-based hydrogels are currently attracting much interest for their fundamental properties such as tunable functionality, biocompatibility, and high degree of swelling.<sup>6, 7</sup> Various polysaccharides have been investigated for hydrogel formulations, typically dextran,<sup>8-10</sup> alginate,<sup>11-13</sup> chitosan,<sup>14-16</sup> and starch.<sup>17, 18</sup>

Heteropolysaccharides or hemicelluloses, although mostly unexplored as a raw feedstock for many polymeric materials applications until recently, can nevertheless be as useful as related polysaccharides and have significant potential as a material resource for hydrogel preparation/application. For instance, xylan-based hydrogel has already shown potential for biocompatibility because of its reported non-cytotoxic effect.<sup>19</sup> However, there have only been few examples that have described the feasibility of using hemicelluloses such as galactoglucomannan to formulate hydrogels.<sup>20-22</sup>

Xylans are the most common hemicelluloses and considered to be the major non-cellulosic cell wall polysaccharide component of angiosperms (e.g., trees, grasses, and cereals) where they exist in many different compositions and structures.<sup>23</sup> Indeed, xylans' structure exhibits a  $\beta$ - (1 $\rightarrow$ 4) linked D-xylosyl backbones, with various side groups or chains attached to the O-2 and/or O-3 of the xylosyl residues. These side chains mainly consist of  $\alpha$ -D-glucuronic acid, 4-O-methyl- $\alpha$ -D-glucuronic acid and some neutral sugars units ( $\alpha$ -L-arabinofuranose,  $\alpha$ -D-xylopyranose or  $\alpha$ -D-galactopyranose). Among the common side groups are also acetyl groups, phenolic, ferulic and coumaric acids.<sup>24</sup>

Relatively pure xylans and 4-O-methyl- $\alpha$ -D-glucuronoxylans have been used in various industrial and non-industrial applications including biomedical applications.<sup>25</sup> They have even been reported to inhibit the growth rate of tumors, probably with respect to the indirect stimulation of the nonspecific immunological host defense.<sup>26, 27</sup> Xylan-based films were also reported to present a hydrogel-like behavior with high swelling capacity.<sup>28,</sup>

29

The aim of this work is to fabricate, characterize, and explore hydrogels prepared from xylans extracted from hardwood as viable drug delivery vehicles. The study emphasizes on the effect of the acetyl groups by comparing xylans with different structural features, e.g., presence or absence of the acetyl groups. For hydrogels preparation, xylan backbones were conjugated with 2-hydroxyethylmethacrylate (HEMA) and the obtained hydrogels were characterized in terms of their morphology, swelling, and rheological properties. They were used as matrices to examine the potential for the delivery of an anticancer drug, viz., doxorubicin, a representative anthracycline antibiotic and one of the most widely used anticancer drugs available, that has demonstrated high antitumor activity.<sup>30</sup>

## Results and Discussion

### *Extraction and derivatization of the xylans*

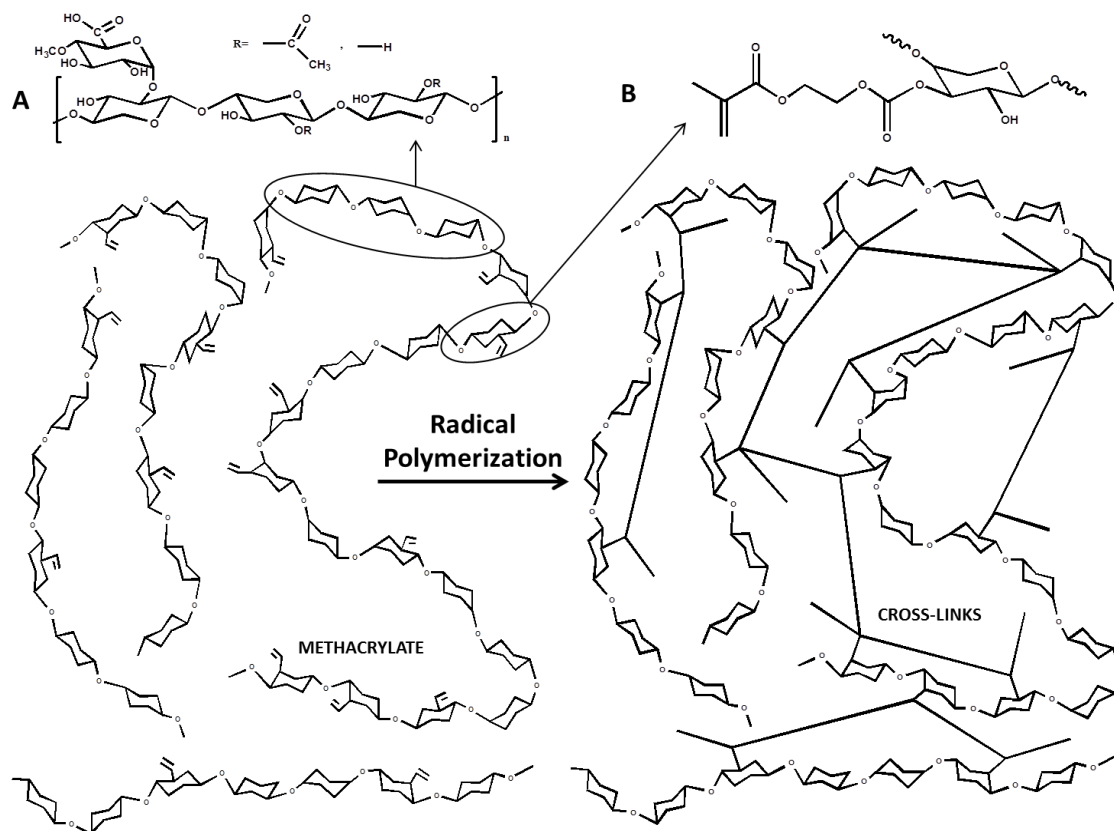
First, acetylated and non-acetylated xylans were extracted from *Eucalyptus urograndis* using DMSO at 50°C and potassium hydroxide 24% (w/v) at room temperature respectively. As expected, the sugar composition showed a abundance of xylose concentration for both type of extractants with the presence of other minor monosaccharides such as glucose, mannose, rhamnose and galactose. In fact, the molar ratio of xylose to the other minor sugars detected was 0.83:0.17 for non-acetylated xylan and 0.89:0.1 for acetylated xylans which is well within the accepted range as found for the same xylans.<sup>31, 32</sup> The respective structures of the isolated xylans were confirmed by NMR with representative recorded spectra in Figure 1. The acetylated xylans had a degree of acetylation of approximately 0.63 as determined by <sup>1</sup>H-NMR which corroborated the values already published for this wood specie.<sup>33</sup> Similarly, the 4-*O*-methylglucuronic acids (MeGlcA) contents were determined by <sup>1</sup>H-NMR from which it was found that these xylans had a ratio of 1.2 units of MeGlcA for every 10 xylose units. This value was approximately the same for both xylans.

The molecular weights of the extracted xylans were evaluated by Size Exclusion Chromatography (SEC). Acetylated xylans showed higher molecular weights in the range of 33.7 kDa, while the molecular weight of non-acetylated counterparts was 28.3 kDa. These results suggest that a slight degradation of alkali-extracted xylans due to  $\beta$ -elimination may have occurred during the extraction. The chromatography profiles also demonstrated a unimodal Gaussian distribution suggesting a relative structural homogeneity of isolated polysaccharides resulting from extensive purification based on solubilization-precipitation and dialysis which are known to separate small chains. This observation is supported by the low polydispersity indices that were approximately 1.06 for acetylated xylans and 1.33 for non-acetylated xylans.

In general, hydrogels as a class of polymeric-based materials represent a compositional motif best characterized as a 3D network and their preparation thus requires a cross-linking of polymer chains. To this end, the extracted xylans were first covalently modified with 2-[(1-imidazolyl)formyloxy]ethyl methacrylate (HEMA-Im),<sup>34</sup> to produce hydroxyethyl methacrylate derivatized xylan (xylan-HEMA) (Scheme 1). This attached monomer further serves as a reactive site to cross link the chains during the radical

polymerization. By increasing the amount of attached HEMA-Im in the xylans' backbone, i.e., the degree of substitution, an increase in the junction points (cross-linking density) is expected. However, it is already known that the conjugation of HEMA to the polysaccharides via the formation of ester carbonate bounds may undergo hydrolytic scission affecting the swelling of the gel, the release of entrapped drugs and depending on the extent of the hydrolysis of the esters bonds, it can result in the dissolution of the gel.<sup>9</sup>

35



**Scheme 1.** Representation of the xylan-based hydrogels formation by radical polymerization of the methacrylate groups. Chemical structures of (A) xylan polymer and (B) xylan-HEMA.

The HEMA-Im, previously prepared similarly to what has been reported, was coupled to the hydroxyl groups of xylans. The reaction time was varied from 6 to 120 h to achieve different degrees of substitution (DS) of HEMA on xylan backbone that allows for tuning the density of the 3D network. The success of this reaction was confirmed by <sup>1</sup>H-NMR and examples of recorded spectra are in Figure 1. The attachment of HEMA

moieties was evidenced by the presence of the signals at chemical shifts  $\delta$  6.05 and  $\delta$  5.71 ppm that are attributed to the vinyl proton.

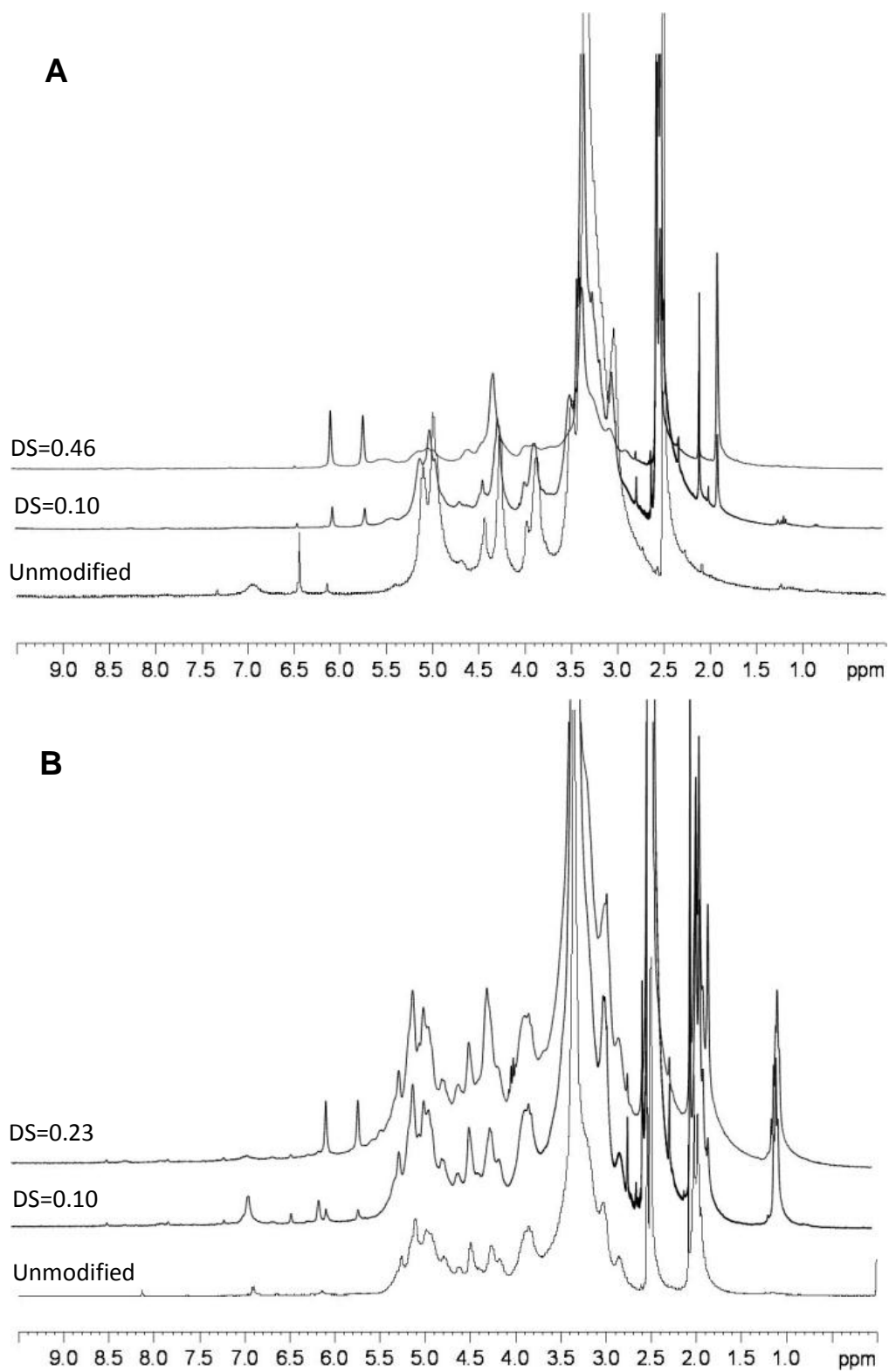


**Figure 1.**  $^1\text{H}$ -NMR spectra of unmodified and HEMA-Im-modified non-acetylated (A) and acetylated xylans (B).

The DS was determined by relating the intensity of the vinyl proton signals to the intensity of signals of the acetyl groups for acetylated xylan or 4-*O*-methyl glucuronic acid for non-acetylated xylan, respectively. Figure 2 illustrates the variation of DS with reaction time. The results clearly indicate that the resulting DS varied from 0.020 to 0.23 for acetylated xylans and from approximately 0.10 to 0.46 for non-acetylated samples over reaction times from 6 h to 120 h. The higher DS (~ 0.46) achieved for non-acetylated xylan when compared to the acetylated ones is most likely due to the presence of more available hydroxyl groups because of the absence of acetyl groups. The presence of acetyl groups in acetylated xylans may have prevented the reaction of their vicinal hydroxyl groups due to steric hindrance (this factor can limit the diffusion of HEMA-Im to hydroxyl groups). This factor again may have affected also the rate of the reaction which can be easily recognized in Figure 2. In the case of non-acetylated xylans the maximum DS (~0.46) was reached after approximately 24 h and longer times did not lead to any substantial further increases in the DS;<sup>34, 36</sup> while the maximum DS achieved for the acetylated samples (e.g., 0.23) was achieved 72 h later.

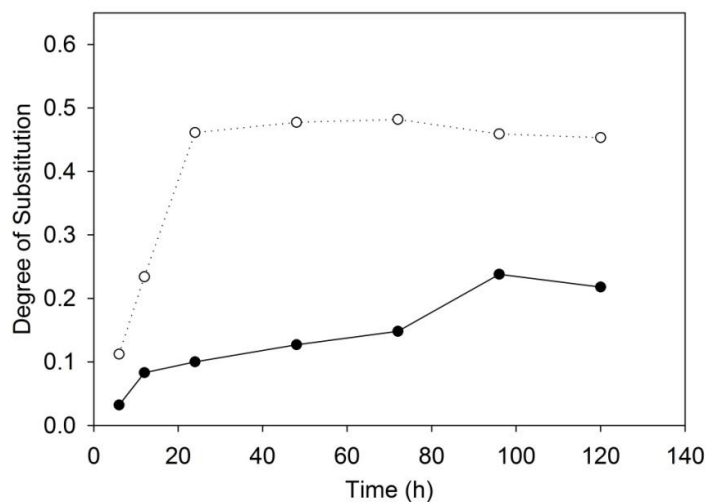


**Figure 2.** Variation of the degree of substitution for non-acetylated (○) and acetylated (●) modified xylans with HEMA-Im as a function of reaction time.

#### *Morphology, bounded water and rheological properties*

These modified xylans were used to manufacture the hydrogels, and HEMA was used as co-monomer to accomplish the cross-linking between the double bond of xylan

chains via a radical polymerization. Hydrogels with two compositions, namely 40:60 and 60:40 of xylans:HEMA were prepared and xylans with different DS were used for each type of xylan; however, thereafter, to accentuate the remarkable activity of these materials, the focus of the results obtained will be on the two DS, i.e., low and high as shown in Table 1.

Table 1. The composition and content of the bounded water of hydrogel-based xylans.

Xylan type	Degree of Substitution	Ratio xylan:HEMA	Bounded Water (%)
Acetylated	0.10	60:40	51
Acetylated	0.23	60:40	59
Acetylated	0.10	40:60	50
Acetylated	0.23	40:60	55
Non-acetylated	0.10	60:40	66
Non-acetylated	0.46	60:40	72
Non-acetylated	0.10	40:60	56
Non-acetylated	0.46	40:60	64

The amount of bounded or associated water on swollen hydrogels is demonstrated in Table 1. The uptake water molecules first disrupt the intermolecular hydrogen bonds and then hydrate/bind the most polar, hydrophilic sites. These molecules are distributed homogeneously throughout the polymer.

The results showed that hydrogels produced with non-acetylated xylans had a higher bounded water content than those made from acetylated xylans. The absence of acetyl groups confers the structure greater hydrophilicity and therefore, a higher concentration of water molecules are able to bind to the polymer. Moreover, when the ratio of xylan:HEMA is increased from 40:60 to 60:40, it is possible to observe an enhancement in the bounded water in the hydrogels and this behavior is more striking in the non-acetylated xylan, in accordance with the level of polymer used.

The resulting hydrogels were examined in terms of their morphology, swelling and deswelling behaviors, and rheological properties. The hydrogels present different macroscopic morphologies; the gels made from non-acetylated xylan were soft, whereas the ones made from the acetylated xylans were harder to solid-like gels. Figure 3 shows

typical SEM micrographs for the resulting gels. All formulations provided gels with porous structures where the size of the pores seems to be affected by both the type of xylans and their DS which provides a semi-quantitative way to ascertain the density junction points in the network. Open structures with larger pores were obtained with non-acetylated xylans which is in contrast to the case of acetylated samples that formed hydrogels with smaller pores. Furthermore, the structure became densely packed because the pores become smaller when the degree of substitution increased in both xylans. This fact was more pronounced in the case of highly substituted acetylated xylan-based hydrogels that showed a more firm morphology. This observation could be related to the presence of acetyl groups that confer to them a more “hydrophobic” character and therefore lead to enhanced affinity.

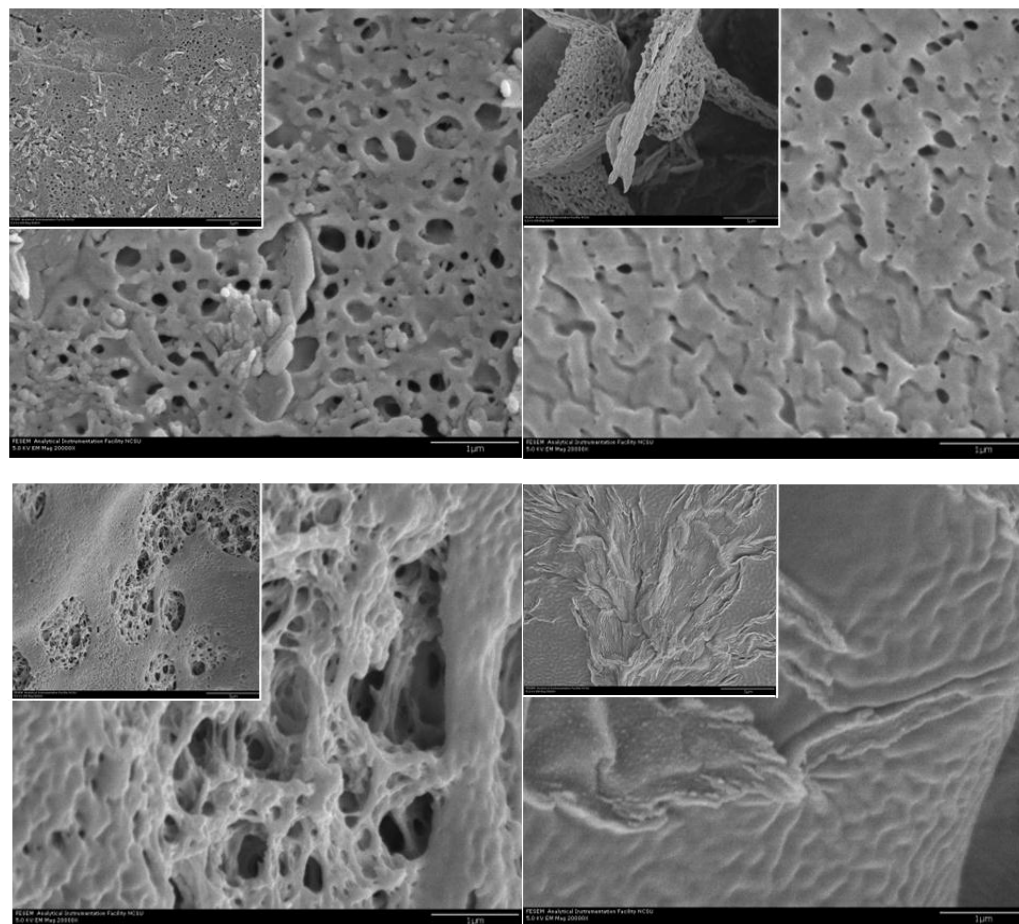


**Figure 3.** SEM images of xylan based hydrogels with xylan to HEMA of 60:40 (Top: non-acetylated xylan (left DS of 0.10 and right 0.46) and Bottom acetylated xylans (left DS of 0.10 and right 0.23))

The rheological properties are strongly related to the number of effective intermolecular cross-links formed in the hydrogels as has been suggested from previous studies.<sup>37-39</sup> Hence, the mechanical behavior of the gel depends mainly on the architecture of the polymer network. Frequency sweep tests are typically used to evaluate the stability of 3D cross-linked networks.<sup>40</sup> The rheological properties of the resulting hydrogels were studied for all different compositions. The measurements were done on the hydrogels as taken from the reaction media, and the relative water content was around 80% for all samples.

Figure 4 shows the rheological properties (storage moduli,  $G'$ , and loss moduli,  $G''$  and viscosity) of hydrogels based on acetylated or non-acetylated xylans having different DS as a function of the applied oscillating frequency.  $G'$  and  $G''$  of all hydrogels obtained from non-acetylated xylans exhibited a frequency-independent behavior at very low frequencies (in the range of 0.01-2 Hz for low DS and 0.01-1Hz for high DS) which is indicative of a stable, cross-linked network. However, at higher frequencies, all hydrogels showed an increase in  $G'$  and  $G''$ , and this behavior is more striking in the case of high DS and/or low xylans content (40%). Moreover, higher cross-linking density, resulting from higher DS or lower xylans content (because the same amount of the co-monomer was used), contributes to a sharp increase in the modulus. In fact, at higher frequencies, polymer chains, in highly cross-linked networks, fail to rearrange themselves rapidly upon the imposed stress and therefore stiffen up. Similarly, the change of the viscosity upon the applied stress demonstrated the same trend. The rheological properties of the resulting hydrogels seem to be also greatly influenced by the presence of the acetyl groups. Indeed, a significant increase in the stiffness of the hydrogels was observed because the storage modulus increased more than 1000-fold from approximately 0.6 MPa to more than 390 MPa in the case of hydrogels made with a high amount (60%) of highly substituted xylans (0.46 for non-acetylated vs 0.23 for acetylated). For all samples, the storage shear modulus  $G'$  is higher than the loss shear modulus  $G''$  over the entire frequency range which indicates that the elastic response of the material is stronger than the viscous response. In addition, the elastic modulus of the acetylated xylan based hydrogels exhibited a predominantly frequency-independent profile, especially those made from highly substituted xylans, throughout the range of applied frequencies which confirm their solid-like gel structures. Indeed, similar results were reported with hydrogels based on acetylated

galactoglucomannan extracted from softwood (*Picea abies*).<sup>41</sup> Acetylated xylan based hydrogels are mildly cross-linked networks with a large free volume that allows them to respond nearly instantaneously and reversibly to external stresses with a rapid rearrangement of the polymer segments. When comparing the same DS and the same HEMA content, gels made with acetylated xylans appear to be more stiff and their  $G'$  demonstrates a frequency independence compared to those made with non-acetylated xylans that convincingly demonstrates their mildly cross-linked architecture even at the same DS.

This peculiar behavior is most likely related to the occurrence of the entanglement of xylan chains when acetyl groups are absent. Quite possible there exists a contribution of water molecules to such an entanglement-driven gelation in the case of non-acetylated xylans. Indeed, it is well known that through hydrogen bonding water molecules can be absorbed to xylan chains. These water molecules induce self-assembling of the backbone of xylan in a three-fold, left-handed conformation.<sup>42, 43</sup> Such helix forming phenomenon is well described in several other polysaccharides like  $\beta$ -(1 $\rightarrow$ 3)-linked D-xylans,<sup>44</sup> and  $\beta$ -(1 $\rightarrow$ 3)-linked D-glucans.<sup>45-47</sup> In the case of xylan-based hydrogels, the presence of bonded water molecules may contribute to the cross-linking which “indirectly” increases the density of network junction points in the case of non-acetylated xylan based hydrogels. The presence of acetyl groups in the case of acetylated counterparts prevents such absorption. The amount of bounded water was in fact estimated by DSC measurements and as reported in Table 1, the total content of non-freezable bound water (bounded to HEMA copolymer and xylan backbone), is slightly higher in the case of non-acetylated xylans for hydrogels prepared under the same conditions (DS and HEMA content) which to a great extent confirms the earlier hypothesis.

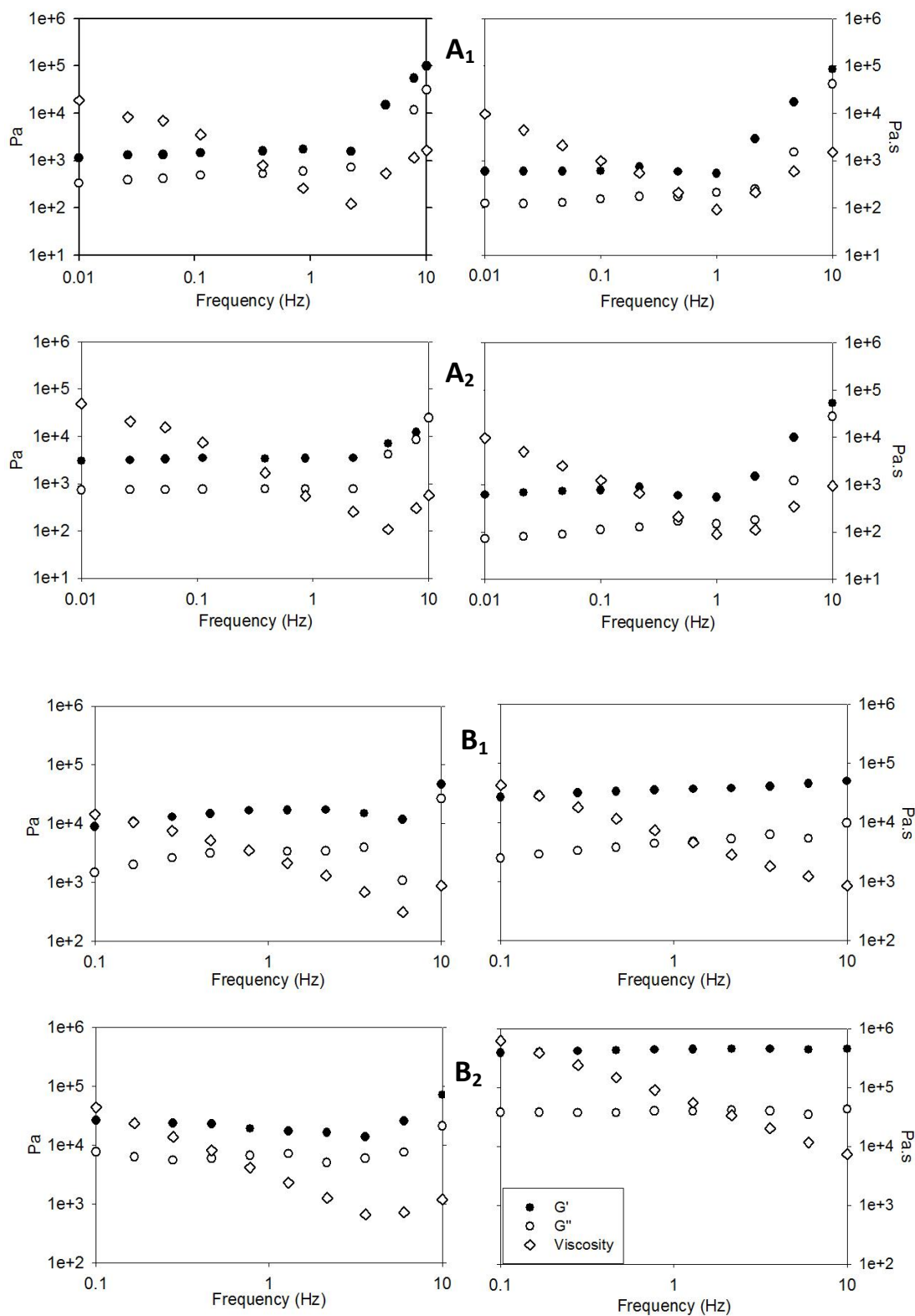


**Figure 4:** Rheological behavior of hydrogels based on (A<sub>i</sub>) non-acetylated (left DS=0.10 and right DS=0.46) (B<sub>i</sub>) acetylated (left DS=0.10 and right DS=0.23) xylans with different xylan:HEMA ratios (*i*=1, 40:60 and *i*=2, 60:40).

### *Swelling behavior*

The cross-linking density of the network seems to also affect the water uptake (swelling) behavior of the hydrogels; a less dense network confers more free volume to hydrogels and consequently the ability to absorb more water. The swelling behavior of a hydrogel is an important parameter for drug release because it determines the optimal concentration of the drug loading. To check the stability of the hydrogels regarding the dissolution caused by hydrolysis of esters bounds,<sup>35</sup> the gels were immersed in water at 37°C for 15 days. The swelling ratio was recorded from 0.25 hours to 24 hours of immersion in water at 37°C. As expected for polymethacrylate esters hydrogels, the hydrogels produced were very stable and no dissolution was observed in any of the hydrogels, as expected according to previous work.<sup>9</sup> Figure 5 shows the results of the swelling behavior of hydrogels made from different types of xylans having various DS. These results demonstrate that all gels swell, by immersion in water medium, very quickly as they reach equilibrium after approximately only 1 hour. However, the extent of the swelling seems to be greatly affected by the type and DS of xylans and consequently the density of the hydrogel network. As expected, non-acetylated xylan-based hydrogels were able to uptake more water than their acetylated counterparts as evidenced by the swelling ratio (Qs) reaching up to 4-fold. In fact, the presence of the acetyl groups confers a hydrophobic character to the hydrogels and consequently prevents water absorption. The swelling ratio obtained for the acetylated xylan is comparable to what has been reported for the acetylated galactoglucomanan. Conversely, the DS of the xylan does not appear to affect strongly the swelling behavior of hydrogels made from acetylated xylans. However, hydrogels made with low DS exhibit higher water swelling in the case of non-acetylated xylans. These findings reflect that a decrease density of the hydrogel network resulting from low DS lead to gels with large free volumes which enable them to absorb more water if their hydrophilic-hydrophobic balance is not severely compromised by the presence of substituents such as acetyl groups.

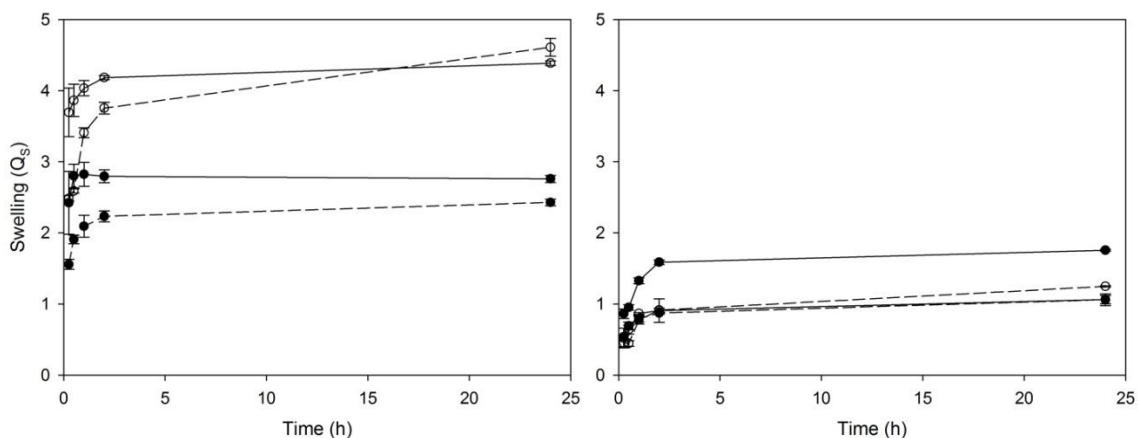


**Figure 5.** Variation of swelling ratios versus time of hydrogels based on non-acetylated (left) and acetylated (right) xylans (solid line 40:60 and dashed line 60:40 of xylan:HEMA and (○) DS 0.1 (●) DS 0.46 for non-acetylated or 0.23 for acetylated xylan, respectively) (average  $\pm$  SD,  $n=2$ )

#### *Post-acetylated xylan based hydrogels*

In order to confirm the effect of the acetyl groups on hydrogel properties, non-acetylated xylans, previously extracted with alkali solution, were post-acetylated with acetic anhydride in presence of pyridine. The success of the acetylation was confirmed by  $^1\text{H-NMR}$ , as shown in Figure 6B, and the achieved degree of acetylation was of 0.38 as determined by NMR.

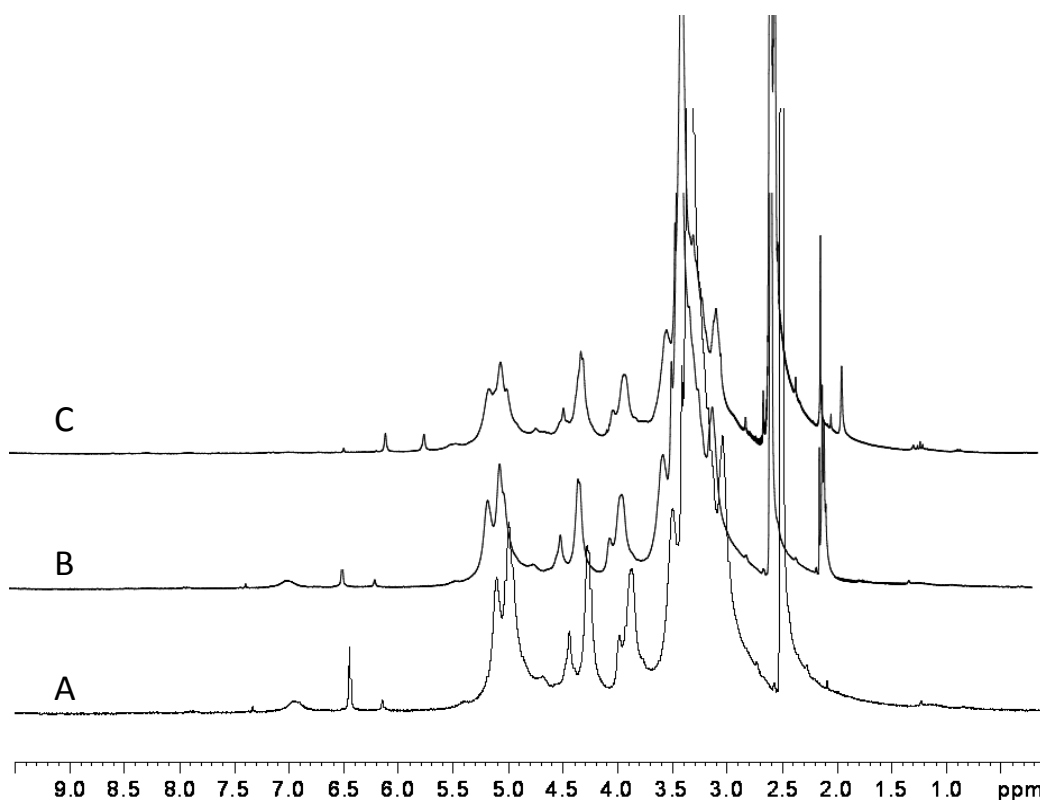


**Figure 6.**  $^1\text{H}$ -NMR spectra of (A) unmodified, (B) post-acetylated and (C) HEMA-Im-modified non-acetylated xylans.

Hydrogels were produced from post-acetylated xylans by following the same route previously described. They were first modified by HEMA monomer and the success of this grafting was also confirmed by NMR (see Figure 6C). The modification of xylan with HEMA-Im was carried out to achieve the same  $\text{DS}_{\text{HEMA}}$  of 0.10. Hydrogels were further prepared based on the previous modified post-acetylated xylans and only the hydrogel composition xylan:HEMA ratio was 60:40 was studied. The hydrogels made from the post-acetylated xylans present a macroscopic consistency similar to those prepared from acetylated xylans. Although the degree of acetylation obtained by the post reaction is less than for naturally acetylated xylans, based on the quantitative acetyl groups determined by  $^1\text{H}$  NMR, rheological measurements reported in Figure 7A showed clearly a behavior unlike what has been previously seen in the case of hydrogels based on naturally acetylated xylans (Figure 4B<sub>2</sub> left). In fact the  $G'$  and  $G''$  exhibited a predominantly frequency independent behavior in addition to a great increase of the stiffness ( $G' = 16.9$  MPa) compared to hydrogels based on non-acetylated xylans ( $G' = 3.1$  MPa). Likewise, the swelling behavior of hydrogels based on post-acetylated xylans is similar to the naturally

acetylated xylans based hydrogels as the water uptake leveled off below  $Q_s=2$  compared to more than  $Q_s=4$  obtained in the case of non acetylated xylans based hydrogels. These results confirm clearly the effect of acetyl groups of the physical properties of the xylan based hydrogels.

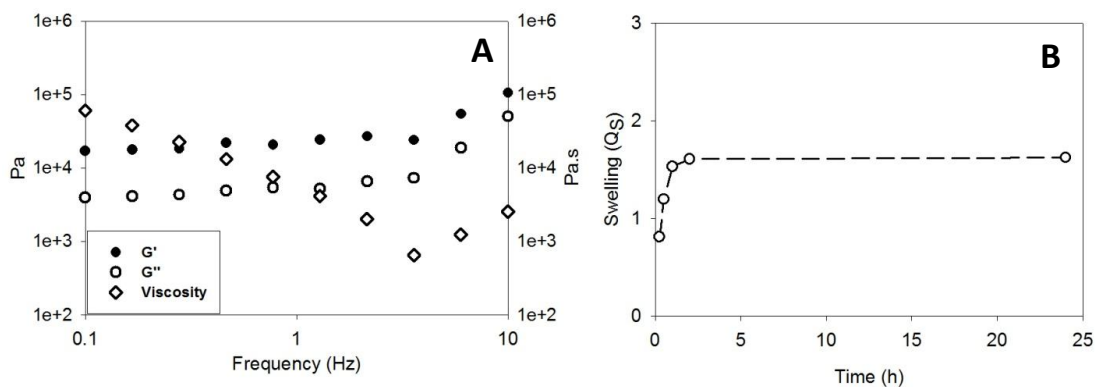


**Figure 7.** A) Rheological behavior and B) variation of swelling ratio versus time of hydrogels based on post-acetylated xylan ( $DS_{\text{HEMA}}= 0.10$  and xylan:HEMA ratio 60:40)

### *Drug release*

The release of doxorubicin from different xylan-based hydrogels was investigated under simulated pH that closely approximated the gastrointestinal tract environment. Thus, two representative pH were used, namely 7.0 and 2.5 for the release study and the results are depicted in Figure 8.

The two types of hydrogels showed different profiles as hydrogels made from non-acetylated xylans leveled off between 30-60% depending on the DS and xylan content used. This behavior is directly opposed to what was observed for hydrogels made from acetylated xylans in which more than 80% of drug was released for high DS and high xylan content. This effect may be attributed to the diffusion of the drug caused by rapid gel swelling and also the release of drug that is adsorbed towards the surface of the gel matrix.<sup>48</sup> This drug adsorption could be reduced by the presence of acetyl groups which enhance its delivery from hydrogels derived from acetylated xylans. The higher and faster release of doxorubicin in low DS hydrogels may also be explained because of the presence of larger pores, observed by SEM, especially in acetylated hydrogels.<sup>49</sup>

The ratio of doxorubicin released was not affected by changing the pH; however, the release rate from all hydrogels was faster at lower pH and two reasons for this behavior could be posited: 1) less stability of xylans at lower pH and 2) protonation of the hydroxyl groups of the xylan at lower pH accelerates the swelling, consequently accelerating the release of doxorubicin. Similar behavior was reported in hydrogels based on polyethylene glycol (PEG).<sup>50</sup>

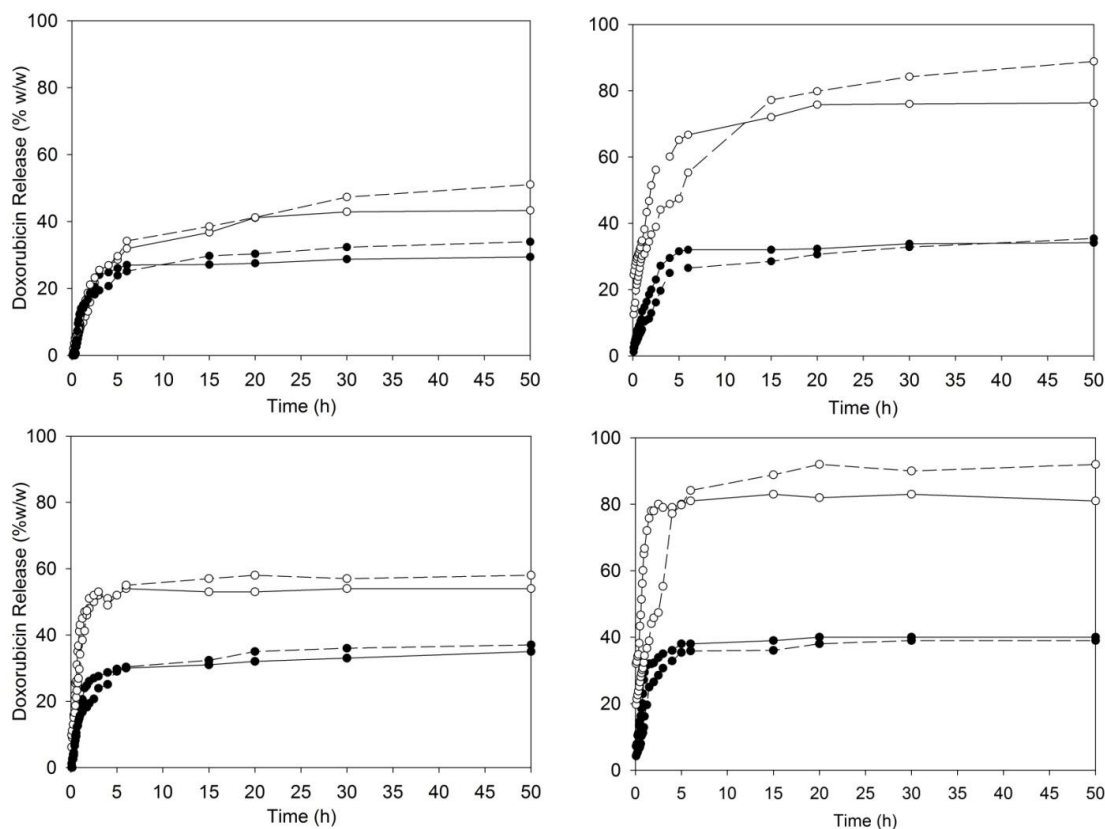


**Figure 8.** Doxorubicin release from non-acetylated xylan (left) and acetylated xylan (right) based hydrogels as function of time in different pH (top pH 7 and bottom pH 2.5) (solid line 40:60 and dashed line 60:40 of xylan:HEMA and (○) DS 0.1 (●) DS 0.46 for non-acetylated or 0.23 for acetylated xylan respectively)

## Conclusion

In this work, it was demonstrated the success of preparing hydrogels from xylan, the most abundant non-cellulosic-based polysaccharide found in the plant kingdom, but also the overall richness/tunability of the delivery system based on the chemical functionality of the substrate. This renewable resource was extracted from *E. urograndis*

by two different processes that ultimately provided xylans with and without acetyl moieties. Subsequently, xylan/Poly(2-hydroxyethylmethacrylate)-based hydrogels were prepared after facile crosslinking induced by methacrylic monomers using standard radical polymerization. Herein is demonstrated for the first time the effect of xylan-based acetyl substituents on the morphology and physical properties of a novel polysaccharide-based hydrogel biomaterial which was also confirmed by the post-acetylation of non acetylated xylans. Most importantly, the presence of acetyl groups introduced compactness and high stiffness to the hydrogels which ultimately reduced their water swelling capacity and moreover, significantly enhanced their drug release properties as evidenced by the time release profile obtained for a representative drug, i.e., doxorubicin.

## **Material and Methods**

*Materials.* Doxorubicin Hydrochloride (99%) was purchased from Tocris Bioscience, N,N'-carbonyldiimidazole (CDI, 97%), 2-hydroxyethylmethacrylate (HEMA, 99%), triethylamine (TEA, 99.5%), ammonium peroxodisulfate (98%), sodium perodisulfate (98%), sodium sulfate (99%), potassium hydroxide (99%), hydrogen peroxide (30%) were all obtained from Sigma-Aldrich. Acetic acid (99.5%) and formic acid (99%) were purchased from Acros Organics. All reagents were used as received. Organic solvents (dimethylsulfoxide (DMSO, 99.5%), ethyl acetate (99%), anhydrous chloroform, ethanol (99%), methanol (99%), acetone (99.9%) were all obtained from Sigma-Aldrich and used as received without any further purification.

*Isolation of xylans.* The xylans used in this work were extracted from hardwood *Eucalyptus urograndis* specimens. First, extractives-free sawdust of wood samples were subjected to delignification with peracetic acid solution (pH 4.5) at 15%, as previously published,<sup>51</sup> to yield so-called holocellulose. Acetylated xylans were solvent-extracted from the holocellulose by DMSO (1:25 (w/v) holocellulose-to-DMSO ratio) at 50°C, for 12 h, with stirring under nitrogen atmosphere. The DMSO dissolved xylans were acidified with formic acid to pH 2 and precipitated with an excess of ethanol. The xylans were then recovered by centrifugation, washed extensively thoroughly with methanol in order to remove DMSO and dried at room temperature under vacuum. Non-acetylated xylans were alkali-extracted from the holocellulose by using KOH solution (24%) at room temperature, for 24 h, with stirring under nitrogen atmosphere. After acidification to pH 2, the extracted

xylans were recovered as previously described. Xylan chemical structure from eucalyptus is shown in Figure A3.1 (appendix).

*Xylan Acetylation:* Acetylation of the xylan extracted with alkali was carried out with pyridine: acetic anhydride (1:1) at 25°C for 48 hours.<sup>52</sup> The acetylated xylans were recovered by evaporation of the acetylation mixture several times (pyridine/Ac<sub>2</sub>O) with ethanol.

*Sugar analyses.* Sugar compositions of the extracted xylans were determined by high performance liquid chromatography (HPLC) analysis after acid hydrolysis of the polymers. Xylans were first pre-hydrolyzed by 72% (w/v) sulfuric acid at room temperature during 2h followed by sulfuric acid (4% w/v) catalyzed hydrolysis at 120°C during 1h.<sup>53</sup> The resulting solutions were diluted with ultra-pure water to the desired concentration and filtered through 0.2 µm nylon filter (Milipore, Billerica, MA) before chromatography analysis. They were then analyzed by using a Dionex ICS 3000 IC system equipped with a CarboPac PA1 cartridge, eluent generator (EG50) and electrochemical detector (ED50). The mobile phase was 18 mM hydroxide (OH<sup>-</sup>) and all analyses were conducted with a column temperature of 25°C.

*Size Exclusion Chromatography (SEC).* The isolated xylans were dissolved in a small amount of 8% LiCl solution in N,N-dimethylacetamide (DMAC) HPLC grade at 70-80 °C and further diluted with DMAC to a concentration of about 0.4%. The SEC analysis was carried out by PL-GPC 110 system (Polymer Laboratories, UK) equipped with four PLgel 10µm MIXED B 300x7.5 mm columns and pre-column type PLgel 10µm. The columns, injector and Infra-red detector were maintained at 80°C during the analysis. The eluent (0.5% LiCl solution in DMAC) was pumped at a flow rate of 1.0 mL/min. The analytical columns were calibrated with pullulan standards (Polymer Laboratories) in the range 0.8-100 kDa.

*Hydrogel Synthesis.* Xylan-based hydrogels were prepared through a three-step procedure.<sup>34, 54, 55</sup> Figure A.3.2 (Appendix) shows a scheme followed for producing hydrogels. The first step involves the preparation of 2-[(1-imidazolyl)formyloxy]ethyl methacrylate (HEMA-Im) which was synthesized as already reported by Ranucci et al.<sup>56</sup> by reacting 20.3g (156 mmol) of 2-hydroxyethyl methacrylate (HEMA) with 50.67 g (312 mmol) of N,N'-carbonyldiimidazole (CDI) in 80 mL of anhydrous CHCl<sub>3</sub> at room temperature during 1h. The organic phase was then neutralized and washed with several

portions of water and dried over  $\text{Na}_2\text{SO}_4$  before removing the solvent. HEMA-Im was, in the second step, covalently coupled with the xylans. Briefly, 1.5 g of each xylan and 2.0 g of HEMA-Im were dissolved in 60 mL of DMSO under stirring. 250  $\mu\text{L}$  of triethylamine was added to initiate the reaction and the mixture was left at  $50^\circ\text{C}$  under stirring during time period between 6 and 120 h depending on the targeted degree of substitution (DS). The product was precipitated in ethyl acetate, extensively washed and centrifuged and finally dried. The DS was determined by  $^1\text{H-NMR}$  spectroscopy as described below (see Table 1).

Finally, xylan-based hydrogels were prepared with different compositions using HEMA as a co-monomer. Hydrogels with two weight ratio of xylans to HEMA (60:40 and 40:60) were prepared. In a typical experiment, prescribed amount of xylans was dissolved in small volume of deionized water and the corresponding amount of HEMA was added, and the resulting mixture then was thoroughly stirred. Catalytic amounts of water solutions of ammonium peroxodisulfate and sodium pyrosulfite were then added to initiate the cross-linking and solution was transferred quickly to a cylindrical mold before gelation. The mold was sealed with Parafilm<sup>TM</sup> and the mixture was left at room temperature for at least 6 h before analysis. The incorporation of doxorubicin was realized simultaneously with the cross-linking by adding the desired amount of doxorubicin to the mixture before initiating the cross-linking. No crosslinking of the doxorubicin was detected based on the chemistry of the crosslinking reaction and gravimetric experiments.

*$^1\text{H-NMR}$  Measurements.* Modified and unmodified xylans were dissolved in  $\text{D}_2\text{O}$  or  $\text{DMSO-}d_6$  spectra were recorded on an AC 500 MHz Bruker spectrometer at 303K in a 5 mm o.d. tube (internal acetone  $^1\text{H}$  ( $\text{CH}_3$ ) at 2.1 ppm relative to  $\text{Me}_4\text{Si}$ ). The DS of modified xylans was determined from  $^1\text{H-NMR}$  spectra. For that, the area of the acetyl peak ( $\delta$  2.0 ppm – 3H), 4-O-methyl glucuronic acid peak (4-O-MeGlcA) ( $\delta$  5.3 ppm – 1H) and vinyl C-H peaks ( $\delta$  5.71 and  $\delta$  6.05 ppm – 1H each) were integrated; the obtained value for the vinyl peaks were relating to the acetyl peak for acetylated xylan and to the 4-O-MeGlcA peak for non-acetylated xylan. The DS of the non-acetylated xylan was determined in  $\text{D}_2\text{O}$  due to the quality of the 4-O-MeGlcA peak.

*Hydrogel Swelling ratio measurements.* Gels were previously freeze-dried, and then they were immersed in an excess of deionized water at  $37^\circ\text{C}$ . At various time, the samples were withdrawn from the water medium and weighed. The swelling,  $Q_s$ , was then calculated

from:  $Q_s=(W_s-W_d)/W_d$ , where  $W_d$  is the weight of the dry gel prior to swelling and  $W_s$  is the weight at the swollen state.

*Scanning Electron Microscopy (SEM).* The morphology of the hydrogels was controlled by field emission scanning electron microscopy (FE-SEM) using a JEOL 6400F microscope operated with an accelerating voltage of 5 kV and a working distance of 15 mm, and a 30  $\mu$ m objective aperture. A small hydrogel sized sample was affixed onto conductive carbon tape and mounted on the support and then sputtered with an approximately 25 nm layer of gold/palladium (60/40).

*Bounded water content.* Non-freezable bound water content ( $W$  in the swollen hydrogel) was determined using differential scanning calorimetry (TA Instruments DSC Q100). Portions of hydrogels (5-10 mg) were cut from the pre-equilibrated swollen gels, placed in the pre-weighted aluminum pan, sealed, cooled to  $-20^\circ\text{C}$  and maintained at temperature for 5 min. The temperature was raised to  $-10^\circ\text{C}$  at a heating rate of  $1^\circ\text{C}/\text{min}$  and the sample was maintained isothermally until the heat flow returned to the baseline value. Subsequent heating steps to higher temperatures ( $-5, 0, 5^\circ\text{C}$ ) were then successively performed. The free and freezable water content ( $W_f$ ) was calculated from the sum the endothermic enthalpies corresponding to the melting of water by using the following equation:

$$W_f = \Delta H \times (1 + W_t) / \Delta H_w$$

where  $W_f$  is the free and freezable water content,  $W_t$  total water content estimated by gravimetry after the swollen of the gels,  $\Delta H$  is the sum of enthalpies from the DSC thermogram. The value of  $\Delta H_w$  is the melting enthalpy of pure water at the corresponding fusion temperature and can be estimated using the following equation:

$$\Delta H_w = \Delta H_w^0 - \Delta c_p \Delta T$$

where  $\Delta H_w^0$  is the pure water enthalpy at  $0^\circ\text{C}$ ,  $\Delta c_p$  is the specific heat capacity between the liquid water and solid ice,  $\Delta T$  is the freezing point depression. Non-freezable bound water content ( $W_b$ ) was estimated by subtracting the free and freezable water content from the total water content:  $W_b = W_t - W_f$

*Rheological Properties.* Viscoelastic measurements for determination of  $G'$  (shear storage modulus) and  $G''$  (shear loss modulus) were performed on a StressTech model rheometer (Reologica Instruments). Cylindrical discs (diameter= 8 mm and height=4mm)

were cut from the hydrogels as prepared and the experiments were carried out by using a parallel plate geometry with a diameter of 8 mm. A dynamic frequency sweep test was performed at 25°C with each sample at 5% of strain within a frequency range from 10 to 0.1 Hz and 10 to 0.01 Hz for hydrogels made from acetylated xylans and non-acetylated xylans, respectively.

*Doxorubicin Release from Xylan-Based Hydrogels.* Drug release analysis from the hydrogels was performed after immersing the samples in a water bath at 37°C under 50 rpm stirring and where the pH was previously adjusted at pH at 2.5 and 7. Samples were withdrawn at different time intervals over a time period of 50 h of the gel to remove spontaneous released doxorubicin. The released doxorubicin (chemical structure shown in Figure A.3.3 – Appendix) was measured using a Lambda 3B UV/VIS spectrophotometer (Perkin Elmer, Norwalk, CT) at 486 nm.

## ACKNOWLEDGMENTS

We would like to gratefully acknowledge the CNPq (Conselho Nacional de Desenvolvimento Científico e Tecnológico) for the generous provision of a research fellowship to TCFS that allowed parts of this work to be realized. We would also like to acknowledge the NC State Metal Workshops for their support that helped us to develop the mold for the hydrogel. Finally, portions of this work would not have been possible without the generous support of a Higher Education Challenge Grant administered by USDA (Cooperative Agreement No. 2006-38411-17035).

## REFERENCES

1. J. Jagur-Grodzinski, *Polym. Adv. Technol.*, 2010, **21**, 27-47.
2. W. Cai and R. B. Gupta, in *Kirk-Othmer Encyclopedia of Chemical Technology (5th Ed.)*, ed. S. Arza, John Wiley & Sons, Inc, Hoboken, NJ, 2005, vol. 13, pp. 729-754.
3. T. R. Hoare and D. S. Kohane, *Polymer*, 2008, **49**, 1993-2007.
4. K. Pal, A. K. Banthia and D. K. Majumdar, *Des. Monomers Polym.*, 2009, **12**, 197-220.
5. B. V. Slaughter, S. S. Khurshid, O. Z. Fisher, A. Khademhosseini and N. A. Peppas, *Adv. Mater.*, 2009, **21**, 3307-3329.

6. J. K. Oh, D. I. Lee and J. M. Park, *Prog. Polym. Sci.*, 2009, **34**, 1261-1282.
7. M. S. Lindblad, J. Sjöberg, A.-C. Albertsson and J. Hartman, in *Materials, Chemicals, and Energy from Forest Biomass*, ed. D. S. Argyropoulos, American Chemical Society, Washington, DC, 2007, vol. 954, pp. 153-167.
8. M. Giannuzzo, M. Feeney, P. Paolicelli and M. A. Casadei, *J. Drug Delivery Sci. Technol.*, 2006, **16**, 49-54.
9. W. N. E. van Dijk-Wolthuis, J. A. M. Hoogeboom, M. J. van Steenberg, S. K. Y. Tsang and W. E. Hennink, *Macromolecules*, 1997, **30**, 4639-4645.
10. S. R. Van Tomme and W. E. Hennink, *Expert Rev. Med. Devices*, 2007, **4**, 147-164.
11. A. Barbetta, E. Barigelli and M. Dentini, *Biomacromolecules*, 2009, **10**, 2328-2337.
12. H. Park, S.-W. Kang, B.-S. Kim, D. J. Mooney and K. Y. Lee, *Macromol. Biosci.*, 2009, **9**, 895-901.
13. H. Park and K. Y. Lee, *Nat.-Polym. Biomed. Appl.*, 2008, 515-532.
14. R. A. A. Muzzarelli and C. Muzzarelli, in *Handbook of Hydrocolloids (2nd Edition)*, eds. G. O. Phillips and P. A. Williams, Woodhead Publishing Ltd., Cambridge, UK, 2009, pp. 849-888.
15. N. Bhattarai, J. Gunn and M. Zhang, *Adv. Drug Delivery Rev.*, 2010, **62**, 83-99.
16. C. Jarry and M. S. Shive, *Smart Mater.*, 2009, 10/13-10/20.
17. Y. A. Aggour, *Starch/Staerke*, 1993, **45**, 55-59.
18. W. M. Kulicke, Y. A. Aggour, H. Nottelmann and M. Z. Elsabee, *Starch/Staerke*, 1989, **41**, 140-146.
19. S. Tanodekaew, S. Channasanon and P. Uppanan, *Journal of Applied Polymer Science*, 2006, **100**, 1914-1918.
20. U. Edlund and A. C. Albertsson, *J. Bioact. Compat. Polym.*, 2008, **23**, 171-186.
21. M. S. Lindblad, E. Ranucci and A.-C. Albertsson, *Macromol. Rapid Commun.*, 2001, **22**, 962-967.
22. J. Voepel, J. Sjöberg, M. Reif, A.-C. Albertsson, U.-K. Hultin and U. Gasslander, *Journal of Applied Polymer Science*, 2009, **112**, 2401-2412.
23. A. M. Stephen, in *The Polysaccharides*, ed. G. O. Aspinall, Academic Press, Orlando, 1983, pp. 98-193.
24. K. C. B. Wilkie, *Adv. Carbohydr. Chem. Biochem.*, 1979, **36**, 215-264.

25. A. Ebringerova and Z. Hromadkova, *Biotechnol. Genet. Eng. Rev.*, 1999, **16**, 325-346.
26. M. Hashi and T. Takeshita, *Agric. Biol. Chem.*, 1979, **43**, 951-959.
27. M. Hashi and T. Takeshita, *Agric. Biol. Chem.*, 1979, **43**, 961-967.
28. I. Gabriellii and P. Gatenholm, *J. Appl. Polym. Sci.*, 1998, **69**, 1661-1667.
29. I. Gabriellii, P. Gatenholm, W. G. Glasser, R. K. Jain and L. Kenne, *Carbohydr. Polym.*, 2000, **43**, 367-374.
30. S. K. Sengupta, in *Cancer Chemotherapeutic Agents*, ed. W. O. Foye, American Chemical Society, Washington DC, 1995, pp. 205-218.
31. D. Evtuguin, J. Tomás, A. S. Silva and C. Neto, *Carbohydr. Res.*, 2003, **338**, 597-604.
32. A. d. S. Magaton, D. Piló-Veloso and J. L. Colodette, *Química Nova*, 2008, **31**, 1085-1088.
33. A. Teleman, J. Lundqvist, F. Tjerneld, H. Stålbrand and O. Dahlman, *Carbohydr. Res.*, 2000, **329**, 807-815.
34. A. A. Roos, U. Edlund, J. Sjöberg, A.-C. Albertsson and H. Stålbrand, *Biomacromolecules*, 2008, **9**, 2104-2110.
35. W. N. E. van Dijk-Wolthuis, M. J. van Steenbergen, W. J. M. Underberg and W. E. Hennink, *Journal of Pharmaceutical Sciences*, 1997, **86**, 413-417.
36. J. Voepel, J. Sjöberg, M. Reif, A.-C. Albertsson, U.-K. Hultin and U. Gasslander, *J. Appl. Polym. Sci.*, 2009, **112**, 2401-2412.
37. G. M. Kavanagh and S. B. Ross-Murphy, *Prog. Polym. Sci.*, 1998, **23**, 533-562.
38. S. B. Ross-Murphy, *Polym. Gels Networks*, 1994, **2**, 229-237.
39. S. B. Ross-Murphy, *Polym. Networks*, 1998, 288-315.
40. K. S. Anseth, C. N. Bowman and L. Brannon-Peppas, *Biomaterials*, 1996, **17**, 1647-1657.
41. M. Söderqvist Lindblad, A.-C. Albertsson, E. Ranucci, M. Laus and E. Giani, *Biomacromolecules*, 2005, **6**, 684-690.
42. H. Chanzy, M. Dube and R. H. Marchessault, *Polymer*, 1979, **20**, 1037-1039.
43. I. Nieduszynski and R. H. Marchessault, *Biopolymers*, 1972, **11**, 1335-1344.
44. H. Saito, J. Yamada, Y. Yoshioka, Y. Shibata and T. Erata, *Biopolymers*, 1991, **31**, 933-940.

45. H. Saito, M. Yokoi and Y. Yoshioka, *Macromolecules*, 1989, **22**, 3892-3898.
46. H. Saito, Y. Yoshioka, M. Yokoi and J. Yamada, *Biopolymers*, 1990, **29**, 1689-1698.
47. H. Saito, M. Yokoi and J. Yamada, *Carbohydr. Res.*, 1990, **199**, 1-10.
48. K. L. Shantha and D. R. K. Harding, *Int. J. Pharm.*, 2000, **207**, 65-70.
49. P. M. de la Torre, Y. Enobakhare, G. Torrado and S. Torrado, *Biomaterials*, 2003, **24**, 1499-1506.
50. H. Saito, A. S. Hoffman and H. I. Ogawa, *J. Bioact. Compat. Polym.*, 2007, **22**, 589-601.
51. D. Evtuguin, J. Tomás, A. S. Silva and C. Neto, *Carbohydrate Research*, 2003, **338**, 597-604.
52. E. Adler, G. Brunow and K. Lundquist, *Holzforschung*, 2009, **41**, 199-207.
53. T. Ehrman, *Method for determination of acid-soluble lignin in biomass.*, National Renewable Energy Laboratory, Golden, CO., 1996.
54. M. Soderqvist Lindblad, A.-C. Albertsson, E. Ranucci, M. Laus and E. Giani, *Biomacromolecules*, 2005, **6**, 684-690.
55. M. S. Lindblad, E. Ranucci and A.-C. Albertsson, *Macromolecular Rapid Communications*, 2001, **22**, 962-967.
56. E. Ranucci, G. Spagnoli and P. Ferruti, *Macromolecular Rapid Communications*, 1999, **20**, 1-6.

## CHAPTER 4

### A FACILE APPROACH FOR THE SYNTHESIS OF XYLAN-DERIVED HYDROGELS

*Teresa C. Fonseca Silva,<sup>1,2</sup> Ilari Filpponen,<sup>2</sup> Youssef Habibi,<sup>2</sup> Jorge Luiz Colodette,<sup>1</sup> and  
Lucian A. Lucia<sup>2</sup>*

<sup>1</sup>Departamento de Química, Universidade Federal de Viçosa, Viçosa, MG, 36570-000;  
Brazil

<sup>2</sup>Laboratory of Soft Materials & Green Chemistry, Department of Forest Biomaterials,  
North Carolina State University, Raleigh, North Carolina 27695-8005

E-mail: [lucian.lucia@ncsu.edu](mailto:lucian.lucia@ncsu.edu)

**Abstract.** Xylan polysaccharides from *Eucalyptus urograndis* wood were obtained by controlled extraction processes in order to obtain them with and without acetyl groups. Xylans extracted were structurally characterized by NMR and subsequently used without previous modification to prepare xylan/Poly(2-hydroxyethylmethacrylate)-based hydrogels in one-step by radical polymerization of HEMA. Heteronuclear 2D NMR (HSQC) confirmed traces of lignin, probably from the forming lignin carbohydrate complex (LCC). The generation of double bonds mainly in lignin fragments during the delignification step with peracetic acid (PAA) under mild conditions was the justification for the crosslinking. The hydrogels were produced using two composition ratios of xylan to HEMA (60:40 and 40:60) and further characterized by means of their morphology, swelling and rheological properties. The presence of acetyl groups leads to reduced capacity for water uptake. All hydrogels showed great homogeneity, elasticity and softness.

**Keywords:** hardwoods; hydrogels; renewable resources; xylans

## Introduction

Hydrogels are three-dimensional stable networks formed from cross-linked hydrophilic polymers to form insoluble polymeric materials.<sup>[1, 2]</sup> They have received increasing interest over the last several years in part due to their hydrophilicity, soft tissue-mimicking consistency, high permeability to metabolites and oxygen, and resilience. Furthermore, hydrogels have been the material of choice for such applications as witnessed by work in cartilage or tendons, in bio-adhesives, in tissue engineering, as ocular lenses, or as drug delivery matrices.<sup>[3-5]</sup>

Natural polysaccharide-based hydrogels are currently attracting much interest for their fundamental properties such as tunable functionality, biocompatibility, and high degree of swelling<sup>[6]</sup>. We have demonstrated recently the overall richness/tunability of the delivery system based on the chemical functionality of xylan polysaccharide. Moreover, xylan-based acetyl substituents have effect on the morphology, rheology and swelling of this polysaccharide-based hydrogel biomaterial.<sup>[7]</sup>

Although various polysaccharides have been investigated for hydrogel formulations, hemicelluloses have significant potential as a material resource for hydrogels preparation.<sup>[7, 8]</sup> Xylans are the most common hemicelluloses and considered to be the major noncellulosic cell wall polysaccharide component of angiosperms.<sup>[9]</sup> Indeed, xylans' structure exhibits a  $\beta$ - (1 $\rightarrow$ 4) linked D-xylosyl backbones, with various side groups or chains attached to the O-2 and/or O-3 of the xylosyl residues depending on the species and/or the extraction method. Different xylan structures are shown in Figure 1. These side chains mainly consist of  $\alpha$ -D-glucuronic acid, 4-O-methyl- $\alpha$ -D-glucuronic acid and some neutral sugar units ( $\alpha$ -L-arabinofuranose,  $\alpha$ -D-xylopyranose or  $\alpha$ -D-galactopyranose). Among the common side groups are also acetyl groups, phenolic, ferulic and coumaric acids.<sup>[10]</sup> Moreover, it has been proved already the association of hemicelluloses with lignin (LCC) through covalent linkages,<sup>[11-14]</sup> which confers to the xylans versatile characteristics. Recent studies found that all lignin in wood exist chemically linked to polysaccharides and chemical treatments are not able to separate them completely and so the material properties of the polymeric hemicelluloses have not been recognized yet.<sup>[15, 16]</sup>

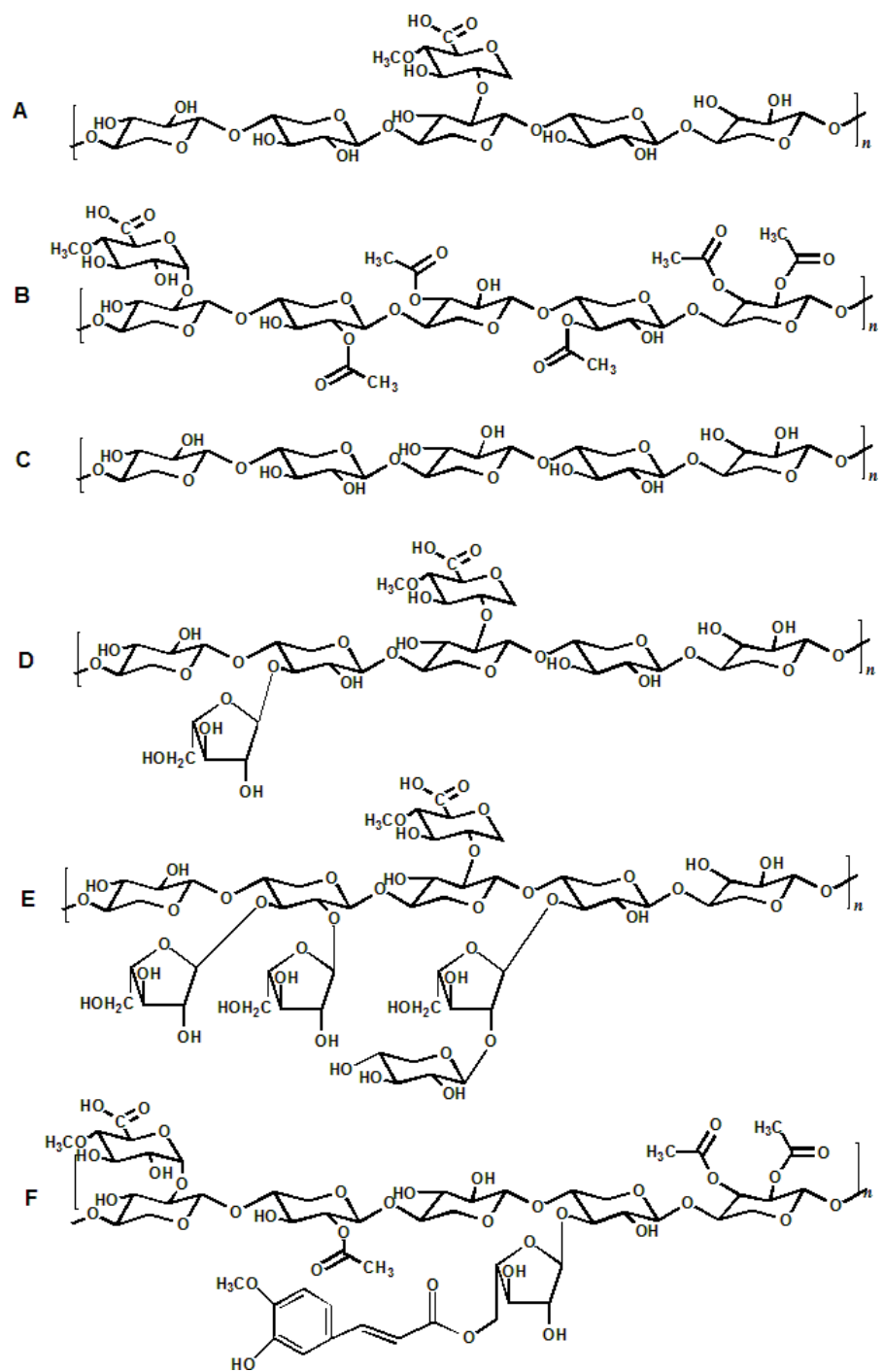


*Figure 1.* Examples of xylan structures presenting different side groups composition: A) methylglucuronic acid (MeGlcA), B) MeGlcA and acetyl groups, C) no side groups, D) MeGlcA and furanose, E) MeGlcA and furanose/xylose and F) MeGlcA, acetyl groups and furanose/lignin.

Whereas many approaches to modify polymers or even use various synthetic polymers to develop advanced gels with tailored properties have been considered, xylans themselves seem to have the potential to perform the requirements to produce such hydrogels due to their multi-branches, avoiding long and tedious process as well as the necessity to employ organic solvents sometimes under severe conditions.

Based on that, a facile one-step route hydrogel exploiting renewable resources (typical by-products from wood industry) was performed without previously grafting of vinyl groups by radical polymerization with 2-hydroxyethylmethacrylate (HEMA).

The aim of this work was to produce xylan-based hydrogels in a facile approach, using as a raw material xylans extracted from *Eucalyptus urograndis* species following two different ways in order to give xylans/hydrogels with different structural features. The obtained hydrogels were characterized in terms of their morphology, swelling and rheological properties.

## **Experimental Part**

### **Materials**

2-hydroxyethylmethacrylate (HEMA, 99%), ammonium peroxodisulfate (98%), sodium perodisulfate (98%), sodium sulfate (99%), potassium hydroxide (99%), hydrogen peroxide (30%) were all obtained from Sigma-Aldrich. Acetic acid (99.5%) and formic acid (99%) were purchased from Acros Organics. Organic solvents (ethanol (99%), methanol (99%), acetone (99.9%)) were all obtained from Sigma-Aldrich and used as received without any further purification.

### **Isolation and Characterization of Xylan**

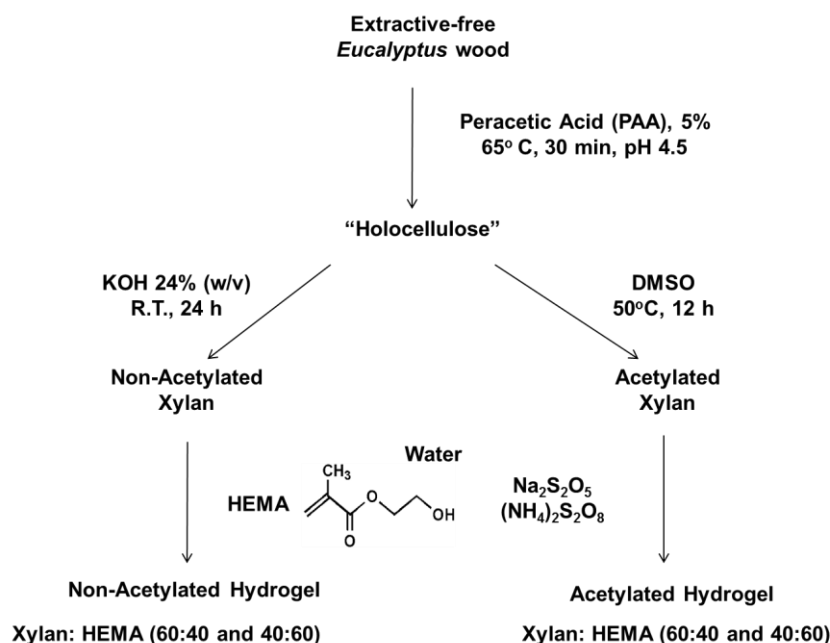
The xylans used in this work were extracted from hardwood *Eucalyptus urograndis* specimens. First, extractives-free sawdust of wood samples were subjected to delignification under mild conditions with 5% v/v peracetic acid (PAA) solution (pH 4.5), at 65°C for 30 minutes to yield so-called holocellulose. Acetylated xylans were solvent-extracted under stirring from the holocellulose by using DMSO for 12 hours at 50°C and non-acetylated xylans were alkali-extracted with KOH solution 24% (w/v) for 24 hours at room temperature according to the literature.<sup>[7]</sup>

Isolated xylans were characterized in terms of sugar composition and heteronuclear HSQC NMR. Sugar compositions were determined by high performance liquid chromatography (HPLC) analysis after acid hydrolysis of the polymers. Xylans were first pre-hydrolyzed by 72% (w/v) sulfuric acid at room temperature for 2 h followed by sulfuric acid (4% w/v) catalyzed hydrolysis at 120°C for 1 hour. <sup>[17]</sup> The resulting solutions were diluted to the desired concentration and filtered through a 0.2 µm nylon filter before chromatography analysis. They were then analyzed by using a Dionex ICS 3000 IC system equipped with a CarboPac PA1 cartridge, an eluent generator (EG50) and an electrochemical detector (ED50). The mobile phase was 18 mM hydroxide (OH<sup>-</sup>) and all analyses were conducted with a column temperature of 25°C.

<sup>1</sup>H and Heteronuclear HSQC NMR spectra were recorded on an AC 500 MHz Bruker spectrometer at 303K. Sodium 3-(trimethylsilyl)propionate-*d*<sub>4</sub> was used as internal standard (δ 0.00) and the operations conditions of NMR were set according to reported previously. <sup>[18]</sup>

### **Hydrogel Synthesis and Characterization**

Xylan-based hydrogels were prepared using HEMA as a co-monomer and varying the weight ratio of xylan to HEMA (60:40 and 40:60). In a typical experiment, 225 or 100 mg of xylan was dissolved in 1.4 mL of deionized water. Then, 150 µL of HEMA was added, and the resulting mixture was then thoroughly stirred. 30µL of water solutions of ammonium peroxodisulfate and sodium pyrosulfite, both at 2% (w/v) were then added to initiate the cross-linking and solution was transferred quickly to a cylindrical mold before gelation. The mold was sealed with Parafilm<sup>TM</sup> and the mixture was left at room temperature for at least 6 h before analysis. Scheme 1 represents the steps used for hydrogel production.



*Scheme 1.* Isolation of xylans from eucalyptus and preparation of xylan-based hydrogels.

The formed hydrogels were characterized according to their rheological properties, morphology and swelling. Rheological measurements were performed on a StressTech model rheometer (Reologica Instruments) for determination of  $G'$  (shear storage modulus) and  $G''$  (shear loss modulus). Cylindrical discs (diameter = 8 mm and height = 4 mm) were cut from the hydrogels as prepared and the experiments were carried out by using a parallel plate geometry with a diameter of 8 mm. Dynamic frequency sweep test was performed at 25°C with each sample at 5% of strain within a frequency range from 10 to 0.1 Hz for both types of xylan-based hydrogels produced.

The morphology of the hydrogels was controlled by field emission scanning electron microscopy (FE-SEM) using a JEOL 6400F microscope operated with an accelerating voltage of 5 kV and a working distance of 15 mm, and a 30  $\mu\text{m}$  objective aperture. A small hydrogel sized sample was affixed onto a conductive carbon tape and mounted on the support and then sputtered with an approximately 25 nm layer of gold/palladium (60/40).

Hydrogel swelling ratio measurements were performed by freeze-drying the gels and then immersed them in an excess of deionized water at 37°C. At various time, the samples were withdrawn from the water medium and weighted. The swelling ( $Q_s$ ), was then calculated from:  $Q_s = (W_s - W_d) / W_d$ , where  $W_d$  is the weight of the dry gel prior to swelling and  $W_s$  is the weight at the swollen state.

## Results and Discussion

### Isolation and Characterization of Xylans

First, rich-carbohydrate material, so-called holocellulose, was extracted from *Eucalyptus urograndis* by using PAA 5% for 30 minutes at 65°C and pH 4.5, as seen in Scheme 1. The mild conditions carried out for delignification aimed to produce xylan-linked lignin fragments and therefore, providing partially free double bounds that would be useful for hydrogel production. After PAA usage step, acetylated and non-acetylated xylans were obtained using DMSO at 50°C and potassium hydroxide 24% (w/v) at room temperature, respectively.

Xylans obtained were characterized by NMR (<sup>1</sup>H and 2D heteronuclear HSQC) and sugar composition. As expected, the sugar composition showed a predominance of xylose concentrations for both types of extractants with the presence of other minor monosaccharides such as glucose, mannose, rhamnose and galactose. In fact, the molar ratio of xylose to the other minor sugars detected was 0.82:0.18 for non-acetylated xylan and 0.87:0.13 for acetylated xylans, which is similar to previous results for the same xylans.<sup>[19, 20]</sup> Even after extensive purification based on solubilization-precipitation and dialysis, the xylans obtained presented signals of lignin residue, what was confirmed by the means of NMR. Both the degree of acetylation and 4-O-methylglucuronic acid (MeGlcA) contents were determined by <sup>1</sup>H-NMR and the values were approximately 0.61 and 0.10 which corroborated the values already published for this wood specie.<sup>[21]</sup> The value for MeGlcA was approximately the same for both xylans.

2D heteronuclear HSQC spectra are presented in Figure 2. Figura 2A refers to non-acetylated xylan as the acetyl group signal at  $\sim \delta$  2.0/20 ppm is absent. Previous works have demonstrated characteristics signals of xylans main chain extracted from eucalyptus between  $\sim \delta$  3.2 and 5.0 ppm in a <sup>1</sup>H NMR.<sup>[18, 20]</sup> Variations in this range may occur due to the presence of branches such as MeGlcA and acetyl groups. However, the presence of signals between  $\sim$  5.7 and 7.0 ppm clearly indicates the presence of double bounds possible found due to the presence of lignin fragments attached to xylans chain after modification during the mild delignification with PAA.

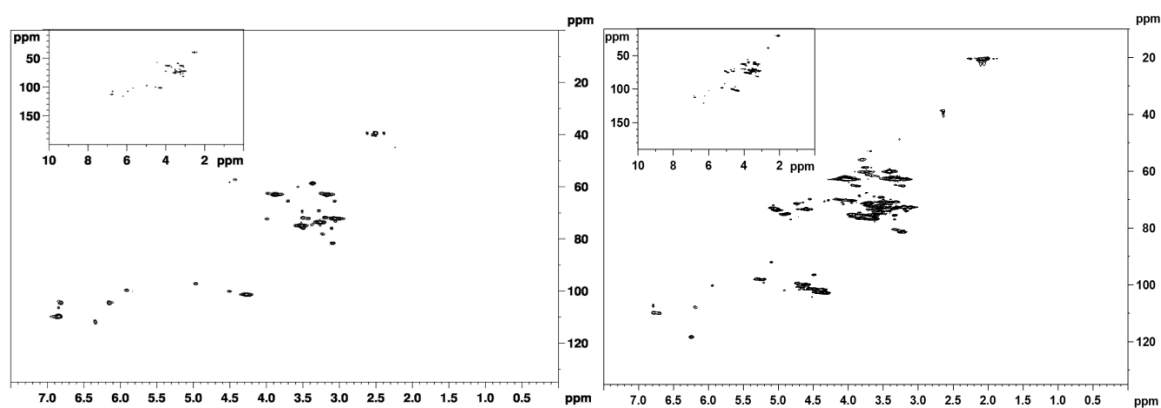


Figure 2. 2D NMR – HSQC spectra of xylans extracted from eucalyptus under mild conditions using PAA. A) Non-acetylated xylan and B) Acetylated xylan

Indeed, the reaction between PAA and wood is relatively selective for lignin and just slightly changes can be seen in carbohydrates structures. Some of the believed types of linkage between lignin-carbohydrate in wood are presented in Figure 3. [14, 22] Once these xylans' structures are mostly likely found as components of the holocellulose, their linkages persist as they are extracted, except the ester linkages when KOH 24% (w/v) is used as extractant.

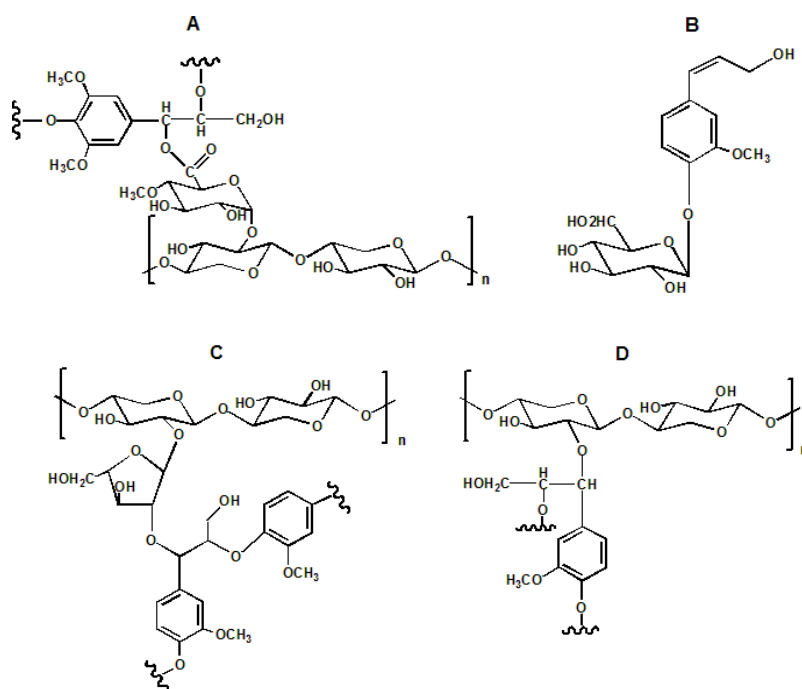


Figure 3. Main lignin-carbohydrate linkages. A) ester, B) phenyl glycoside, C) and D) benzyl ether.

Double bonds can be created mainly by reacting lignin substructures with PAA. Among these reactions, oxidative cleavage of the aromatic rings of the lignin leads to lactones (Fig. 4A) and muconic acids (Fig. 4B) as well as maleic acids (Fig. 4C). The later may be likely formed from *p*-quinones generated from the oxidation of syringyl and guaiacyl units.<sup>[23]</sup> Previous study on lignin compounds has identified vinyl-phenol and vinyl-benzene (Fig. 4D) as products of a reaction in acidic reaction with hydrogen peroxide.<sup>[24, 25]</sup> Random reactions of carbohydrates with hydroxyl radical also generate an unsaturation and a ketone introduction, promoting fragmentation of the carbohydrate main chain (Fig. 4E).

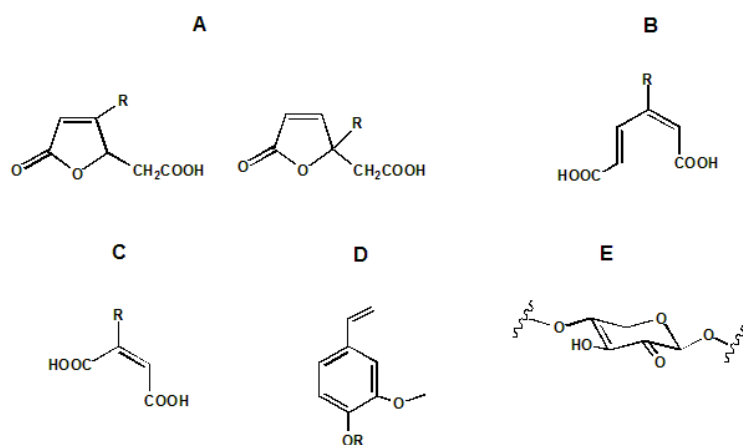


Figure 4. Some products of the reaction of lignin (A-D) and carbohydrate (E) with PAA.

HSQC spectra (Fig. 2) corroborate with the formation of unsaturated fragments as proposed in Figure 4. Signals observed at 5.9/98 ppm, 6.3/116 ppm for non-acetylated xylan (Figure 2A) and 6.0/102 ppm, 6.4/119 ppm for acetylated xylan (Figure 2B) were attributed to hydrogen linked to the double-bond carbon.

### Preparation and Characterization of xylan-based hydrogel

Four hydrogels samples were prepared using both types of xylans extracted from eucalyptus wood with two weight ratio of xylans to HEMA (60:40 and 40:60). In general, hydrogels as a class of polymeric-based materials represent a compositional motif best characterized as a 3D network and their preparation thus requires a cross-linking of polymer chains. Therefore, the generation of reactive sites to serve as junctions points for further crosslinking is required. With this in mind, the presence of fragments of lignin

covalently linked to the xylan chain would serve as a reactive site for posterior use of HEMA as co-monomer to accomplish the cross-linking and finally form a hydrogel without any modification in the xylan structure. The resulting hydrogels were examined in terms of their morphology, swelling and rheological properties.

### **Morphology and rheological properties**

The morphology provided a relatively homogenous network for the resulting hydrogels both with and without acetyl groups (Figure 5), thus contributing to the elasticity of the network.<sup>[26]</sup> The uptake water molecules hydrate and bind the most hydrophilic sites, generating homogenous distribution throughout the polymer.<sup>[27]</sup> Open structures with more free space were obtained with acetylated hydrogels whereas the non-acetylated hydrogels displayed smaller porous and agglomerates along the hydrogels network probably due to contribution of water molecules to such an entanglement-driven gelation in the case of non-acetylated xylan.<sup>[7]</sup> The ratio xylan: HEMA did not affect the morphology of the hydrogels and so, the ratio xylan: HEMA of 60:40 is displayed on Figure 5 in both cases.

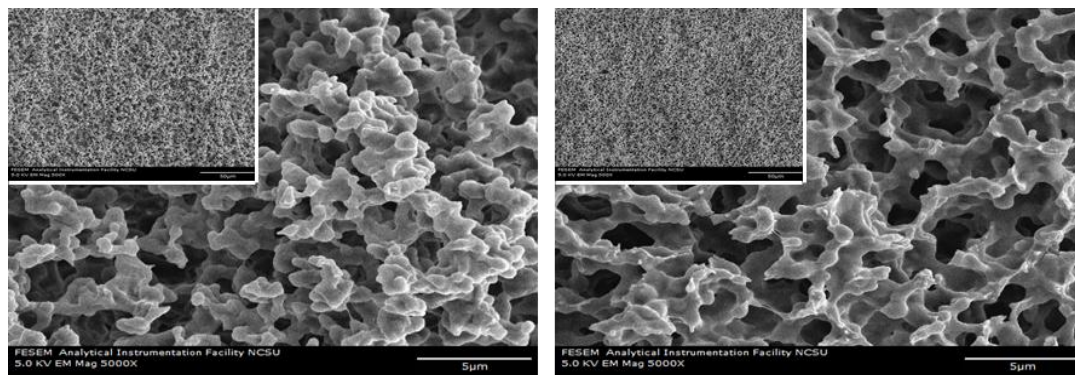


*Figure 5.* SEM images of xylan based hydrogels with xylan to HEMA ratio of 60:40. (Left: non-acetylated xylan. Right: acetylated xylan)

Rheological properties of the resulting hydrogels were studied as taken from the reaction media in all different compositions (Figure 6). For all samples, the storage modulus  $G'$  is higher than the shear modulus  $G''$  over the entire frequency range indicating that the elastic response of the material is stronger than the viscous response. In addition, all hydrogels exhibit a frequency-independent behavior at lower frequencies, indicating stable,

cross-linked network. At higher frequencies, acetylated xylan-based hydrogels maintained the behavior whereas hydrogels fabricated with non-acetylated xyans displayed an increasing in the modulus, especially at xylan: HEMA ratio of 60:40. As previously reported by our group,<sup>[7]</sup> the reason attributed for such behavior is related to a highly cross-linked polymer which would fail under stress and rapidly stiffen. Therefore, is reasonable to consider that the extraction of xyans with sodium hydroxide may better maintain and/or form more available unsaturated sites compared to the extraction carried out with DMSO at 50 °C.

Comparing both types of xyans in terms of hydrogel production, the acetyl group plays a crucial role on the rheological properties. Acetylated xylan-based hydrogels provided greater storage modulus, increasing about 10-fold in both ratios studied (40:60 and 60:40). In fact, the morphology of acetylated xylan-based hydrogels is more open and therefore, provides a large free volume and mildly cross-linked network, which allows them to respond nearly instantaneously and reversibly to external stresses with a rapid rearrangement of the polymer segments. As a result, acetylated hydrogels provided slightly higher stiffness than their counterpart and so, solid-like structures were produced.

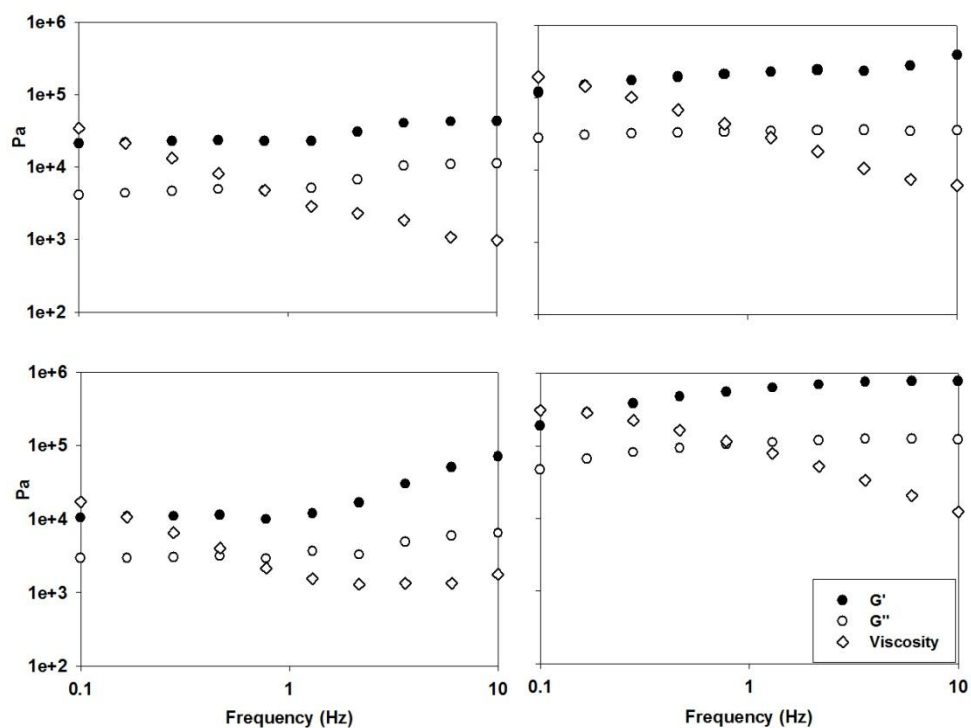
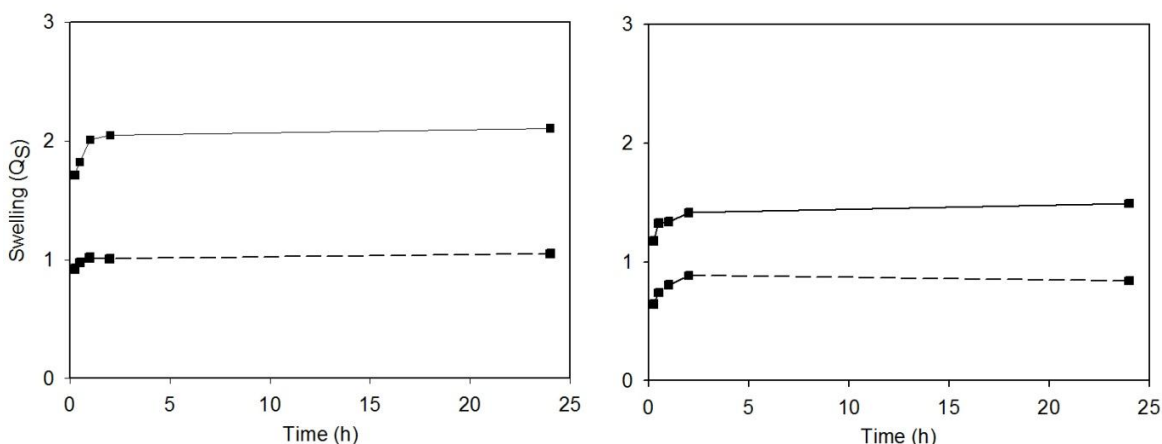


Figure 6: Rheological behaviors of hydrogels based on non-acetylated (left) and acetylated xyans (right) with different xylan:HEMA ratios (top 40:60 and bottom 60:40).

## Swelling behavior

The water uptake (swelling) of the hydrogels were also affected by the cross-linking density of the network. Open structures, with more free volume have greater ability to absorb more water. The swelling ratio was recorded from 0.25 hours to 24 hours of immersion in water at 37°C. The hydrogels produced were very stable and no dissolution was observed in any of them. Figure 7 shows the results of the swelling behavior of all hydrogels produced from different types of xylans. All the hydrogels swell very quickly (approximately one hour) after immersion in water medium. However, hydrogels produced with non-acetylated xylans were able to uptake more water than their acetylated counterparts as evidenced by the swelling ratio ( $Q_s$ ) reaching almost 2-fold. The hydrophobicity of the acetylated xylan based-hydrogels might be attributed to the presence of acetyl groups which prevents water absorption. Different ratios also affect the swelling of the hydrogels. For both acetylated and non-acetylated based hydrogels, less amount of xylan (40%) caused greater water uptake and this effect is more striking in the case of non-acetylated xylans.



*Figure 7:* Variation of swelling ratios versus time of hydrogels based on non-acetylated (left) and acetylated (right) xylans (solid line 40:60 and dashed line 60:40 of xylan:HEMA)

## Conclusion

Hydrogels were successfully prepared from eucalyptus xylan (with and without acetyl groups) in a facile approach induced by methacrylic monomers using standard radical polymerization. Delignification step was performed with PAA under mild conditions generating open quinoidal structures attached to the xylan chain that were the starting structures proposed for radical polymerization using HEMA as a co-monomer.

The presence of acetyl groups provided open hydrogel network, slightly stiff hydrogels and reduced their water swelling capacity.

**Acknowledgements:** We thank the *CNPq (Conselho Nacional de Desenvolvimento Científico e Tecnológico)* for the generous provision of a research fellowship to TCFS. We would also like to thank Dr. *Hanna S. Gracz* for the assistance with the NMR experiments.

## References

- [1] J. Jagur-Grodzinski, *Polym. Adv. Technol.* **2010**, *21*, 27.
- [2] W. Cai, R. B. Gupta, "Hydrogels", in *Kirk-Othmer Encyclopedia of Chemical Technology (5th Ed.)*, S. Arza, Ed., John Wiley & Sons, Inc, Hoboken, NJ, 2005, p. 729.
- [3] T. R. Hoare, D. S. Kohane, *Polymer* **2008**, *49*, 1993.
- [4] K. Pal, A. K. Banthia, D. K. Majumdar, *Des. Monomers Polym.* **2009**, *12*, 197.
- [5] B. V. Slaughter, S. S. Khurshid, O. Z. Fisher, A. Khademhosseini, N. A. Peppas, *Adv. Mater.* **2009**, *21*, 3307.
- [6] J. K. Oh, D. I. Lee, J. M. Park, *Prog. Polym. Sci.* **2009**, *34*, 1261.
- [7] T. C. F. Silva, Y. Habibi, J. L. Colodette, L. A. Lucia, *Soft Matter* **2011**, *7*, 1090.
- [8] M. S. Lindblad, E. Ranucci, A.-C. Albertsson, *Macromol. Rapid Commun.* **2001**, *22*, 962.
- [9] A. M. Stephen, "Other plant polysaccharides.", in *The Polysaccharides*, G.O. Aspinall, Ed., Academic Press, Orlando, 1983, p. 98.
- [10] K. C. B. Wilkie, *Adv. Carbohydr. Chem. Biochem.* **1979**, *36*, 215.
- [11] G. Gellerstedt, A. Majtnerova, L. Zhang, *Comptes Rendus Biologies* **2004**, *327*, 817.
- [12] N. Takahashi, T. Koshijima, *Wood Science and Technology* **1988**, *22*, 231.

- [13] C. Laine, T. Tamminen, B. Hortling, *Holzforschung* **2005**, 58, 611.
- [14] D. Fengel, G. Wegener, "*Wood Chemistry, Ultrastructure, Reactions*", Berlin, 1984, p. 167.
- [15] M. Lawoko, G. Henriksson, G. Gellerstedt, *Holzforschung* **2006**, 60, 162.
- [16] I. Gabriellii, P. Gatenholm, *J. Appl. Polym. Sci.* **1998**, 69, 1661.
- [17] T. Ehrman, "Method for determination of acid-soluble lignin in biomass.", in *Laboratory Analytical Procedures*, National Renewable Energy Laboratory, Golden, CO., 1996, p. No. 004/.
- [18] D. Evtuguin, J. Tomás, A. S. Silva, C. Neto, *Carbohydrate Research* **2003**, 338, 597.
- [19] D. Evtuguin, J. Tomás, A. S. Silva, C. Neto, *Carbohydr. Res.* **2003**, 338, 597.
- [20] A. d. S. Magaton, D. Piló-Veloso, J. L. Colodette, *Química Nova* **2008**, 31, 1085.
- [21] A. Teleman, J. Lundqvist, F. Tjerneld, H. Stålbrand, O. Dahlman, *Carbohydr. Res.* **2000**, 329, 807.
- [22] T. Koshijima, T. Watanabe, "*Association between lignin and carbohydrates in wood and other plant tissues.*", Springer-Verlag, Berlin, 2003.
- [23] L. B. Brasileiro, J. L. Colodette, D. Piló-Veloso, *Química Nova* **2001**, 24, 819.
- [24] T. Zhu, J. F. Kadla, H. m. Chang, H. Jameel, *Holzforschung* **2005**, 57, 44.
- [25] T. Kishimoto, J. F. Kadla, H. m. Chang, H. Jameel, *Holzforschung* **2005**, 57, 52.
- [26] A. S. Hoffman, *Adv. Drug Delivery Rev.* **2002**, 54, 3.
- [27] X. Qu, A. Wirsen, A. C. Albertsson, *Polymer* **2000**, 41, 4589.

**CHAPTER 5**  
**A QUANTITATIVE MOLECULAR STRUCTURE-PYROLYTIC ENERGY**  
**CORRELATION FOR HARDWOOD LIGNINS**

*Teresa Cristina Fonseca Silva,<sup>1,2</sup> Ricardo Bailerini dos Santos,<sup>3</sup> Hasan Jameel,<sup>3</sup> Jorge Luiz Colodette,<sup>1</sup> and Lucian A. Lucia<sup>2\*</sup>*

<sup>1</sup>Departamento de Química, Universidade Federal de Viçosa, Viçosa, MG, 36570-000; Brazil

<sup>2</sup>Laboratory of Soft Materials & Green Chemistry, Department of Forest Biomaterials, North Carolina State University, Raleigh, North Carolina 27695-8005; USA

<sup>3</sup> Department of Forest Biomaterials, North Carolina State University, Raleigh, North Carolina 27695-8005; USA

\*Corresponding author: E-mail: lucian.lucia@ncsu.edu; Tel.:(919) 515-7707

**ABSTRACT**

The molecular structures of the milled wood lignins (MWL) and technical lignins (TL) obtained from four hardwood species (*E. urograndis*, *E. nitens*, *E. globulus* and cottonwood) were quantified by <sup>13</sup>C-NMR in tandem with their thermal responses as obtained by TGA and DSC. Both MWLs and TLs showed similar DSC curves with two exothermic peaks (referred to as 1 and 2). Also, maximum temperatures for MWL peaks were higher than for TL with an average of 20°C and 10°C for the first and second peak, respectively. Even though calculated enthalpies for MWLs were higher because of their purities, TLs had reasonable relationships between heat values and lignin substructures. TL had a positive correlation between condensed structures and the enthalpy value between 413 – 428°C, but negative relationships were found at the latter temperature window for lignin substructures such as methoxyl groups, S/G and aliphatic OHs. These findings have important ramifications for the overall efficiency and energetics of thermochemical biomass transformations.

*Keywords:* Hardwood, milled wood lignin, technical lignin, thermal analyses, <sup>13</sup>C-NMR.

## 1. Introduction

Lignin is among the most prevalent biological materials on the planet and comprises 20-30% of the dry weight of woody plants, displaying high structural complexity. Indeed, the lignin structure exhibits a seemingly random (highly polydisperse), highly cross-linked polymeric network characterized by monomeric phenylpropane units cross-linked through ether linkages and carbon-to-carbon bonds. In addition to the multiplicity of lignin forms potentially available based on their origin, lignin structures vary within the same species and specimen according to isolation method.

The most commonly used lignin isolation method requires milling of the plant material followed by extraction with dioxane-water to provide what is referred to as milled wood lignin (MWL) [1]. Although MWL is considered the most representative type of lignin to study due its alleged similarity with native lignin in the wood cell wall, it has been demonstrated, not surprisingly, that chemical changes during the isolation process must be considered for structural veracity, especially with respect to lignin purity (carbohydrate contamination). Many methodologies have been proposed, for example, to remove carbohydrates chemically linked to lignin (e.g., lignin-carbohydrate complexes) and enhance the purity of MWL [2]. A reasonable method of extracting lignin is by precipitating the alkali-dissolved lignin from the viscous chemical waste medium produced during the kraft wood pulping process (the nominal “black liquor”) with mineral acid. The chemical structure of lignin, called technical lignin (TL), is not surprisingly modified along the process and TL is no longer identical to the native lignin found in the original wood. In fact, TL is largely recovered as a byproduct in the pulp industry to be used either as a solid fuel or additive in fuel oil.

Developing a better understanding of TL structures would be extremely helpful to exploit the potential of lignin as a renewable and readily available feedstock. Such utilization of lignin has attracted considerable interest from the “bio”-energy perspective. The use of renewable resources has emerged as a powerful alternative to fossil fuels because not only does it provide a local solution to energy dependence, but it helps to minimize environmental impacts by closing the green house gas (CO<sub>2</sub>) loop. Recent bioenergy engineering advances have increased the desirability of the utilization of biomass products to provide energy rich solutions [3]. For example, because pyrolysis is considered one of the promising thermochemical conversion routes, a more thorough

understanding of the thermochemistry of biomass may expedite its use for large scale transformations. It has been shown that biomass pyrolysis can be divided into several stages: moisture evolution, hemicellulose decomposition, cellulose decomposition, and lignin decomposition [4]. Thus, knowledge of the thermochemical response (pyrolysis characteristics) of each component is crucial for optimizing biomass conversion.

In this work, milled wood lignin and technical lignin from four hardwood species (*E. urograndis*, *E. nitens*, *E. globulus* and *P. trichocarpa*) were isolated. The eight lignin samples were then comprehensively characterized using  $^{13}\text{C}$ -NMR [5]. The pyrolysis behavior of the lignin samples was studied using thermogravimetric analysis and differential scanning calorimetry (TGA and DSC), i.e., according to their weight loss and energy changes during heating, respectively. The results from the TGA and DSC were compared and correlated to the quality and quantity of lignin substructures from  $^{13}\text{C}$ -NMR.

## 2. Material and Methods

### 2.1. Materials

Hardwood species cottonwood (*Populus trichocarpa*), and three eucalyptus varieties (*E. urograndis*, *E. nitens* and *E. globulus*) were used as the raw material to obtain isolated milled wood lignin (MWL) and related technical lignin (TL) from black liquor. The proposed lignin structure from eucalyptus is shown in Figure A.5.1. (Appendix)

MWL was isolated by a slightly modified Björkman procedure [1] described as follows: 40-60 mesh wood sawdust fraction from appropriate wood chips was extracted with 0.3% NaOH solution over 1 h (liquid-to-wood ratio = 50:1) under reflux. The extracted wood was thoroughly washed with hot distilled water until the filtrate reached neutral pH and it was dried at 30°C under vacuum. Alkaline extracted wood sawdust was ball milled using a planetary ball mill (Pulverisette 7, Fritsch). After the necessary milling time achieved a 30% yield, the wood sawdust was suspended in 96:4 dioxane:water (v:v) and agitated for 12 h at 40°C. The mixture was centrifuged and the liquid phase collected. This operation was done in triplicate. Then, the filtrates were combined, roto-evaporated to remove the solvents, and finally dried in a vacuum oven. No purification step was necessary because the lignin isolated from the alkaline extracted wood had a low sugar content (< 3%).

TL was isolated from black liquor after kraft pulping of the species by precipitating it at pH 2.5 and then extracting with diethyl ether. [6]. Kraft pulping was performed at the following conditions: 150°C, an active alkali of 40%, and a sulfidity of 25%. High alkaline charge was used to avoid alkali consumption by carbohydrates, extractives, and labile lignin structures.

## 2.2. Chemical/Structural Analysis of Lignin

<sup>13</sup>C-NMR spectra of the lignin preparations in DMSO-*d*<sub>6</sub> were recorded on a Bruker AVANCE 500 MHz spectrometer at 300 K using a 90° pulse width, a 1.4 s acquisition time, and 1.7 s relaxation delay. Chromium (III) acetylacetonate (0.01 M) was added to the lignin solution to provide complete relaxation of all nuclei. A total of 20,000 scans was collected. The integral over the spectral 162-102 ppm region was set as the reference, assuming that it includes six aromatic carbons and 0.12 vinylic carbons. In this way, the integral values divided by 612 gave results equivalent to a hundred aromatic rings (Ar).

Carbohydrate composition was determined by standard chromatographic methods after acid hydrolysis. In a typical experiment, 0.1 g of sample was hydrolyzed with 1.5 mL of 72% (w/v) sulfuric acid at room temperature for 2 h followed by sulfuric acid (3% w/v)-catalyzed hydrolysis at 120°C for 1.5 h. The resulting suspensions were diluted with ultra-pure water to the desired concentration and filtered through a 0.2 μm nylon filter (Milipore, Billerica, MA) before chromatography. They were then analyzed by using a Dionex ICS 3000 IC system equipped with a CarboPac PA1 cartridge, an eluent generator (EG50), and an electrochemical detector (ED50). Water was used as eluent at the flow rate of 1.0 mL/min, and the column temperature was 18°C. A post-column base containing 40 mM NaOH was added in to improve the detection by pulsed amperometry.

Klason lignin and acid soluble lignin were determined for each species using the extractive free wood meal [7]. The sum of Klason lignin and acid soluble lignin was reported as total lignin content.

## 2.3. Thermal Analysis of Lignin

The pyrolysis of the MWL and TL obtained from all species was carried out in a thermogravimetric analyzer (TGA, Q500, TA Instruments). The samples masses were 10-

15 mg and were heated up to 600°C at a linear temperature ramp of 10°C min<sup>-1</sup> under both purified nitrogen and air. A differential scanning calorimeter (DSC, Q100, TA Instruments) equipped with a cooling unit (RCS, Refrigerated Cooling System) was used to determine enthalpies (1 – 5 mg sample masses). The samples were placed in sealed aluminum pans and a linear temperature ramp of 10 mL·min<sup>-1</sup> was used from room temperature and 500°C. Data were analyzed using TA Instruments Universal Analysis Software. Experiments were done in duplicate for TGA analysis and triplicate for DSC (error less than 2% on TGA and 10% on DSC).

### 3. Results and Discussion

Lignin content of the hardwoods was estimated as total lignin (Klason and soluble lignin) whose values were found to be 25.5, 26.6, 23.9 and 21.5% for *E. nitens*, *E. urograndis*, *E. globulus*, and cottonwood, respectively. Considering soluble lignin to be as a small portion of the total (less than 4%), these results are similar to the Klason lignin contents found in previous published reports for other hardwoods species (18 – 23%) [8]. However, other than the content of lignin in wood, it is well known that its structural composition has a pronounced effect on delignification reactions, pulping yields, and thermal degradation [4, 9]. For this reason, two types of lignin (MWL and TL) were isolated to quantitatively assess their chemical structure by <sup>13</sup>C-NMR and energy and mass changes during lignin pyrolysis by DSC and TGA, respectively.

MWL is considered to be representative of the whole native lignin in the plant and therefore, the objective for using MWL in pyrolysis is to create a baseline. Under the pulping conditions, the residual lignin after kraft pulping was found to be 2.0% for cottonwood and *E. urograndis* and 1.4 % for *E. globulus* and *E. nitens*. TLs were precipitated with aqueous sulfuric acid and extracted with diethyl ether without further purification [6]. Sugar analyses revealed high levels of carbohydrate content, mainly xylans. The total sugar contents of the sampled lignins were 13.5, 14.6, 22.6 and 17.6% for *E. nitens*, *E. urograndis*, *E. globulus* and cottonwood, respectively.

#### 3.1. Lignin Quantification by <sup>13</sup>C-NMR

<sup>13</sup>C NMR is a powerful tool that provides valuable qualitative and quantitative structural information. The technique presents advantages such as relatively short

experimental acquisition, high accuracy, and a small amount of sample compared to traditional wet chemistry techniques. Previous NMR lignin characterizations for MWL, technical, and residual lignin in hardwoods have shown promise [5, 10-14]. The lignin substructures determined by  $^{13}\text{C}$ -NMR are shown in Figure 1.

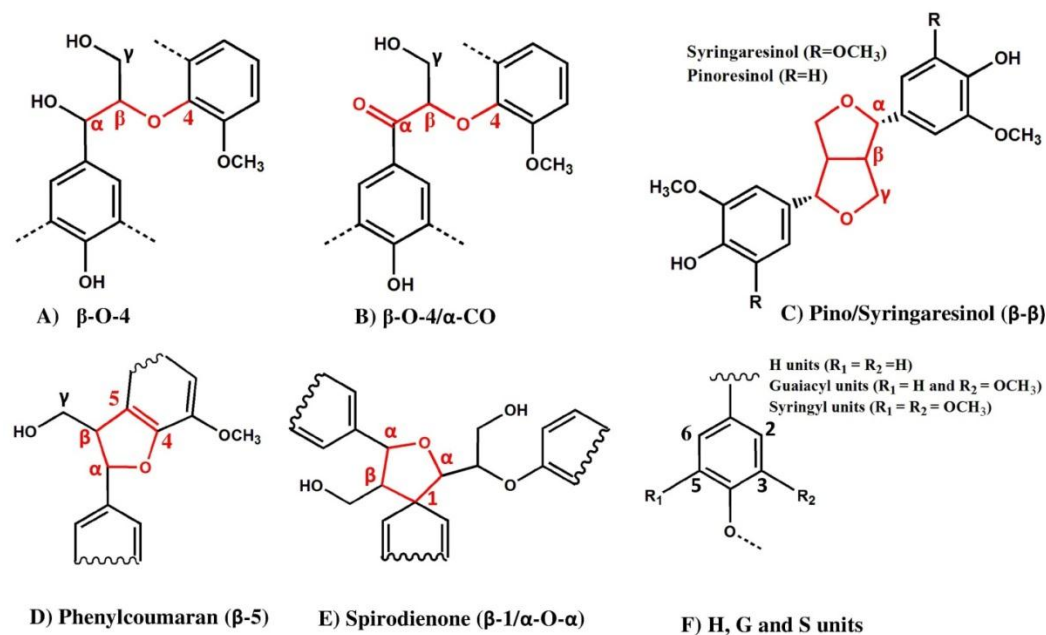


**Figure 1.** Lignin substructures determined by  $^{13}\text{C}$  NMR.

Carbohydrates signals could be found at their corresponding anomeric correlations ( $\text{C}_1\text{-H}_1$ ) between 99-102/4.0-4.5 ppm for TL estimated by HSQC NMR (Figure 2B) and also  $^{13}\text{C}$ -NMR (Figure 3). Even though it is believed that the linkage between carbohydrates and lignin in plant cell walls is covalent, it is not possible at this point to assume the presence of such linkages. For MWL, anomeric correlations of carbohydrates were not detected (Figure 2A) and these results are in good agreement with sugar analysis because less than 3% of carbohydrates were detected for the studied species. Table 1 shows the values found by  $^{13}\text{C}$ -NMR, whereas Figure 3 shows the spectra for MWL and TL of *E. globulus*. It is worth mentioning again that MWL represents a “true” representation of lignin in wood, while TL instead is a degraded one. Such a finding was corroborated by the resolved spectrum for MWL (Figure 3A) versus TL (Figure 3B). Thus, the pulping process and the isolation process have already demonstrated that there exists a great difference between MWL and TL structures.

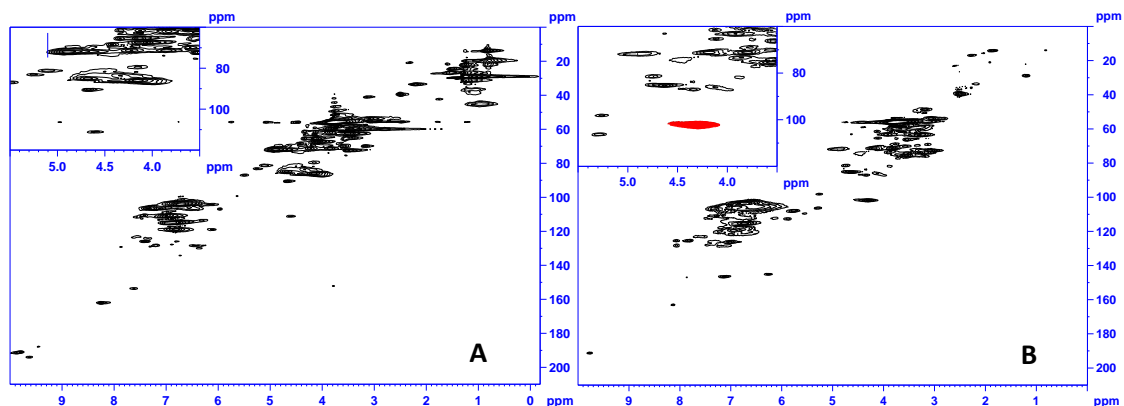


**Figure 2.** HSQC spectra of MWL (A) and TL (B) for *E. globulus*. In red, presence of anomeric correlation present in the carbohydrates.

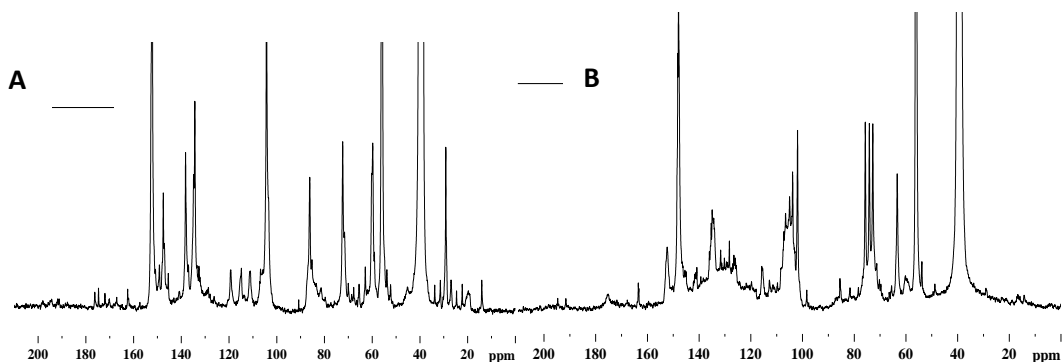


**Figure 3.** NMR spectra of MWL (A) and TL (B) for *E. globulus*.

Oxidized lignin structures ( $\beta$ -O-4/ $\alpha$ -CO) (Figure 1B) were detected in both types of lignin which upon further analysis indicate significant lignin structural variations (using the two-tailed Student's *t* test at 95% significance). Although the milling experiment was not supposed to oxidize lignin (it was done under an inert atmosphere and low heat generation), higher amounts of  $\beta$ -O-4 linkages having  $\alpha$ -CO group were found for MWL. Such results may be attributable to mechanically induced oxidation, whereas oxidation during lignification in plant may also generate such structures for lignins right in syringyl units [10]. Most of the native structures identified in MWL such as  $\beta$ - $\beta$  substructures (pino/syringaresinol) (Figure 1C) and  $\beta$ -5 (phenylcoumaran) (Figure 1D) are still found in TLs. The abundance of phenylcoumaran substructures is rather low and it presents no significant difference between MWL and TL.  $\beta$ - $\beta$  substructures were found to be slightly

higher for MWL (Table 1) confirming the permanence of these substructures after the pulping process [6].

**Table 1.** Content of lignin substructures quantified by  $^{13}\text{C}$  NMR of MWL and TL isolated from four hardwood species

Substructures	<i>E. urograndis</i>		<i>E. nitens</i>		<i>E. globulus</i>		Cottonwood	
	MWL	TL	MWL	TL	MWL	TL	MWL	TL
<b><math>\beta</math>-O-4/<math>\alpha</math>-CO</b>	2	1	3	1	4	1	3	0
<b><math>\beta</math>-O-4</b>	62	8	59	5	61	6	55	6
<b>Phenylcoumaran</b>	2	1	3	2	2	2	4	1
<b>Pino/syringaresinol</b>	9	7	10	8	10	7	8	7
<b>Spirodienone</b>	3	2	3	2	3	2	4	3
<b>Ar-CHO</b>	3	2	3	1	3	1	4	1
<b>Al. COOR</b>	1	9	6	8	7	7	4	10
<b>Methoxyl groups</b>	164	114	174	140	175	142	151	128
<b>Total OH</b>	153	121	157	134	161	135	142	121
<b>Aliphatic OH</b>	128	52	131	66	136	67	118	56
<b>Primary OH</b>	75	27	74	29	80	30	66	29
<b>Secondary OH</b>	53	25	57	36	56	37	52	27
<b>Phenolic OH</b>	24	69	24	68	21	68	19	65
<b>Deg. Condensation</b>	20	36	15	27	17	27	16	32
<b>S/G</b>	1.76	1.08	2.59	2.2	2.73	2.3	1.41	1.16

The spirodienone structure ( $\beta$ -1/ $\alpha$ -O- $\alpha$ ) might also be present in native lignin (Figure 1E) [15]. The higher amounts of these substructures in the MWL compared to TL can be explained due to the conversion of the linkage to  $\beta$ -1, under acid conditions (black liquor precipitation stage, pH 2.5) [16].

MWL of hardwood species has a higher proportion of  $\beta$ -O-4 linkages than TL (Figure 1A), relatively lower proportion of phenolic groups, and lower proportion of condensed structures (carbon-carbon linkages). During alkaline pulping,  $\beta$ -O-4 ether linkages are cleaved, leading to an increased content of phenolic groups and also reactions resulting in elimination of terminal methyloyl groups (-CH<sub>2</sub>OH) [13]. As a result, residual and dissolved kraft lignins have greater amounts of phenolic groups than native wood (MWL). At the same time, condensed linkages resist alkaline cooking conditions [17].

MWL has a greater abundance of methyloyl groups ( $\gamma$ -carbons). During pulping, a reduction in the methyloyl group is expected due to elimination of formaldehyde (CH<sub>2</sub>O). Total OH groups, consisting of aliphatic and phenolic groups, is higher for MWL than for TL and the reason for this can be attributed to the greater quantity of MWL aliphatic groups available primarily from the primary hydroxyl groups (methyloyl groups).

Taking in account that during kraft pulping delignification reactions (mainly ether cleavage reactions) can be counter-balanced to some extent by a number of different condensation reactions, it is not surprising that the content of methoxyl groups found in the TL is rather low compared to MWL, while the degree of condensation of the TL is higher. The extent of the condensation reactions is dependent on pulping conditions such as temperature and heating time [13]. Methoxyl group contents in the Eucalyptus in this study are high in agreement with previous work [11].

Signals of H units (Figure 1F) were found to be low as has been previously reported in Eucalyptus lignins [18]. In terms of H units and S/G ratios, no significant difference (using the two-tailed Student's t test at 95% of significance) was observed between MWL and TL, even with a large variation between the values for H units. S and G units (Figure 1F) were estimated to give molar S/G ratios of these lignin types and the results are in Table 1. The major difference in hardwoods is the ratio of S/G.

Considerable variation in kraft pulping performance for different hardwood species has been reported [19-21]. A study with model compounds has indicated easier cleavage of  $\beta$ -aryl ethers in syringyl lignins versus guaiacyl lignins [22]. Because  $\beta$ -O-4 is the

dominant linkage pattern in lignin and appears to greatly correlate with the S/G ratio, investigation of the S/G effect on kraft pulping of hardwoods have been extensively studied [19-21]. The influence of S/G ratio on pulping yield of *E. globulus* wood species led to the use of lignin S/G ratio as a selection parameter in clonal breeding programs for pulpwood production [23].

It was noticed that TL has a lower S/G value than MWL (Table 1) which is due to the higher reactivity of the S units during the pulping. The current S/G values for MWL are in agreement with S/V values found for the hardwood species determined by nitrobenzene oxidation [24] (S/V - *E. globulus*: 4.17; *E. nitens*: 3.28; *E. urograndis*: 2.01; cottonwood: 1.58).

### 3.2. Pyrolysis of Lignins in TGA/DSC

#### 3.2.1. TGA experiments

Figure 4 shows typical TGA experimental results for MWL and TL undergoing pyrolysis under a nitrogen atmosphere. The samples were heated from room temperature to 600°C at a rate of 10°C min<sup>-1</sup>. A considerable amount of char (~ 30%) remained which can resist temperatures as high as 900°C [4, 25]. The TGA weight-loss curves decay until approximately 100°C due to moisture evaporation and are stable between 100 and about 180°C.

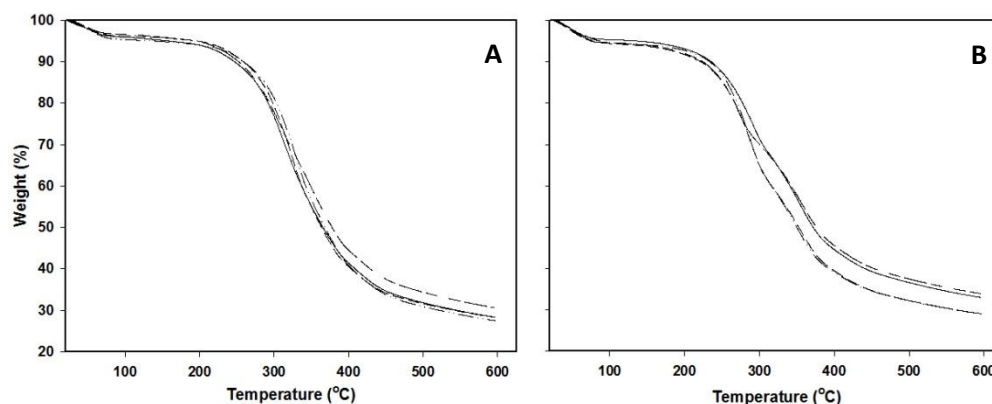


**Figure 4.** TGA curves. (A) MWL and (B) TL. *E. urograndis* (—), *E. nitens* (---), *E. globulus* (- · - ·), cottonwood (- - -).

In keeping with the drivers for this work, differences have been obtained between the pyrolysis behavior for MWL and TL. Figure 4 shows greater thermal stability for TL versus MWL. It is known that the difference in the stability of the lignins may be attributed to their preparation as well as to the presence of chemical characteristics such as degree of condensation [26, 27]. Unlike the TGA curves for TL, MWL curves are smooth for all species. This behavior could be likely explained based on the sugar content difference between the two types of lignin. The higher sugar content (13.5 – 22.6%) for TL might create inflection points in the TGA curves due to the thermal decomposition of the carbohydrates (xylans) present in the samples. Previous work using DSC has attributed an exothermic peak at 275°C – 300°C to the pyrolysis of hemicelluloses [4, 28] which is in agreement with the temperature of the inflection points in the TL TGA curves (Figure 4B).

TLs from *E. urograndis* and cottonwood have shown TGA curves with similar patterns and were thermally more stable than the other two species. Comparing *E. urograndis*/cottonwood species with *E. globulus*/*E. nitens* in terms of chemical structure, it can be observed (Table 1) that the first two samples have a higher degree of condensation as well as lower S/G molar ratio, which may confer higher thermal stability to these samples.

### 3.2.2. DSC experiments

A further advantage of DSC analysis is that it is a direct analysis, not requiring pretreatment. DSC curves for all samples show similar tendencies when temperatures are lower than 200°C as reported previously [4] and therefore the range 30°C – 200°C was not shown on the thermograms (Figure 5). An endothermic peak was found at about 100°C for all samples which can be attributed to the evaporation of water.

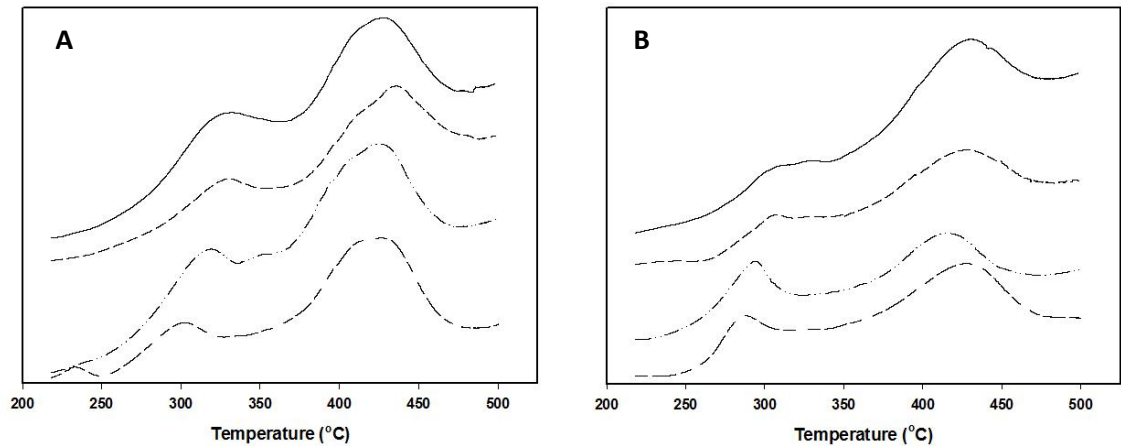


**Figure 5.** DSC curves (A) MWL and (B) TL. *E. urograndis* (—), *E.nitens* (---), *E. globulus* (- - -), cottonwood (- - -).

Beyond 200°C, two exothermic peaks were found for both types of lignin (Figure 5) and the peak temperatures for each DSC curve are shown in Tables 2 and 3, for MWL and TL respectively. MWL has its peak temperature at 301 – 327°C (peak 1) and at 424 – 434°C (peak 2), while peaks between 286 – 307°C and 413 – 427°C were characteristic for TL. The average values of peak temperature for MWL increased by a factor of 20 and 10 for peak 1 and 2, respectively, compared to TL. The larger shifts observed for temperature of peak 1 might be attributed to the sugar content of lignin. This fact can be ascertained by noting the peak temperatures of 1 for TL extracted from cottonwood and *E. globulus*. Because the amount of samples for the DSC experiments were similar, the shifts to lower temperatures observed in Table 2 and Figure 5B for those species are likely related to the content of sugar (xylans) recovered from black liquor at the end of pulping.

Taking into account the amount of carbohydrates in TL and the fact that hemicelluloses display peak temperatures varying from 275 to 370°C [4, 28], the first peak of TL can be attributed mainly to the degradation of hemicelluloses [4, 29, 30].

Great differences in the thermal responses of lignin and wood derivatives have been reported. DSC curves of Björkman lignin (MWL), for example, revealed three maxima at 330, 485, and 555°C, while two peaks at 350 (more pronounced) and 505°C were found for Klason lignin [31]. MWL and lignin-carbohydrate complexes (LCC) have presented DSC peaks at temperatures of 530°C and 475°C, respectively. By removing hemicelluloses

from LCC through acid hydrolysis, peak temperatures shifted from 475 to 520°C. Although higher top temperatures have been assigned to lignin pyrolysis, many studies involving lignin pyrolysis have shown peak temperatures in the range of 250 – 365°C, including Klason and alkali-extracted lignin [4, 25, 26, 28, 32]. Note that in this study, DSC experiments were conducted at temperatures only up to 500°C, which might have neglected any peak above this set temperature. At temperatures higher than 500°C, however, it is assumed that lignin has secondary pyrolysis events [4]. In fact, in this study, the DSC curves showed good similarity to wood powder and a mixture of lignin and cellulose (50:50) set as reference for thermal analysis of soil organic matter, which presented two exothermic peaks with maxima at 320 and 420°C [28, 30].

Even though it was found that the MWLs have rather low carbohydrate contents (< 3.0%), peak 1 attributed to hemicellulose pyrolysis from DSC curves is well pronounced (Figure 5A). The reason attributed to this behavior is based on a possible modification of polysaccharides during the isolation/purification process such as oxidation of hydroxyl groups on carbohydrates into carboxylic groups. In fact, previous work has attributed the first peak to decarboxylation [33, 34]. HSQC NMR (Figure 2) provides semi-quantitative evidence for the higher level of carboxylic groups on MWL (190-192/9.7-10 ppm).

It was reported that alkaline degradation of cellulose occurs even under mild time/temperature conditions leading to many products. Therefore, it is not unexpected that amorphous polysaccharides such as xylans are more prone to rapid molecular weight loss, degradation, and subsequent generation of many types of organic acids under alkali-extraction [35].

### **3.3. Analysis of the enthalpy and correlation with lignin substructures/content**

In order to correlate lignin substructures/content to thermal characteristics, enthalpies of each peak were calculated from the area under the DSC curves and are listed in Tables 2 and 3 for MWL and TL, respectively. The exothermic peaks found in this work were coincident with results found for soil organic matter fractions. The first peak was attributed to the liberation of aliphatic compounds and decarboxylation and the second one to the decomposition of aromatic moieties such as lignin dimers [30].

No significant difference ( $P < 0.05$ ) was found between MWL and TL from the enthalpy values for Peak 1. However, TL enthalpies of Peak 1 showed good correlation

with sugar contents. TL from *E. globulus* showed the highest sugar content, while *E. nitens* and *E. urograndis* showed the lowest.

In general, MWL had higher enthalpies (Peak 2) than TL (Table 1 and 2), but the driving factors behind this behavior were not due to lignin chemical structures. Instead, MWL samples are more pure than TL and this fact reflects in a higher heating value. Earlier studies reported a good linear correlation between lignin contents and heat of combustion (expressed as higher heating value - HHV) of fourteen biomass fuels, but there were no direct relationships between HHV and the holocellulose for the same lignocellulosic fuels [36].

**Table 2.** Enthalpy values ( $\pm$ SD) and peak top temperatures for MWL.

Species	Peak 1		Peak 2	
	$-\Delta H^{\circ}$ (J g <sup>-1</sup> )	Temperature (°C)	$-\Delta H^{\circ}$ (J g <sup>-1</sup> )	Temperature (°C)
<i>E. urograndis</i>	74.6 $\pm$ 13.9	321.8	181.0 $\pm$ 17.3	424.7
<i>E. nitens</i>	44.8 $\pm$ 3.9	327.0	152.6 $\pm$ 9.8	434.1
<i>E. globulus</i>	47.1 $\pm$ 2.1	312.1	212.0 $\pm$ 7.6	424.6
<b>Cottonwood</b>	36.8 $\pm$ 3.9	301.2	221.8 $\pm$ 11.6	425.7

**Table 3.** Enthalpy values ( $\pm$ SD) and peak top temperatures for TL.

Species	Peak 1		Peak 2	
	$-\Delta H^{\circ}$ (J g <sup>-1</sup> )	Temperature (°C)	$-\Delta H^{\circ}$ (J g <sup>-1</sup> )	Temperature (°C)
<i>E. urograndis</i>	22.7 $\pm$ 1.8	307.2	149.9 $\pm$ 12.4	425.5
<i>E. nitens</i>	23.6 $\pm$ 1.2	305.8	105.1 $\pm$ 10.1	423.7
<i>E. globulus</i>	55.5 $\pm$ 3.6	293.4	104.4 $\pm$ 8.3	413.5
<b>Cottonwood</b>	45.4 $\pm$ 4.1	286.0	139.2 $\pm$ 12.2	427.5

Because the enthalpy value for Peak 2 is attributed to the decomposition of aromatic moieties such as lignin, enthalpy values and substructures' quantity estimated by <sup>13</sup>C-NMR were subjected to correlation analyses. MWL did not show any significant correlation (at  $P < 0.05$ ) either positive or negative to the enthalpy values, while TL showed significant relationships.

Among all the correlations, the degree of condensation was the only measurement that had positive interaction with enthalpy values for Peak 2. Even though it was suggested that peak(s) at temperatures above 500°C were likely correlated to the degree of condensation [31], it was found that a fairly close relationship existed between those parameters ( $R^2=0.96$ ) at temperatures under 500°C (Peak 2) during pyrolysis (Figure 6A). Indeed, some authors have demonstrated that lignin is transformed to a more thermally stable form via condensation reactions during low-temperature heating [37]. Earlier work found that thermal behavior during pyrolysis depends upon the degree of condensation present in the initial lignin. Carbon-carbon linkages have shown to be more resistant to pyrolytic bond breakage than ether bonds [27, 37]. For example, methoxyl groups (-OCH<sub>3</sub>) connected to the aromatic ring of lignin are readily cleaved under pyrolysis conditions and demethoxylation of -OCH<sub>3</sub> was found to occur from 370 to 420°C [27]. In the present work, methoxyl groups showed negative correlation with the enthalpy calculated for Peak 2 for TL ( $R^2=0.93$ ) as could be seen in Figure 6B. Taking into account that higher methoxyl contents in TL correlate with a lower degree of condensation (correlation not shown), a lower pyrolysis temperature was revealed. With this in mind, the basis of the relationship between S/G ratio and enthalpy values (Figure 6C) is reasonable; as expected, it was found that a positive correlation existed between S/G and methoxyl groups (not shown). The  $R^2$  found for S/G versus  $\Delta H$  was 0.98 (Figure 6C).

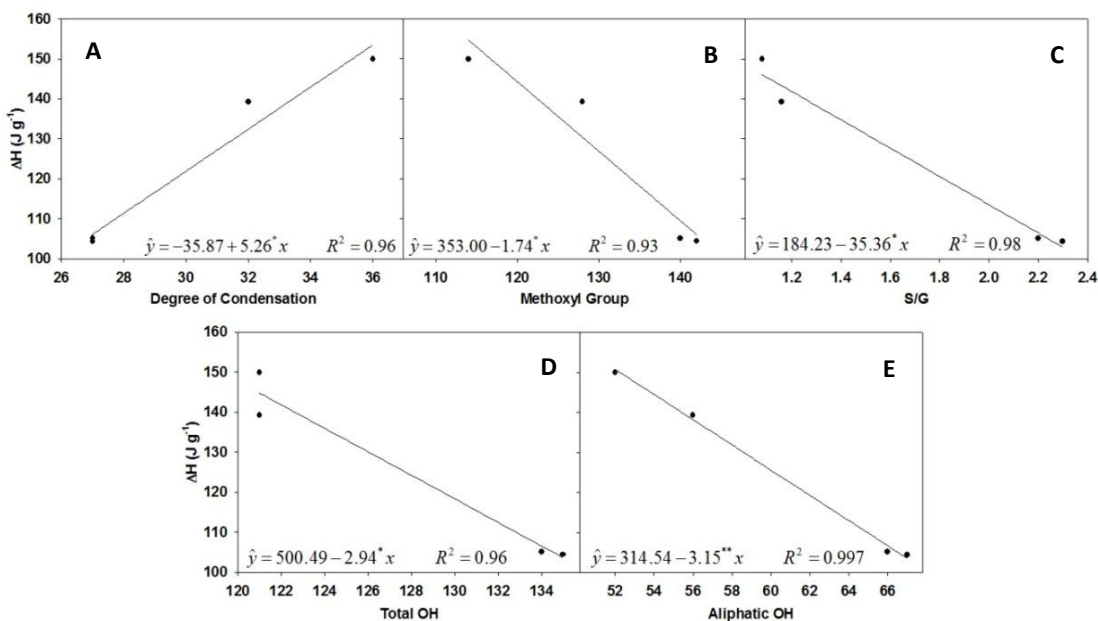


**Figure 6.** Correlation of <sup>13</sup>C NMR and DSC enthalpy results for Peak 2 of TL.

A negative correlation was found between enthalpy and total OH (Figure 6D). Total OH comprises aliphatic and phenolic OH units, but the phenolic OH content in TL had no significant difference among the hardwood species studied. This fact, therefore, indicates a negative contribution of aliphatic OH units to enthalpy (Figure 6E). Earlier studies have found OH groups in char from lignin at 550°C and attribute it to phenolic OH because they display higher thermal stability than aliphatic OH units. In the same work, increasing aromatic character is observed beyond 450°C by losing hydroxyl and aliphatic groups under such temperatures [38].

The results show greater regression values for aliphatic OH and enthalpy. In fact, the loss of OH groups through dehydration along with reactions such as decarboxylation and demethoxylation, contributes to increase aromatic carbon content and therefore degree of condensation.

Overall, the lignin structures (especially in TL) that are driving the amount of energy released during pyrolysis were reflected in the quantities of syringyl and guaiacyl moieties. S/G ratio determines lignin methoxyl content and also degree of condensation. These findings merit substantial consideration when assessing pyrolysis efficiency because they demonstrate that the lignin substructural qualities such as S/G ratio and carbon-carbon condensation greatly influence the thermodynamics of the process.

#### **4. Conclusions**

The ratio of syringyl and guaiacyl in TL was found to be the driving force for enthalpy variation in the hardwoods studied. As S/G decreases, methoxyl content is reduced and the degree of condensation in lignin rises. The reduction in methoxyl content was shown to increase the enthalpy, whereas increasing the degree of condensation of lignin was shown to have a positive correlation with the energy associated with the lignin pyrolysis of the different species.

Reducing the quantity of OH moieties present in lignin causes an increase in enthalpy values, whereas enhancing the degree of condensation of TL through dehydration, decarboxylation, and demethoxylation reactions contributes to increased aromatic carbon content and therefore cause the observed reduction in OH moieties.

Hardwood species with a higher degree of condensation (lower S/G ratios) were found to be thermally more stable than those with lower degrees of condensation. No significant difference ( $P < 0.05$ ), however, was found between MWL and TL for enthalpy values for Peak 1 (DSC). However, TL enthalpies of Peak 1 had good correlation with sugar contents; specifically, Peak 1 for MWL was associated with decarboxylation of the aliphatic structures from carbohydrates arising from the isolation/purification process. Thus, MWL showed higher enthalpies (Peak 2) than TL due its purity in terms of freedom from sugar contamination.

### **Acknowledgments**

We would like to gratefully acknowledge the CNPq (Coordenação de Aperfeiçoamento de Pessoal de Nível Superior) for the generous provision of a research fellowship to T.C.F.S. that allowed part of this work to be realized.

### **5. References**

- [1] Björkman A. Studies on finely divided wood. Part 1. Extraction of lignin with neutral solvents. *Svensk Papperstidn* 1956;59:477.
- [2] Brunow G. *Methods to Reveal the Structure of Lignin*: Wiley-VCH Verlag GmbH & Co. KGaA; 2005.
- [3] McKendry P. Energy production from biomass (part 1): overview of biomass. *Bioresource Technology* 2002;83:37.
- [4] Yang H, Yan R, Chen H, Lee DH, Zheng C. Characteristics of hemicellulose, cellulose and lignin pyrolysis. *Fuel* 2007;86:1781.
- [5] Capanema EA, Balakshin MY, Kadla JF. Quantitative characterization of a hardwood milled wood lignin by nuclear magnetic resonance spectroscopy. *Journal of Agricultural and Food Chemistry* 2005;53:9639.
- [6] Pinto PC, Evtuguin DV, Neto CP, Silvestre AJD. Behavior of *Eucalyptus globulus* lignin during kraft pulping. I. Analysis by chemical degradation methods. *Journal of Wood Chemistry and Technology* 2002;22:93
- [7] Dence CW. The determination of lignin In: Springer-Verlag, editor. *Methods in Lignin Chemistry*. Berlin; 1992.

- [8] Rencoret J, Gutiérrez A, del Río JC. Lipid and lignin composition of woods from different eucalyptus species. *Holzforschung* 2007;61:165.
- [9] Leroy V, Cancellieri D, Leoni E. Relation between forest fuels composition and energy emitted during their thermal degradation. *Journal of Thermal Analysis and Calorimetry* 2009;96:293.
- [10] Zhang A, Lu F, Liu C, Sun R-C. Isolation and characterization of lignins from *Eucalyptus tereticornis* (12ABL). *Journal of Agricultural and Food Chemistry* 2010;58:11287.
- [11] Evtuguin DV, Neto CP, Silva AMS, Domingues PM, Amado FML, Robert D, et al. Comprehensive study on the chemical structure of dioxane lignin from plantation eucalyptus globulus wood. *Journal of Agricultural and Food Chemistry* 2001;49:4252.
- [12] Liitiä TM, Maunu SL, Hortling B, Toikka M, Kilpeläinen I. Analysis of technical Lignins by two- and three-dimensional NMR spectroscopy. *Journal of Agricultural and Food Chemistry* 2003;51:2136.
- [13] Robert DR, Bardet M, Gellerstedt G, Lindfors EL. Structural changes in lignin during kraft cooking Part 3. On the structure of dissolved Lignins. *Journal of Wood Chemistry and Technology* 1984;4:239
- [14] Balakshin MY, Capanema EA, Chen C-L, Gracz HS. Elucidation of the structures of residual and dissolved pine kraft lignins using an HMQC NMR technique. *Journal of Agricultural and Food Chemistry* 2003;51:6116.
- [15] Brunow G, Lundquist K. On the acid-catalysed alkylation of lignins. *Holzforschung* 1991;45:37.
- [16] Zhang L, Gellerstedt G. NMR observation of a new lignin structure, a spiro-dienone. *Chemical Communications* 2001:2744.
- [17] Gierer J. Chemical aspects of kraft pulping. *Wood Science and Technology* 1980;14:241.
- [18] Ikeda T, Holtman K, Kadla JF, Chang H-m, Jameel H. Studies on the effect of ball milling on lignin structure using a modified DFRC method. *Journal of Agricultural and Food Chemistry* 2001;50:129.
- [19] Pinto PC, Evtuguin DV, Neto CP. Effect of Structural Features of Wood Biopolymers on Hardwood Pulping and Bleaching Performance. *Industrial & Engineering Chemistry Research* 2005;44:9777.

- [20] Bose SK, Francis RC, Govender M, Bush T, Spark A. Lignin content versus syringyl to guaiacyl ratio amongst poplars. *Bioresource Technology* 2009;100:1628.
- [21] Santos RB, Capanema EA, Balakshin M, Chang H-M, Jameel H. Effect of hardwood lignin structure on the kraft pulping process. TAPPI Peers Conference. Norfolk, VA; 2010.
- [22] Tsutsumi Y, Kondo R, Sakai K, Imamura H. The Difference of Reactivity between Syringyl Lignin and Guaiacyl Lignin in Alkaline Systems. *Holzforschung* 1995;49:423.
- [23] del Río JC, Gutiérrez A, Hernando M, Landín P, Romero J, Martínez ÁT. Determining the influence of eucalypt lignin composition in paper pulp yield using Py-GC/MS. *Journal of Analytical and Applied Pyrolysis* 2005;74:110.
- [24] Chen C-L. Nitrobenzene and cupric oxide oxidations. In: Lin SY, Dence CW, editors. *Methods in Lignin Chemistry*. New York: Springer-Verlag Berlin Heidelberg; 1992.
- [25] De Chirico A, Audisio G, Provasoli F, Schieroni AG, Focher B, Grossi B. Differential scanning calorimetry and thermal gravimetric analysis of lignin blended with triglycidyl isocyanurate. *Die Angewandte Makromolekulare Chemie* 1995;228:51.
- [26] Ramiah MV. Thermogravimetric and differential thermal analysis of cellulose, hemicellulose, and lignin. *Journal of Applied Polymer Science* 1970;14:1323.
- [27] Gardner DJ, Schultz TP, McGinnis GD. The pyrolytic behavior of selected lignin preparations. *Journal of Wood Chemistry and Technology* 1985;5:85
- [28] Tsujiyama S-i, Miyamori A. Assignment of DSC thermograms of wood and its components. *Thermochimica Acta* 2000;351:177.
- [29] Tsujiyama S-i. Differential scanning calorimetric analysis of the lignin-carbohydrate complex degraded by wood-rotting fungi. *Journal of Wood Science* 2001;47:497.
- [30] Lopez-Capel E, Sohi SP, Gaunt JL, Manning DAC. Use of thermogravimetry-differential scanning calorimetry to characterize modelable soil organic matter fractions. *Soil Science Society of America Journal* 2005;69:136.
- [31] Reh U, Kraepelin G, Lamprecht I. Use of differential scanning calorimetry for structural analysis of fungally degraded wood. *Applied and Environmental Microbiology* 1986;52:1101.

- [32] Murugan P, Mahinpey N, Johnson KE, Wilson M. Kinetics of the pyrolysis of lignin using thermogravimetric and differential scanning calorimetry methods. *Energy & Fuels* 2008;22:2720.
- [33] Leinweber P, Schulten HR. Differential thermal analysis, thermogravimetry and in-source pyrolysis-mass spectrometry studies on the formation of soil organic matter. *Thermochimica Acta* 1992;200:151.
- [34] Leinweber P, Schulten HR, Horte C. Differential thermal analysis, thermogravimetry and pyrolysis-field ionisation mass spectrometry of soil organic matter in particle-size fractions and bulk soil samples. *Thermochimica Acta* 1992;194:175.
- [35] Knill CJ, Kennedy JF. Degradation of cellulose under alkaline conditions. *Carbohydrate Polymers* 2003;51:281.
- [36] Demirbas A. Relationships between lignin contents and heating values of biomass. *Energy Conversion and Management* 2001;42:183.
- [37] Evans RJ, Milne TA, Soltys MN. Direct mass-spectrometric studies of the pyrolysis of carbonaceous fuels: III. Primary pyrolysis of lignin. *Journal of Analytical and Applied Pyrolysis* 1986;9:207.
- [38] Sharma RK, Wooten JB, Baliga VL, Lin X, Geoffrey Chan W, Hajaligol MR. Characterization of chars from pyrolysis of lignin. *Fuel* 2004;83:1469.

## OVERALL CONCLUSIONS

Biomass components (cellulose, hemicelluloses and lignin) were successfully studied and exploited for achievement of the biorefinery model. The main focus of this work was the utilization of xylans, the most common hemicellulose in hardwoods. For that, deeply investigation on the effects of xylans' chemical features was accomplished in order to produce advanced products with tailored properties.

Chemically modified xylans were deposited on cellulose pulp and among the parameters studied, temperature and type of uronic acid linked to the xylan chain played an important role during adsorption. Xylans were also used to successfully produce advanced materials such as hydrogels. The presence of acetyl moieties led to stiffer hydrogels which have a reduced capacity for water uptake and high drug delivery ratios differently of the non-acetylated xylan-based hydrogels. A development of a new hydrogel in a facile path was also accomplished by using mild delignification conditions. Aerogels from nanofibrillated cellulose were also produced and modifications on cellulose structure were able to generate high strength-materials. Finally, lignin from kraft liquor was isolated and studied according to its chemical structure and enthalpy changes during heating. Correlations between structures and enthalpy values were found, which allows further studies in order to modify the lignin structure to improve thermal processing.

## APPENDIX

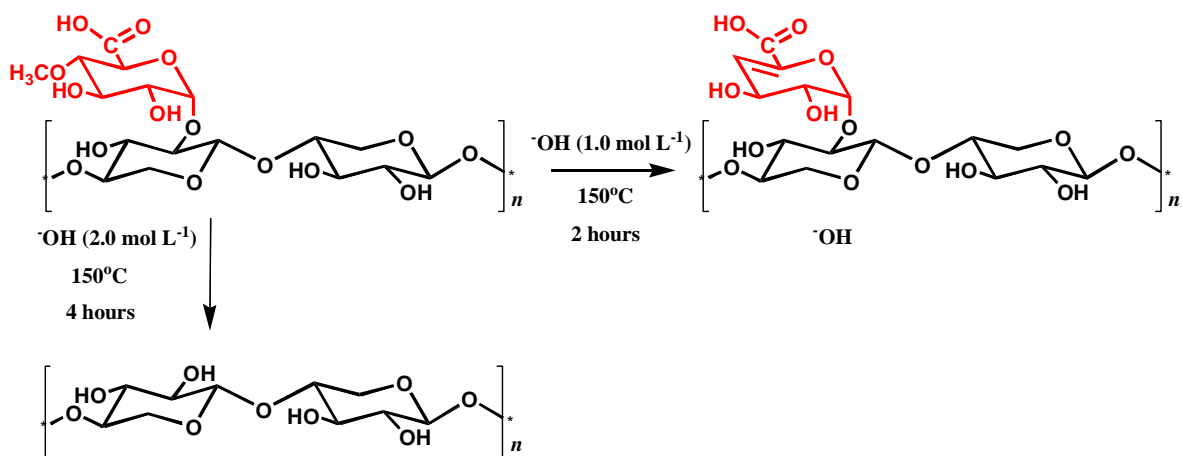


**Figure A.1.1.** Formation of different xylan structures features by alkaline treatment.

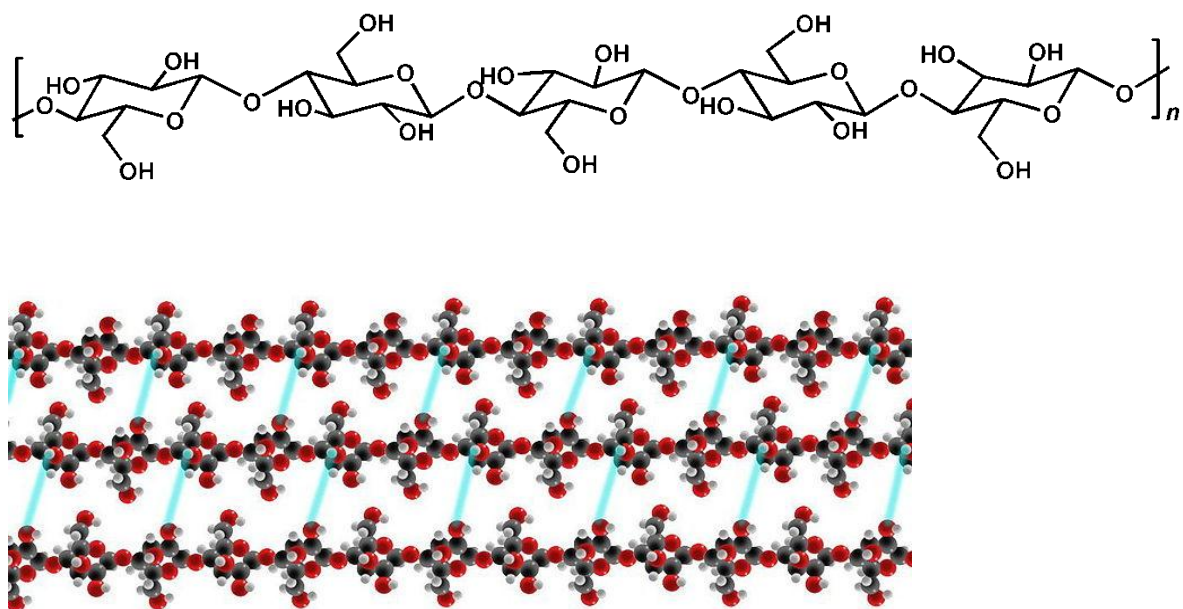


**Figure A.2.1.** Cellulose structure

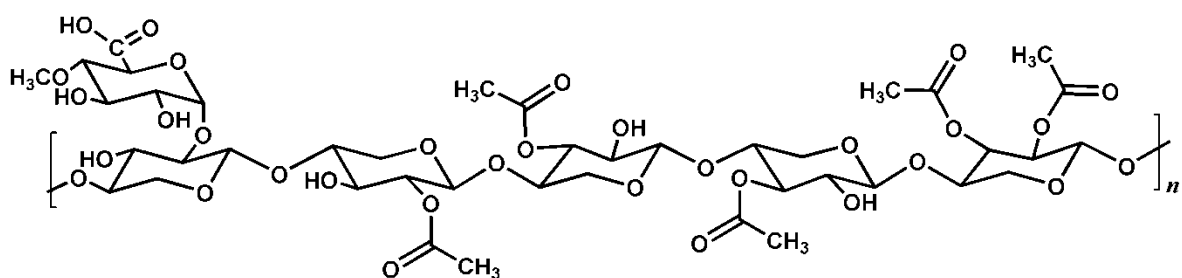


**Figure A.3.1.** Typical xylan structure from *Eucalyptus urograndis*: 4-*O*-methyl-(glucurono)xylans.

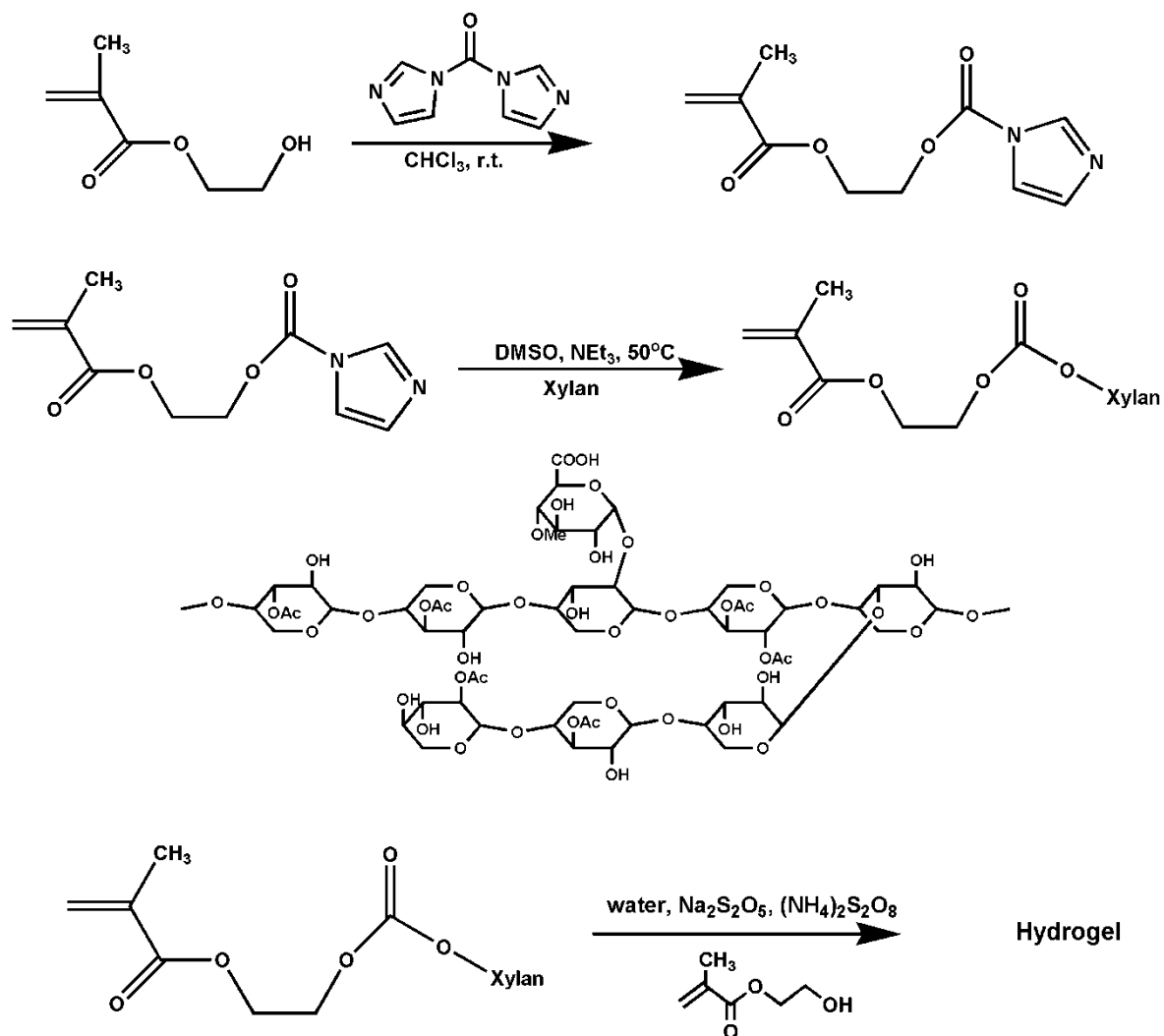


**Figure A.3.2** Procedure for synthesis of Xylan-Based Hydrogels.

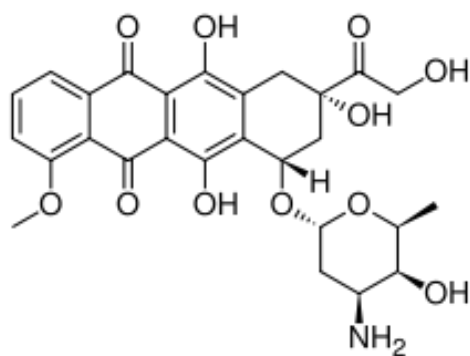


**Figure A.3.3** Chemical structure of doxorubicin.

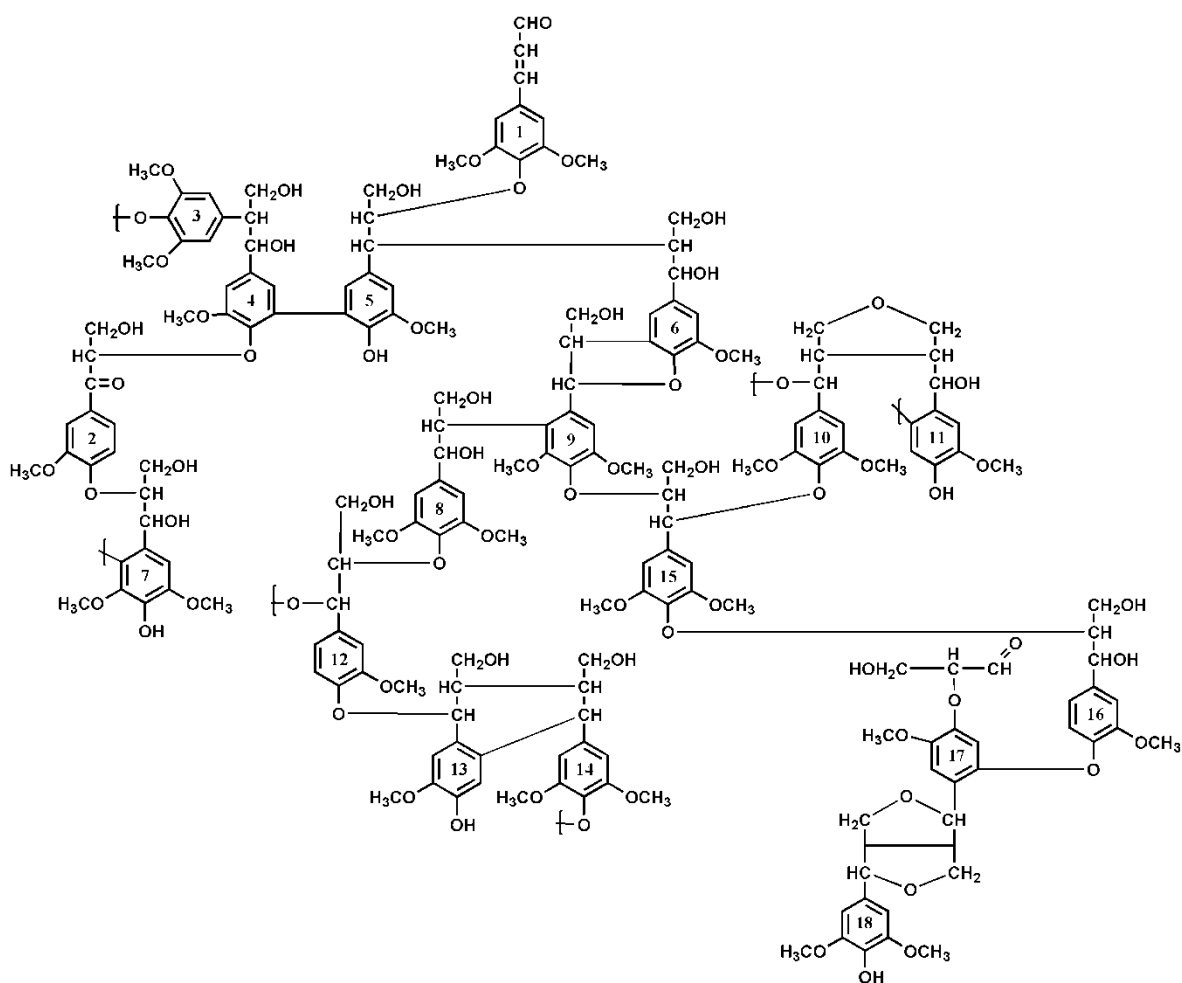


**Figure A.5.1** Proposed structure for *Eucalyptus grandis* lignin.